2001

Use of a mass consistent wind model to investigate areas of enhanced rainfall

Brian Stephen Reinbold
San Jose State University

USE OF A MASS CONSISTENT WIND MODEL TO INVESTIGATE AREAS OF ENHANCED RAINFALL

A Thesis

Presented to

The Faculty of the Department of Meteorology

San Jose State University

In Partial Fulfillment

of the Requirements for the Degree

Master of Science

By

Brian Stephen Reinbold

December, 2001

UMI Number: 1407315

APPROVED FOR THE DEPARTMENT OF METEOROLOGY

Alison F.C. Bridger

Dr. Alison F. C. Bridger

Scot Rafkin

Dr. Scot Rafkin

Douglas M. Sinton

Dr. Douglas Sinton

APPROVED FOR THE UNIVERSITY

Joseph J. Pesek

ABSTRACT

USE OF A MASS CONSISTENT WIND MODEL TO INVESTIGATE AREAS OF ENHANCED RAINFALL

By Brian S. Reinbold

This study uses a mass consistent wind model, WOCSS (Winds on Critical Streamline Surfaces), to calculate rainfall enhancement along the Santa Cruz Mountains of California. Rainfall and vertical velocity values are correlated to determine if WOCSS may be used as a quick and accurate diagnostic tool.

Results of the study show that correlation values were satisfactory for areas with sufficient meteorological data, and poor where data is limited. Improvements made to the analysis, including hourly sounding input, increasing available wind data near rainfall sites, and using the moist adiabatic lapse rate to determine stability through saturated layers will likely increase model accuracy. At this time WOCSS does not show the necessary accuracy to be used as a diagnostic tool to determine rainfall enhancement across areas of complex terrain.

ACKNOWLEDGMENTS

I would like to thank my thesis advisors Dr. Alison Bridger, Dr. Scot Rafkin and Dr. Doug Sinton for giving me the knowledge and guidance necessary to undertake and complete this thesis project.

I wish to also thank my father for all his encouragement through the years and for not letting me give up during difficult times.

Lastly I want to recognize my wife Shannon for having tremendous patience, love and support during both my time away from her at San Jose State and the final push to finish this thesis project.

TABLE OF CONTENTS

LIST OF TABLES

LIST OF FIGURES

1.0 Introduction

Diagnosing rainfall amounts over areas of complex terrain has proven to be a very difficult task. Generally, regional and mesoscale numerical models, used to forecast weather, do not have the resolution necessary to accurately depict complex terrain features. These models parameterize microphysical processes, and break the domain into a grid with varying horizontal resolutions. Current National Center for Environmental Prediction (NCEP) models have a suite of regional and mesoscale models including the Nested Grid Model (NGM), Regional Spectral Model (RSM), Medium Range Forecast Model (MRF) and Aviation Model (AVN). The NGM is run with a horizontal resolution of about 48km and the RSM has a resolution closer to 29km. The MRF and AVN use a triangular grid with resolutions of about 0.49 degrees in both latitude and longitude (www.ncep.noaa.gov). Another model run at NCEP is the Eta model. Different versions of the Eta are run at varying horizontal resolutions ranging from 29km for the mesoscale Eta to 48km for the regional Eta model.

Other mesoscale models used to study rainfall patterns near complex terrain are the MM5 and the NCEP Eta10 (Colle et. al. 1999, 2000). While the Eta10 runs at a horizontal resolution of 10km, the MM5 uses a nesting technique and can achieve resolutions under 5km.

An average terrain value is calculated for each grid box throughout the domain, regardless of the model used. Higher resolution models will obviously capture more of the small-scale features of the terrain, providing a more realistic simulation. Lower resolution prognostic models (larger grid boxes) have a tendency to underpredict rainfall over complex terrain (Mass et. al. 1990). This underprediction can have important implications over the mountains of the Western US in winter, when heavy rain and flooding can occur.

It seems reasonable that the solution to the rainfall underprediction would be to increase the resolution of the models. The problem is that as the resolution of these numerical models is increased, large amounts of computing power and time are required to calculate the microphysical parameters in each grid box. As a result, the higher the resolution, the more time each run will take to complete. During heavy rainfall or runoff events, critical warning time may be lost waiting for these complex mesoscale model runs to finish. Also, recent studies (Colle et. al. 1999, 2000) show that higher resolution prognostic models tend to overpredict rainfall on the windward side of a terrain barrier while underpredicting precipitation along the lee side.

Another approach to rainfall prediction is the use of simplified model analysis without complex dynamics or microphysics. An example of this approach is the Rhea Orographic Precipitation Model (OPM) (Rhea 1978, 1996, 1997). The model uses sounding information (including temperature, moisture, and wind information) to calculate Quantitative Precipitation Forecasting (QPF) over areas of complex terrain. It uses a 5km-resolution grid and 12 vertical levels from 1000 to 450mb at 50mb increments. Each grid point represents a parcel of air in which the moisture content is calculated from the input parameters. Wind speed at each level is derived from the sounding, and a constant 700mb wind direction is assumed throughout the domain. The wind speed and direction determine the advection of each parcel for every time step. By keeping track of moisture parameters such as condensation, evaporation, and precipitation efficiency during advection of the parcel over terrain, QPF can be calculated. Results from this model analysis were very encouraging for diagnosing the distribution of rainfall over Northern California mountain areas (Rhea 1978, 1996).

Our study will utilize a simplified model analysis similar to Rhea's for the purpose of determining how accurately rainfall enhancement can be diagnosed. The Winds on Critical Streamline Surfaces (WOCSS) model, developed by Ludwig (1988), interpolates observed winds to very high resolution in areas of complex terrain. WOCSS uses flow-following coordinates and inputs terrain, wind, and sounding information to calculate an array of horizontal winds along each flow surface. The static stability of the flow determines whether the flow will pass over the terrain or be deflected around it (Ludwig et. al. 1991). During more unstable conditions, more of the flow will pass over a terrain barrier.

There are no moisture parameters in the WOCSS model analysis. In our study, a different technique is used (compared to the Rhea approach) to diagnose rainfall patterns in areas of complex terrain. Using the calculated array of horizontal winds from WOCSS, a vertical velocity field (w) can be found using the following relationship:

$$w = V_H \bullet \nabla Z_{sfc} \qquad (1)$$

where V_H is the horizontal wind along the flow surfaces and Z_{sfc} is the height of the terrain. Areas of positive vertical velocity, or upward motion, should enhance rainfall on the windward portion of the terrain. Conversely areas of negative vertical velocity, along the lee side of the barrier, tend to have less precipitation.

The horizontal advection of the raindrops needs be taken into account when attempting to correlate vertical motion patterns with rainfall distribution. Factors such as the growth of the droplets within the cloud and the fall speed of the mature drops will allow a portion of the enhanced precipitation to fall downwind of the region of enhanced vertical velocity. A simple technique will be developed and incorporated into the analysis to estimate the effect of the raindrop transport. This technique, called the Cone Method, will account for the downwind droplet advection of the raindrops by incorporating a certain number of upstream vertical velocity grid points, from a given reference point, into the analysis. Thus, enhancement of rainfall may occur some distance downwind of the enhanced upward vertical motion. The Cone Method will be tested extensively using varying cone sizes to determine if an optimal value exists.

The goal of our study is to see if there is a high correlation between the vertical velocity field produced by WOCSS and the observed rainfall enhancement in the Santa Cruz Mountains of California. Rainfall from stations in the Santa Cruz Mountains will be compared to stations in valley locations (e.g. San Jose) so that rainfall enhancement can be determined. Rainfall at valley locations away from the terrain will represent the overall synoptic-scale precipitation, and will be assumed to have little to no orographically-produced rainfall. For this reason, a location in the mountains, under the influence of positive orographic vertical motion, should experience higher rainfall compared to the valley location. This orographic precipitation gives rise to the rainfall enhancement, or difference in precipitation amount, between a mountain and valley location. Correlations between vertical velocity and enhanced precipitation fields will be calculated as a measure of rainfall enhancement.

Of the factors used to determine the vertical velocity field, the terrain is, perhaps, the most important. Winds along a flow surface determine the angle the flow will interact with the terrain. Winds moving perpendicularly into a mountain range will produce a higher vertical velocity field compared to air moving parallel to the same barrier. A second factor influencing the vertical velocity field is the stability throughout the vertical domain. The stability influences the horizontal wind field produced by WOCSS. When the atmosphere is more stable, the flow will have a tendency to be deflected around the terrain. In more neutral and unstable cases, the air will be more likely to flow over the terrain, producing higher vertical velocity values.

The time period of the study is from 1-7 February, 1998, when a series of strong Pacific storms moved across California producing large amounts of rain. Wind calculations from WOCSS rely heavily on the amount, and accuracy, of the input data (Becker 1992). For this reason, as much data as possible has been used in this study to provide the most accurate w-field. A total of 28 National Weather Service (NWS) surface stations including one buoy off the San Francisco coast were used in the study. The Santa Clara Valley Water District provided hourly rainfall data for 18 rain gauge stations for the entire period. The upper level sounding from Oakland is used as well, with releases at 0000Z and 1200Z daily.

2.0 PAST STUDIES

A. Overview

Determining the enhancement of rain across areas of complex terrain has always been a difficult task. Different approaches have been attempted to try to measure the enhancement that occurs when synoptically-driven precipitation producing flow is forced over a mountain barrier, giving rise to an added orographic precipitation component. Understanding how the flow interacts with the terrain to produce this orographic rainfall enhancement is the key to diagnosing the rainfall distribution across a given mountain basin. The use of mesoscale and regional computer models with complex dynamics, physics and microphysical parameterization has been widely used to try and comprehend wind and precipitation patterns across areas of terrain. Models employed by NCEP like the Eta, AVN, and RSM, are all used to study flow interaction with terrain. Another widely used model is the MM5. The MM5 is a nonhydrostatic regional-scale model with the capability of high-resolution simulations of atmospheric circulation (Archer 1998).

Other methods, including our current study, use simplified models and techniques to describe wind and rain patterns around terrain barriers without the complex and time consuming dynamics and microphysical process included in mesoscale models like the Eta and MM5. These simplified studies include the work of Rhea (1978, 1996, 1997) who developed the OPM in an attempt to determine rainfall patterns across specific mountain basins.

Another simple method that attempts to understand and observe the interaction and enhancement of precipitation across mountainous terrain includes the use of Doppler radar.

The various methods described above used to study and forecast wind and rainfall patterns across complex terrain will be diagnosed in the following sections. The positive and negative aspects of each method will be discussed in an attempt to show that more accurate studies are still needed in order to fully understand and diagnose rainfall distribution across areas of complex terrain.

B. Complex Model Studies

There have been numerous studies in recent years using complex dynamical numerical models to study wind flow interaction around areas of complex terrain, including the aspect of precipitation enhancement. Many of these studies have been performed during the winter months along the West Coast of the United States (Mass et. al. 1990; Colle et al. 1996, 1999, 2000). During this time period, a fully developed westerly jet stream, combined with Pacific moisture, can provide the region with periodic heavy rainfall. The interaction of the flow with the broad mountain areas along the West Coast can greatly enhance the precipitation that occurs.

Past studies show that the general underprediction of precipitation amounts by lower resolution complex computer models could be improved by increasing the resolution (Smith et. al. 1997). A recent study (Colle et. al. 1999) made across the Pacific Northwest may discount this theory to some degree. Two mesoscale models were compared to see which performed better at high resolutions. The study used the National

Center for Atmospheric Research (NCAR) MM5 model and the NCEP Eta10. The MM5 model was run at 36 and 12km while the Eta10 was run at 10km (Colle et. al. 1999). The models were run through the cool season from December 1996 through April 1997. The goal of the study was to compare the models and see which one produced the most accurate distribution of precipitation. Results from the study showed that while the 36km MM5 model tended to distribute rainfall more evenly across both the windward and leeward side of the mountains, the 12km MM5, and especially the Eta10, overpredicted precipitation on the windward side of the terrain, with bias scores of over 200% in many locations. With much of the precipitation falling on the windward side of the terrain, too little was produced on the leeward side. It was also found that this bias was amplified for periods of moderate to heavy precipitation, while minimal during lighter events (Colle et. al. 1999). The paper attributes this windward overprediction and leeward underprediction of precipitation to the microphysics in the models not accurately accounting for the transport of rain and snow produced on the windward slopes downwind to the leeward side. This effect may be amplified in the Eta10 due to the model's flow-blocking scheme having too much influence. Overall the 12km MM5 produced the best windward results, while the 36km MM5 produced the most accurate rainfall bias along the leeward side of the terrain (Colle et. al. 1999).

A second study used the MM5 at 12km and 4km during the same time period as above to see if this windward overprediction of precipitation was amplified or reduced at very high resolutions. The results showed some improvement over the 12km MM5, but the 4km MM5 still produced too much windward precipitation and a 20-40%

underprediction along the leeward side of the Pacific Northwest Mountains (Colle et. al. 2000).

An extreme example of the effects of a landfalling synoptic scale cyclone interacting with coastal topography was the Inauguration Day cyclone, which struck the Pacific Northwest Coast on January 20th 1993 (Steenburgh & Mass 1996). The MM5 was used in this study to simulate the complex wind flow across terrain (Dudhia 1993; Grell et al. 1994). In the case of the Inauguration Day Cyclone, an MM5 simulation was run with a 27km horizontal grid and 9km nesting, along with 28 vertical levels. The model successfully reproduced the pressure perturbations that developed over the Olympic Mountains, and the associated low level jet which brought damaging winds and orographically enhanced rainfall to the Cascade and Olympic Mountains (Steenburgh & Mass 1996).

A similar but more comprehensive multitask study was performed during the months of December in 1993 and 1995. The COAST (Coastal Observation and Simulation with Topography) experiment looked at many aspects of cyclone development and the associated interaction with complex terrain along the West Coast (Bond et. al. 1997). The goal of the study was to collect a large dataset and attempt to model the mesoscale features associated with landfalling storms. Events that may occur include: the formation of low level jets; flow splitting; and enhancement of rainfall from orography (Bond et. al. 1997). Because there are few data sources offshore, the NOAA P-3 research airplane was used to collect data during precipitation events.

One case study was performed along the Oregon coast on December 1, 1995. A cold front moved onshore along the southern Oregon coast, producing enhanced rainfall along the coastal mountains. The MM5 model again was used to try to reproduce the observed enhancement of precipitation in the pre-frontal region. Even with the aid of the P-3 data, and the high resolution MM5 model, the results showed that the heaviest observed precipitation occurred 30km to the north of the MM5 simulated rainfall prediction. Also, the MM5 predicted southwesterly flow along the northern reaches of the domain, which did not match up well with coastal observations taken during the event (Bond et. al. 1997). These deficiencies may be attributed to the inability of the microphysical parameters to accurately model the wind and precipitation fields (Colle et. al. 1999). Other than the aforementioned results, the MM5 accurately depicted the wind flow and rainfall across the region.

Further studies have been made in an attempt to try to improve the understanding and modeling of landfalling cyclones along the West Coast. CALJET (The California Land-Falling Jets Experiment in 1997) set out to improve on the results of COAST in respect to forecasting the distribution of precipitation across the complex terrain of the Northern and Central California coast (Ralph 1997). The primary goal of CALJET was to try to improve the short-term QPF predictions as mid-latitude cyclones come ashore. The experiment used a much more extensive data collection network of instrumentation than the COAST experiment, including 10 profilers and the advanced mobile radar unit Doppler on Wheels. As with the COAST study, the NOAA P-3 aircraft was used, along with data from offshore buoys and the array of available weather station data along the

California coastline. Results from this study showed that the data collected during CALJET may improve short-term 24-hour precipitation forecasts along the Central California coast (Ralph 1997).

An extension of the CALJET study, PACJET (Pacific Coast Jets Experiment), will attempt to learn more about Pacific storms and improve short term 24 hour forecasting of land-falling cyclones (Blier 1999). One goal of PACJET will be to study the effects of topography on landfalling storm systems. The study took place during January and February of 2001 and results are still being analyzed.

Although most of the mountain basins of the United States are located across the western portion of the Country, the lower topographical region of the Appalachian Mountains provide another region to investigate flow interaction and rainfall enhancement. The Tennessee Valley Authority (TVA) manages the flow of the Tennessee River, the fifth largest river in the US, to reduce the threat of flooding and meet the water needs of the region (Mao and Mueller 2000). The TVA uses the NCEP Regional Spectral Model (RSM) as a guide to 48 hour weather forecasts across the region. The RSM has 28 vertical sigma layers, a horizontal resolution of about 21km and contains complex dynamics and microphysics including the Arakawa-Schubert convective parameterization scheme (Mao and Mueller 2000). The model uses polar stereographic projection for analysis and is nested within the lower resolution NCEP Global Scale Model (GSM) reducing lateral boundary concerns. The goal of this study was to verify the accuracy of the RSM in predicting rainfall across the Southern Appalachian Mountains, which is the main water source of the Tennessee River. The model was verified against a network of

243 rain gauges across the area. Results of a year long study of 1996 observed rainfall data versus the RSM model predicted rainfall shows the RSM performed well, with typical correlations of 0.74 (Mao and Mueller 2000).

The use of complex models to study rainfall patterns near areas of terrain is not restricted to the United States. A study in South Africa used the NCEP regional Eta to study a heavy rain event that caused hundreds of lives to be lost due to flooding (Dyson and Van Heerden 2001). The flooding event was tropical in nature and produced nearly 1000mm of rain during the month of February 2000. The study compared the Eta produced rainfall with observations. It was found that the overall rainfall pattern was captured across the region but rainfall amounts were underestimated by up to 50% (Dyson and Van Heerden 2001).

All the experiments presented above used complex models aimed at a better understanding of wind and precipitation patterns across complex terrain. Although most of the studies showed encouraging results, there is room for improvement. It is the hope of our study that the WOCSS analysis scheme is able to provide an accurate assessment of the enhancement of precipitation across a region of complex terrain, without the need for time-consuming and data intensive complex microphysical computer models like MM5, Eta and RSM.

C. Rhea Model

Simplified model techniques can provide another approach to studying wind flow or precipitation enhancement across mountainous terrain. One of these approaches is the use of the Rhea OPM model (Rhea 1978). The OPM is an example of a diagnostic procedure used to analyze precipitation enhancement in complex terrain areas. The OPM assumes steady-state two-dimensional flow to simplify the calculations performed during the analysis. Total rainfall at any given location can be calculated from the addition of the large-scale synoptic-scale precipitation, the forced orographic precipitation, and convective precipitation (Rhea 1978).

The terrain is input into the model with a 5km grid interval resolution. Constant 700mb winds are used throughout a specified domain with directions broken down into 10 degree increments. The precipitation rate is calculated by keeping track of the moisture transport through each layer as it interacts with the terrain. As stated in the introduction, each layer is 50mb thick and the domain stretches from the surface to 450mb. Observed sounding information is used to initialize the moisture, wind and temperature profiles throughout the vertical domain. The same parameters are used for 12 hour blocks of time between each available sounding. For stable conditions (without an inversion) or for neutral conditions, the flow is directed over a given terrain barrier in the model. The model analysis calculates the condensate or liquid water content of the cloud at each level and grid interval for each time step. The associated precipitation or evaporation that takes place depends on the upward or downward movement of air and the relative humidity below the cloud level. The condensate in each 50mb layer that is not precipitated or evaporated is then advected downwind into the next grid box, and the calculation is performed for each successive time step. The total amount of condensation that precipitates during a given time period can then be compared to actual precipitation values over the same time period to demonstrate the accuracy of the model (Rhea 1978).

Rhea (1978) conducted experiments with the OPM in western Colorado to test the accuracy of the model analysis. The time period covered 13 fall and winter seasons for the months of October to March. Only these seasons were used to cut down on the amount of convective precipitation that occurs during the late spring through early fall seasons. Rhea was able to obtain fairly high correlations (ranging from 0.75-0.94 over a 13 year period (Rhea 1978)) between seasonal precipitation predicted by the model and actual precipitation measurements. Because there are only a few precipitation gauges across the domain, and most of the winter precipitation falls as snow across the Rockies, spring stream runoff values were used to verify precipitation amounts for much of the region. It should be noted that these correlation values are for an entire season, and it was determined that as the time period was shortened, the correlation values decreased. QPF calculations over time frames of 24 hours had correlations of only 0.56 to 0.87 (Rhea 1978).

There were some limitations to the model analysis. For example, precipitation derived from convection is not included in the model. While most of the winter precipitation is not convective in nature, some error is possible from the small amount of convective precipitation that occurs during these months. Another possible source of error is from the observations used to initialize the experiment. These include wind speed, temperature and cloud depth taken from the input soundings. These parameters are initially assumed to be constant throughout the domain. Large errors can also occur because only one 700mb wind direction is assumed throughout the domain during each time period of 12 hours (Rhea 1978).

A recent study using the OPM (Rhea 1996) was conducted to see if modifications to the OPM could enhance the accuracy of short-term precipitation forecasts. The study, covering the period January-March 1995, used prognostic sounding data from the NGM, AVN, and Eta computer models as input into the OPM. Eight of the eleven major mountain basins of California were studied. Using a test sounding from a storm period with moist, windy, and warm conditions for that particular region, reference soundings containing temperature, wind speed and moisture depth can be calculated at each grid point throughout the domain. A different reference sounding is calculated for every 10 degree wind direction segment. These 35 reference calculations are made only once for any given mountain basin. These reference sounding were then used to calculate a reference basin average (RBA) precipitation value. Only the wind direction variable could change the value of the RBA for each 24 hour period (Rhea 1996).

To calculate the QPF for each basin, a slightly different procedure was used from previous studies. In this study it was determined that adequate precipitation gauges existed in the 8 mountain basins to represent the region. Unlike the 1978 study, high mountain gauges are now designed to melt snow to give a liquid equivalent precipitation value, eliminating the need for any stream runoff measurements. Also, reference sounding information can be compared to the average predicted sounding from the NGM, Eta and AVN regional and mesoscale models using the 12 to 36 hour forecast period prognostic data. So, for each 24 hour forecast period, a correction factor (CF) is calculated. The CF is calculated by comparing the sounding parameters of temperature, wind speed and moisture content to find the condensation supply rate (CSR) for both the reference and predicted soundings. To compare the two soundings equally, the CSR is vertically summed along a constant sloping surface of 1.2km rise for each horizontal distance of 70km aligned with the 700mb wind. This is done only once for the reference sounding, while the predicted case will change with each new prognostic sounding. Finally the CF is calculated by obtaining a ratio between the CSR of the reference and predicted sounding. Values of CF can range from nearly zero for dry predicted soundings to over one with unusually wet and warm soundings. For example, if the predicted CSR has a higher moisture content than the reference CSR, then the correction factor would be greater than one.

Values of CF are then multiplied by the RBA for each 24 hour period to obtain the predicted QPF for a given basin. A CF greater than one will increase the predicted 24 hour QPF totals. The correlation of predicted QPF to actual basin QPF ranged between 0.70 and 0.87. These are slightly higher correlations than in the 1978 study (Rhea 1996).

Although this scheme is similar in some ways to the WOCSS analysis employed here, there are major differences as well. In the next chapter the WOCSS analysis, precipitation patterns and forecasting schemes are discussed in more detail.

D. Doppler Radar Studies

Doppler radar is an effective way to observe wind and precipitation in the atmosphere. The radar sends out a beam of energy, and particles in the atmosphere reflect a portion of that energy back to the radar site. The size and motion of the particles can be determined at given levels in the atmosphere. The scan angle of the radar beam and the distance from the radar site determine what elevation the beam will detect precipitation.

The Mesoscale Alpine Programme (Chong, et. al. 2000) used a dual-Doppler ground-based radar system to measure real-time winds across the Southern Alps of Europe. The goal of the study was to provide accurate vertical velocity measurements to aviators flying over the treacherous terrain. The study took the horizontal winds measured by the radar and calculated vertical velocity through the use of the continuity equation. The results, verified against sounding data, showed that this dual-Doppler system could accurately model three-dimensional wind flow near complex terrain (Chong, et. al. 2000). The real-time winds could also be used to verify the dynamical accuracy of mesoscale models. This verification would currently be difficult to perform across the mountain basins of the Western US, including the Santa Cruz Mountains, where dual-Doppler radar coverage is limited.

A second study (Westrick 1999) attempted to measure the error in the estimated precipitation amounts produced by Doppler radar across the mountains of the Western US. It was shown that there are currently significant holes in the regional radar coverage due to the blockage of the radar beams by the topography. Raising the scan angle was found to reduce the blocking, however, QPF error increased because the radar scan angle rose above the level where some of the precipitation was forming. During a heavy precipitation event across the Oregon Cascades, the study found a 30-40 percent error between the radar precipitation estimates and ground-based measurements (Westrick 1999). This type of error may also occur across the Santa Cruz Mountains since the San Francisco radar is based at an elevation of 1077 meters.

While using Doppler radar is a good way to observe winds and precipitation currently occurring in the atmosphere, there are some questions to its accuracy around regions of terrain and there are no current uses of Doppler radar as a precipitation forecasting tool.

E. Other Studies

Other studies (Mass 1981; Mass et. al. 1990) have been conducted to more completely understand complex flow interaction phenomena such as flow splitting, enhanced precipitation and strong zones of convergence without the use of computer models.

One study (Mass, 1981) looked at a mesoscale meteorological convergence zone that periodically forms near Seattle from winds blowing off the Pacific Ocean and around the nearly isolated Olympic Mountain barrier. When fully developed, this zone brings enhanced cloud cover and rainfall to the Central and Northern Puget Sound region. The study looked at 10 convergence zone events to deduce the common features involved. The study looked at all the available data, including surface and upper level winds and surface pressure and temperature patterns. It was found that most, if not all, of these convergence events could be predicted simply by looking at *surface* measured wind speeds and directions. In each of the 10 cases where a convergence zone developed, the wind direction ranged between 250 and 320 degrees. Wind speeds during each case were between 6 and 15 knots (Mass 1981). The wind speeds were recorded at a location well exposed to large-scale ocean wind flow and away from the topographical influence of the Olympic Mountains. It was discovered that winds less than 6 knots would be too weak to cause a convergence zone. Stronger winds, or flow with directions outside the range given above, would tend to dominate the mesoscale flow through the Sound, either from a northerly or southerly direction, and not produce any convergence. Although not common, convergence zones around complex terrain are not limited to the Olympic Mountains. A similar event was described by Edlinger and Helvey (1961) for the San Fernando Mountains of Southern California.

A second study (Mass and Ferber 1990) showed some important effects of forced flow over topography. This study focused on looking at pressure perturbations associated with mesoscale wind flow over the Olympic Mountains. To enhance the accuracy of the pressure measurements taken during the experiment, eleven highly sensitive microbarographs were put in place at various locations around the Olympic Peninsula and Puget Sound from the 13 January through 28 June 1988.

The results showed that winds in a 100mb deep layer averaged at 850mb had a high correlation in predicting the times of windward ridging and leeward troughing. Wind directions generally ranged from southwest to northwest off the Pacific, with speeds during the experiment under 20m/s about 95% of the time (Mass & Ferber 1990). Linear theory of wind flow over an isolated bell-shaped mountain predicts that the windward ridge and leeward trough are of equal magnitude. One of the findings of the studies showed that, generally, the windward ridge was weaker than the leeward trough. In the case of the Olympic Mountains, the biggest pressure difference between the windward ridge and leeward trough occurred during times of strong winds and low Froude numbers. The Froude number is an indicator of stability and how wind flow will interact with terrain. Low Froude numbers indicate that most of the flow moves around a barrier, whereas higher Froude numbers (greater than 1) means the flow will be more terrain following. WOCSS uses a similar approach to determine how the flow interacts with the terrain, and how much of the flow moves around a barrier as opposed to over it.

It was determined from the study that for cases with lower Froude numbers there was a larger difference in magnitude between the windward ridge and leeward trough. As the Froude numbers increased to values greater than 1 this difference diminished and was more in line with linear theory. The four quantities examined in this study were wind speed, stability, Froude numbers, and linear theory. Of the four quantities used to describe the pressure perturbations across the Olympic Mountains, the wind speed through a 100mb layer of the atmosphere averaged at 850mb correlated the best (Mass & Ferber 1990).

While studies that forecast certain wind flow and precipitation enhancement through the use of pattern recognition are useful, they are not as accurate or reliable as the other methods previously discussed.

F. Summary

The different methods discussed are all aimed at an accurate determination of flow interaction across areas of complex terrain. While many of the studies have produced good results and low errors, there is still a need for a more accurate analysis of this interaction. This is especially true for rain enhancement. Generally, complex mesoscale or regional prognostic models tend to overpredict rainfall along the windward slopes while producing too little along the leeward portion of the terrain. Simpler methods also exist to determine the rain enhancement across complex terrain. One of the best tools for this is the Rhea OPM.

In order for our study to meet the goal we previously defined, the WOCSS analysis must be able to perform at least as well as some of these other complex models and simplified techniques. If WOCSS can achieve correlations in the range of 0.50 to 0.80, then the WOCSS analysis is providing a fairly accurate assessment of rainfall enhancement across the Santa Cruz Mountains during our study.

3.0 WOCSS ANALYSIS SCHEME

A. Development of WOCSS

Limitations of regional and mesoscale models to produce a quick and accurate solution of wind flow across areas of complex terrain increases the need for fast high resolution wind models. WOCSS not only can reach resolutions as high as one kilometer, it can run very quickly on a microcomputer or workstation, with typical runs taking only a couple of minutes. The WOCSS scheme is a diagnostic model that generates high-resolution output winds via an objective analysis scheme. A prognostic model typically generates a solution by solving a set of complex differential equations. An objective analysis is defined as "a process by which meteorological observations distributed in space and time, and from different observing systems, are combined with other information - predictions from previous analyses, or perhaps climatology - to form a numerical representation of the state of the atmosphere" (McPherson: 151 pp. 1986). The WOCSS analysis solves no differential equations, but instead uses a technique to calculate winds throughout a given domain. The two main assumptions in the analysis scheme are the critical streamline concept, and the adjustment of the winds to nondivergence.

The WOCSS code originated from concepts used by Bhumralkar (1980) and Sherman (1978). Both of these analysis schemes modeled winds across complex terrain using a calculus technique to reach mass consistency throughout the domain. The code that Sherman developed used the standard Cartesian vertical coordinate system, while Bhumralkar used sigma coordinates. Sigma coordinates are useful and widely used because they allow the surfaces to follow the terrain at varying levels from the ground to the top of the domain and they simplify the inclusion of the lower boundary condition. Sigma coordinates are defined by the fractional pressure difference between a particular level and the surface, so that layers can be more numerous in part of the vertical domain and sparse in others (Ludwig et. al. 1991). These terrain following sigma surfaces are most useful when neutral to slightly unstable conditions are present because, in reality, the flow will be more terrain following. In more stable conditions wind flow will tend to move around barriers instead of over them. For stable conditions these sigma surfaces do not represent the wind flow surfaces as accurately because too little flow moves around terrain barriers (Ludwig et. al. 1991). This problem was partially solved by Endlich (1984) when the curvilinear, flow-following, coordinate system was developed and adopted. The main difference between flow-following and sigma coordinates is that flow-following coordinates are objectively defined (user specified) and allow wind flow to intersect the underlying terrain (Ludwig et. al. 1991). A flow surface can be defined as a material surface which can not be penetrated by a rising or sinking parcel during an adiabatic process (sigma surfaces are not material surfaces). Where flow surfaces intersect the terrain the horizontal winds are set to zero, forcing flow to be deflected around terrain barriers. It is assumed that wind components u and v travel along each flow surface with no transfer of air between them (no vertical component to the flow surfaces). It is also assumed that the vertical component (w) is calculated along the slope of the flow surfaces.

By using flow-following coordinates, adjusting the shape of the flow surfaces and setting below ground points to zero as discussed above, there may not be uniform spacing between the surfaces. This can create areas of divergence that then must be removed along the flow surfaces to accurately force the flow around terrain barriers (Bridger et. al. 1994). To achieve this state of non-divergence, a number of techniques can be used. In WOCSS this is handled using an iterative technique, originally developed by Endlich (1967). This iterative method replaced the numerical technique used by Bhumralkar (1980) and Sherman (1978). The technique used in WOCSS consists of a series of iterative adjustments performed on the flow surface winds to reach non-divergence along the flow surfaces. A subjective initial guess of the shape of the flow surfaces is made, and it is assumed that there is no transport of air across the flow surfaces. The horizontal mass flux is then adjusted to non-divergence through the use of the continuity equation (Ludwig 1988). This technique works best when the slope of the flow surfaces is not too large.

Another concern is how to determine the elevation at which air will flow over a terrain barrier as opposed to around it. Ludwig (1988) developed an objective method, called the critical streamline concept. This defines the altitude (Z_{max}) where, for $Z < Z_{max}$ there is not enough kinetic energy for the air parcels to rise over the terrain barrier.

Assuming that wind speed increases with height, the flow above Z_{max} will have enough kinetic energy to pass over the terrain, while the air below does not. The value of Z_{max} is mainly determined by the stability between the flow surfaces.

As air rises up and over a terrain barrier in a neutral or stable environment, some amount of work is required. The height of the terrain, speed of the wind, and stability through the vertical domain determine the amount of work done. The speed of the horizontal wind flow at its original height is equivalent to the available kinetic energy. The lapse rate and terrain height are a measure of the potential energy that can be gained during the lifting process. The critical streamline concept determines the maximum height the flow surfaces can achieve through the equality of the kinetic energy lost and potential energy gained (Ludwig et. al. 1991). The following equation defines this maximum height:

$$Z_{max} - z_0 = V_0(d\Theta/dz * g/\Theta avg)^{-1/2} \quad (2)$$

where Z_{max} = maximum height the air can rise over the terrain, z_0 = initial height, V_0 = surface wind speed, $d\Theta/dz$ = potential temperature gradient, g = acceleration of gravity, and Θavg = average temperature between the layer Z_{max} and z_0. From this equation it can be seen that as the wind speed increases, with no change in the other parameters, more of the air will be forced over the terrain. As the vertical potential temperature gradient (stability) increases, and the atmosphere becomes more stable, the air will not be displaced as far vertically.

There are some limitations to using the critical streamline technique. In neutral to slightly unstable conditions, the flow over the terrain will be terrain following only. Studies (Mass 1981; Mass and Ferber 1990) show that wind flow patterns are more complex during unstable conditions. Also in areas of strong convergence and divergence, the model will not be able to fully achieve non-divergence along the flow surfaces through the WOCSS iterative technique. So flow surfaces near steep terrain or along frontal boundaries will not be accurately represented in the WOCSS scheme (Ludwig et. al. 1991).

B. WOCSS Analysis Procedures

There are a series of steps that the WOCSS analysis goes through during each run. Although the scheme is relatively simple and does not take much computing power, there is still an abundant amount of information to analyze and interpolate. Different subroutines within the WOCSS code perform these steps. The first subroutine reads initial parameters that are important to the function of WOCSS including resolution information, domain size and vertical flow surface information

The vertical coordinate information includes the number of vertical flow levels and the initial distance between flow levels. The standard number of flow surfaces used in the WOCSS analysis is six but a higher number can be used for greater resolution. Other parameters set in this routine help to define the flow surface shapes and changing them can have significant implications on the outcome of the analysis.

Since WOCSS is primarily used in a neutral or stable environment, a boundary layer must be defined. The average and minimum boundary layer thickness is set next.

These two parameters determine the height of the top flow surface, and keep the flow surfaces separated during the analysis. As stated above, the slope factor is also important to the shape of the surfaces. A slope factor of zero will cause the top flow surface to be flat. This is useful in very stable situations where the height of an elevated inversion top does not typically vary across a given region. A slope factor value of one allows the flow surfaces to follow the terrain in the initial guess of the analysis. The boundary layer, if desired, is allowed to slope across the domain.

Next, surface meteorological station data are read into WOCSS. Each station gives wind, temperature and pressure information along with the location.

After all the information is read into WOCSS, the analysis is performed. The first true step of the analysis is to define the elevation of the top and bottom flow surfaces. The average thickness of the boundary layer and the slope factor determine the height of the top layer in the domain. The initial guess of the height of the top of the domain is just a terrain-following surface. The bottom surface is given initially by the height of the terrain only.

Once the first guess flow-following surfaces are defined, the initial winds are calculated on each of the flow surfaces. The lowest level winds are interpolated from surface station wind data. Both surface winds and upper level sounding information are used to interpolate winds to the upper flow surfaces. The interpolation procedure includes weighting the winds according to how close they are to the meteorological observing stations. This scheme has important implications for the results of this study because the number and distribution of surface and upper level sites throughout the domain determines the accuracy of the analysis. A region with few or no wind observations near it will likely show lower accuracy compared to sites with several observations surrounding it.

The next step in the analysis takes the wind and lapse rate data over the lowest terrain heights in the domain to recalculate the height of each flow surface, and determine the maximum rise a flow surface may achieve based on the Froude numbers discussed in Chapter 2. Wind speeds from the five lowest terrain elevations are used to calculate a root mean squared average speed. This speed, used in conjunction with the nearest lapse rate, will determine the maximum flow surface rise. Another important parameter is determined at this point in the analysis: this is the minimum flow surface separation allowed. Not only are the flow surfaces constrained to a maximum slope and a maximum height above the terrain, they must also keep a minimum vertical separation between them. Once these values have been determined over the lowest terrain elevations, a full interpolation is made for each grid point to reshape the flow surfaces.

By reshaping the flow surfaces, areas of divergence are created. The next step in the WOCSS analysis is to remove these areas of divergence. As described in the previous section, the divergence is removed through the use of the continuity equation. The last steps in the analysis are to set the wind speed of all the below ground points (where the flow surfaces intersect the terrain) to zero, and adjust the surface winds to anemometer heights of 10 meters.

Output quantities include the horizontal wind components u and v calculated along the flow surfaces, along with the vertical wind velocity w. The speed units are in knots for horizontal winds and cm/s for the vertical velocity.

C. Past Studies With WOCSS

Since its development in the late 1980's, the WOCSS analysis has been used in several studies (Ludwig 1990, 1991, 1998; Bridger et. al. 1994). These studies tested the accuracy of the model and some of its possible applications.

Even before WOCSS was developed, various studies were performed using similar analysis schemes. One such scheme used Endlich's SRI Complex model for the Diablo Canyon Nuclear Power Plant (Thuillier 1987). It was found that the analysis could accurately produce real-time winds around the nuclear plant and the surrounding complex terrain. Another mass-conserving transport model was tested by Ishikawa (1994). This analysis uses terrain-following surfaces and a calculus-based iterative method to remove divergence. In a test of the wind field during the Chernobyl accident, it was found that the analysis could produce an accurate wind field during the test period (Ishikawa 1994).

One of the first tests with the WOCSS analysis was done using topography and wind data from the Los Angeles Basin (Ludwig et. al. 1991). The Los Angeles area is a unique region with an extensive coastal plain surrounded on three sides by mountains. The region is exposed to the Pacific Ocean to the west, and prevailing onshore breezes, along with a strong marine inversion, can trap pollution for extended periods of time. The experiment used data from December 10, 1987 when an extensive array of meteorological data was available both at the surface and aloft. The weather observations showed mainly light surface winds during the morning with an elevated inversion at around 1000m. By the afternoon the sea breeze had strengthened producing westerly winds that traveled inland. The elevated inversion remained at about the same level, forcing more of the winds through the gaps and canyons of the surrounding terrain. This flow situation was reproduced very well by WOCSS. Other results from the LA Basin study showed that the model has potential uses in providing real-time turbulence fields to low flying aircraft (Ludwig et. al. 1991).

Another study near Vandenberg Air Force Base in California tested the WOCSS analysis against a more sophisticated experimental model (Thykier-Nielsen et. al. 1990). It was shown that WOCSS performed just as well as the more complex model in neutral and stable conditions. This was mainly due to the flow-following critical streamline concept unique to the WOCSS analysis providing an accurate assessment of wind flow across complex terrain.

Another region where the WOCSS analysis has been extensively used is across the San Francisco Bay Area of California, a region of complex coastal geography that includes the Diablo and Santa Cruz mountain ranges. The region also has access to cooler Pacific marine air in the form of a sea breeze that can be channeled through low elevation gaps. This is most prevalent during the summer when the synoptic Pacific high pressure system builds across the eastern Pacific keeping an elevated marine inversion across the Bay Area. In the spring, winter and fall seasons, surface high pressure can occasionally build inland causing offshore winds to be channeled through the East Bay.

Experiments were performed to test the effectiveness of the WOCSS analysis across the Bay Area (Bridger et. al. 1994). The study used different observations of winds and stability to initialize WOCSS. These cases were chosen for their particular synoptic conditions and the large amount of data available at those times. One case of strong northeast wind flow and two with northwest flow were studied. The cases were analyzed with varying amounts of surface data, along with upper data from the sounding taken from the Oakland airport. It was found that the accuracy of the computed winds across the Bay Area improved with increasing numbers of surface observations. The increase in modeled wind accuracy was minimal if the study started with a few stations that could be optimally located throughout the domain (Bridger et. al. 1994). This means that it is not necessarily the number of meteorological surface stations used within the domain, but rather the placement of the stations and accuracy of the wind data that help WOCSS perform at an optimal level. This will be very important in our study due to the limited wind data in the remote parts of the Santa Cruz Mountains.

4.0 WOCSS Correlation Study

A. Study Overview

It is the purpose of this study to show that the WOCSS model can differentiate areas of enhanced rainfall in complex terrain through the computation of the vertical velocity. Areas of positive vertical velocity should correlate to higher rainfall, while those with negative vertical velocity to lower rainfall. In order to compare our correlations, a reference rainfall station away from the terrain must be chosen to represent a location where no enhancement occurs. In our study the best station that fits this criterion is San Jose. San Jose is located in the Santa Clara Valley to the east of the Santa Cruz Mountains. The reference station also needs to be located near the elevated stations of interest in order to limit other errors such as the timing of the rainfall bands and uneven distribution of large-scale precipitation. In the WOCSS analysis no enhancement will occur away from terrain. This is due to the fact that there is no convergence or divergence along the flow surfaces over valley regions thus producing no vertical velocity (w). The rainfall from the reference valley station will be subtracted from the rainfall amounts in mountain locations and the resulting value will be compared with the vertical velocity over the elevated location to determine the correlation. Increasing positive vertical velocities should correlate to greater enhancement of rainfall, meaning the difference in rainfall between an elevated station and San Jose also increases.

The Santa Cruz Mountains of California were chosen for this study due to their complex topography just inland from the Pacific. The mountains parallel the Central Coast running from the southeast to the northwest from eastern Monterey County north to San Mateo County. The higher peaks are over 1000m in elevation providing a barrier to airflow moving off the Pacific.

Figure 1 is a contour map of annual average rainfall map of Northern and Central California. Rainfall generally decreases from north to south along the coast. Rain enhancement is seen across the mountainous region of Northern California including the Coast Range, Shasta region, Santa Cruz Mountains and along the Sierra Nevada Mountains. Due to the rain-shadow effect, much lower rainfall, on the order of 5-10 times less, is seen along the lee side of the mountains. This is clearly seen in Figure 1 across the Central Valley, parts of the Santa Clara Valley and east of the Sierras.

The height of the Santa Cruz Mountain range, combined with its orientation, provides efficient orographic lifting when southwest winds are present. A large difference in annual rainfall exists between the western and the eastern sides of the range. Figure 2 is a section taken from Figure 1 showing the annual rainfall distribution of the Santa Cruz Mountain region in more detail. Annual rain totals range between 30-40 inches along the western base of the Santa Cruz Mountains just north of Monterey Bay. Rainfall amounts are as high as 50 inches along the higher slopes of the central Santa Cruz Mountains and then quickly fall to 15-20 inches across the lee side of the mountains.

B. Synoptic Overview

The time period in our study correlates with an extended period of rainfall during the first week in February of 1998. During this time period an unusually strong westerly jet stream steered a series of mid-latitude cyclones into northern and central California. Waves of moisture associated with surface frontal systems brought moderate-to-heavy rain at times to the mountains and valley areas alike. Figures 3-23 and Tables 1-7 illustrate the weather conditions through the time of the study. Figures 3-16 show satellite pictures at 0000Z and 1200Z each day through the period. Figures 17-23 show surface weather maps during the time period at 1200Z GMT each day from February 1st-7th. The progression of these storms across the Santa Cruz Mountains can be seen in these figures and weather maps. Tables 1-7 list the sounding data from the surface to 700mb. Each table has the two soundings for the day at 0000Z and 1200Z GMT respectively. Each sounding lists the available pressure levels, the corresponding height in meters, temperature, dew point, wind speed, and wind direction.

Figure 17 for 1200Z on February 1st shows a warm front was along the Central California coast with a cold front draped offshore. The warm front spread rain across the Santa Cruz Mountains during the early morning hours. This front moved onshore and dissipated across the Sierra Nevada Mountains through the evening hours. Figures 3-5 confirm this, showing enhanced clouds offshore at 0000Z moving into Central California by 1200Z on Feb. 1st and 0000Z Feb. 2nd. Table 1a shows south to southeast winds up to 700mb at 1200Z. Table 1b shows winds shifting to the southwest by the afternoon indicating the cold front passed to the east of the Bay Area by 0000Z. General onshore flow continued overnight into Feb. 2nd but upper level moisture and dynamics were limited as Central California was between storms.

Figure 18 for 1200Z February 2nd shows a warm front was moving north along the Southern California coast. Figures 6-7 show the next wave of moisture moving into the West Coast Monday Feb. 2nd. By the afternoon the warm front had moved into the Bay Area and moderate to heavy precipitation fell across the region including the Santa Cruz Mountains. Tables 2a and 2b, the Oakland soundings for Monday Feb. 2nd, show winds mainly out of the southeast to south, indicating that the orographic enhancement of the precipitation across the Santa Cruz Mountains would have been minimal.

By the morning of Tuesday February 3rd the second in the series of storms had matured off the West Coast and a cold front swept onto the California coast. The surface pressure off the North Coast fell below 980mb, as shown by Figure 19. Figures 8 and 9 show a large storm system along the West Coast. The soundings for the day, given in Tables 3a and 3b, indicate surface winds had backed to the southeast during the morning but by Tuesday afternoon the winds veered to the southwest. The afternoon sounding indicates that the front and moisture had moved inland to the Sierra Nevada leaving the Santa Cruz Mountains with a decrease in rainfall.

The upper level trough remained along the West Coast from Tuesday night into Wednesday morning. Figure 20 shows that the surface low off the Oregon coast had filled to around 990mb with a trough along the California coast. Figure 10, the satellite image at 1200Z Wednesday February 4th, shows low level clouds across the Bay Area. This is confirmed in the sounding data (Table 4a) indicating that the layers between the surface and 850mb were nearly saturated, with drying near 700mb. By Wednesday afternoon drying occurred near the surface, and the 0000Z sounding (Table 4b) shows a saturated layer around 850mb, with dry conditions at 700mb. The next area of enhanced clouds, shown in Figure 11, was quickly moving towards the West Coast at 0000Z.

Figure 21 indicates the next wave of moisture moving into the West Coast on Thursday February 5th as a strong storm developed well off the Northern California coast. Figures 12 and 13 show a large area of cloud cover (mainly in the form of mid and high level clouds) moved into the Bay Area during the morning. At most locations light rain was falling from these clouds into the afternoon hours. Tables 5a and 5b show that the winds backed to the southeast during the morning and strengthened by the afternoon. The 1200Z and 0000Z soundings are dry below about 900mb but saturated above this level.

The third storm in the series occluded through Friday February 6th with a surface low of 960mb just off the northern coast of California. Figure 22, the surface weather analysis for the day, indicates the front remained offshore through 1200Z. Figure 14 shows this powerful storm system off the coast with abundant clouds and a strong circulation. The soundings for the day, given in Table 6, indicate an unsaturated sounding below 850mb during the morning, with gusty south to southeast winds at 1200Z. By

0000Z, the winds had weakened but remained southeast at the surface as the flow was channeled up the Santa Clara Valley and south Bay. Above the surface, the wind veered to the southwest. Temperatures cooled during the afternoon and the 0000Z sounding was nearly saturated from the surface to 700mb, indicating the cold front had passed through the Bay Area and Santa Cruz Mountains. Figure 15 indicates that clouds across the Santa Cruz Mountains at 0000Z were more convective in nature.

Figure 23 indicates that by 1200Z on February 7th the low had filled, while Figure 16 shows most of the enhanced clouds, associated with the cold front, had pushed to the south and east of the Bay Area. Low level moisture remained across central California at 1200Z with breezy southerly winds. The soundings, shown by Tables 7a and 7b, are unsaturated through much of the layer between the surface, and 700mb and the winds diminished by 0000Z as the pressure gradient along the California coast relaxed.

The study period ends on 2300Z February 7th as most of Central California had begun to dry out. A trough remained along the West Coast, but no shortwave disturbances moved into the Bay Area during February 8-10th, giving much of the region a break from nearly a week of moderate to heavy rainfall.

C. Input Data

A terrain set must be input into WOCSS. The terrain used in this study was taken from a 10 second USGS map of California. The Bay Area region was then extracted out of this dataset to be used in WOCSS. This region includes the Santa Cruz Mountains and surrounding areas. The entire Bay Area and Monterey Bay was included so that more surface stations could be used. Portions of the delta and Northern San Joaquin Valley are included in the domain although they will have little effect on the winds across the Santa Cruz Mountains. The grid was extended offshore in order to incorporate National Weather Service buoys off the San Francisco coast. Unfortunately only one buoy was operational during the time period of the study. The terrain data set also includes the Oakland area in order to use the upper level sounding performed twice a day from the airport. An attempt was made to maximize the number of stations available for the analysis while trying not to inflate the region too far away from the Santa Cruz Mountains.

The domain used is a 300km by 300km in extent, and is shown in Figure 24. Out of that domain a 180km by 240km region is extracted for use in this study. The UTM Coordinates for each corner are 4266N 507E for the northwest corner, 4266N 687E along the northeast corner, 4026N 507E for the southwest corner and 4026N 687E for the southeast corner.

There are a total of 28 surface meteorological stations available for use in this study. A list of them is given in Table 8. The meteorological stations are comprised of 16 National Weather Service sites, 11 Remote Access Weather Stations (RAWS) sites and 1 offshore buoy. The stations are located throughout the domain, most concentrated around the southern portion of the San Francisco Bay. The distribution of stations is shown in Figure 25. Each number in the domain corresponds to a station given in Table 8. Hourly wind and temperature information is extracted from each station to use in the WOCSS analysis. The data must be converted from the RAWS and METAR formats into a simple data file that WOCSS can read.

The upper level sounding is the other important input to WOCSS. Unfortunately there is only one sounding available for the entire Bay Area region. This is taken at the Oakland airport twice a day a 1200Z and 0000Z GMT. Oakland is located to the north of the Santa Cruz Mountains but also lies near the middle of our study domain. This is favorable for our study because the accuracy of the study is improved when the sounding is away from the edge of the domain (Becker 1992).

One important aspect of each sounding is the stability through the vertical domain. As stated in previous chapters, stable soundings will be interpreted differently in WOCSS than neutral soundings. An analysis was done on each sounding to determine the stability at various levels. The stability was determined by taking the difference in the potential temperature, calculated using the dry adiabatic lapse rate, at each level. Most of the soundings were dry up to 925mb before becoming saturated. The cases where the lapse rate was neutral up to 925mb were on Feb. 1st at 0000Z, Feb. 5th at 0000Z, Feb. 6th at 1200Z. All the other soundings were stable up to 850mb using the dry adiabatic lapse rate. Of course some of the soundings were saturated during parts or all, of the vertical rise between the surface and 500mb. Unfortunately WOCSS has no moisture parameters to differentiate between a dry and saturated sounding. This will be a limiting factor to the accuracy of the analysis because WOCSS will inhibit vertical motions in saturated cases causing an unrealistically lower vertical velocity to be output. This is the time when the heavier precipitation is likely to fall possibly increasing the analysis error.

A file containing upper level wind data, is created for each hour during the study. Since a sounding is only provided every 12 hours, the same sounding is used for the time period of 6 hours before and after the sounding time. For example, a 1200Z GMT sounding is used from the time period of 0600Z to 1700Z and a 0000Z sounding is used from 1800Z to 0500Z GMT.

The rain data used in this study was taken from a collection of 18 rain gauges scattered throughout the Santa Cruz Mountains. The gauge data was supplied by the Santa Clara Valley Water District (SCVWD). The rainfall data was analyzed, and some of the stations were removed from the dataset due to missing data. Unfortunately a complete rainfall record could not be retrieved during this critical period of persistent precipitation. Table 9 shows the name of each of the rain station along with the UTM coordinates. Figure 26 is a map of the Santa Cruz Mountains. Each number on the map corresponds to the associated rainfall station listed in Table 9.

With all the input data in the correct format, the WOCSS model is ready to be used. After analyzing the soundings, a boundary layer depth must be entered into the input subroutine along with the slope factors. For this study a boundary layer depth of 3000 meters was used. Since this is a time of neutral or unstable conditions, it was appropriate to use a slope factor of 1 so that the flow surfaces follow the terrain. Also, since only one sounding was used, the boundary layer depth is assumed constant through the domain.

D. Cone Method

A test was performed using the terrain defined in the previous section. All the available surface meteorological station data and upper level Oakland soundings were used to test the vertical velocity field at each rainfall station to look at correlations between the vertical velocity and rainfall enhancement. It was quickly discovered that, since the model does not contain moisture transport parameters, there are numerous stations that should have seen positive correlations but were strongly negative. The main reason for this is that WOCSS does not have any calculation for moisture transport. A portion of the orographic rainfall that develops on the windward side of the Santa Cruz Mountains will be transported and deposited as precipitation along the lee side of the terrain. Some of the precipitation will also evaporate on the lee side due to the downward vertical motion drying the air. When dealing with resolutions of 1km it is important to take into consideration this precipitation transport process from the cloud to the ground.

One way to handle this issue is to devise a procedure in which, depending on the wind speed and direction, a certain number of upstream vertical velocity points are captured and used to represent the grid point where the rainfall station is located. There are a couple of factors that must be taken into account when developing such a technique. Since precipitation is forming and falling from a layer of the troposphere, the higher level droplets will take a longer amount of time to fall from a cloud. Thus, precipitation forming upstream from the station must be considered. If the vertical velocity is greater at these upstream points, then the enhancement of rainfall should be higher as well. A second consideration is the amount of turbulence that will horizontally disperse the raindrops upstream from a particular location. A system that accounts for these properties must be utilized to more accurately define the moisture transport upstream from the rainfall station, and incorporate all of the necessary upstream vertical velocity grid points into the rainfall correlations.

After careful consideration, a cone shaped wedge of variable size was chosen as the best solution to accomplish this task. The cone spreads outward upstream from the rainfall point and can vary in angle and radial distance. A larger angle cone will incorporate more of the vertical velocity grid points. The wind speed and turbulence will determine the angle of the cone. The theory of gaussian plume dispersion is used to determine the cone angle. According to Pasquill's turbulence equations, the angle of the downstream plume of air depends on the wind speed, turbulence and time of transport (Slade 1968). Equation 3 defines the angle of plume dispersion:

$$\sigma = (4.28 * s_y) / (u * t) \qquad (3)$$

where σ = the angle of the plume, s_y = the horizontal dispersion coefficient, u = the wind speed and t = the time of plume transport. The horizontal dispersion coefficient is given by Figure 27 and is calculated from the stability and downwind distance from the source of the plume. Although this equation can not specifically calculate the angle of our cone, the principles defined in the above equation can be applied to the current cone technique. Just as a plume of smoke disperses downwind from a point source, raindrops are mixed by turbulent eddies within a cloud. To interpret the magnitude of the cone angle, it is assumed that the horizontal dispersion coefficient will be a constant as will the time of rainfall transport. So in this study, the only variable that will affect the angle of the cone is the wind speed. As the wind speed increases, the angle of the cone will decrease. Conversely, the cone angle increases with decreasing wind speed. Different angles will be tested to see how the variation in cone angle affects the overall correlations.

The upflow distance of the cone must also be defined. A formulation involving the horizontal wind speed, the fall speed of the drops and the maximum height of orographic precipitation production is used to estimate the number of upflow vertical velocity points that are included in the cone. The fall speed of the precipitation is determined by the droplet diameter. The smallest droplets will take the longest amount of time to fall from the cloud. Raindrop sizes range from around 1mm for the smallest drops to 5mm for the largest drops (Elliott and Shaffer 1962). An average value of the size of the smaller droplets reaching the surface is assumed to be around 1mm. Evaluating the sounding data during times of widespread rainfall showed the average saturated layer was between approximately 1000 and 6000 meters Above Ground Level (AGL). A lack of upper level data points presents the possibility of large errors in this estimate. Given this saturated depth of 5000 meters, the continuous equations for the growth of droplets by collision and coalescence can be used to calculate the time it takes for a growing droplet to fall through this saturated vertical layer. These equations are given below:

$$dr/dz = -(E * w) / (4 * \rho_L) \qquad (4)$$

and

$$dr/dt = (E * w * V_T) / (4 * \rho_L) \qquad (5)$$

where dr/dz = the change in droplet size through a given height, dr/dt = the change of droplet size in a given time, E = the collision efficiency, w = the liquid water content of the cloud, V_T = the terminal velocity of the droplet and ρ_L = the density of liquid. Using a final radius of 1mm, a depth of 5000m for dz and assuming a standard liquid water content of $5x10^{-3}g/m^3$, density of liquid water equal to $1000kg/m^3$ and a collision efficiency of near unity, then the initial radius of the drop can be found at 6000m using Equation 4. It can be shown that this initial radius is 0.5mm. Knowing the initial and final radius of the droplet allows an average terminal velocity to be determined. This terminal velocity is found from Figure 28, showing a theoretical graph of droplet radius vs. fall velocity (Fleagle & Businger, 1980). Assuming a linear acceleration of the droplet starting at 4.0m/s at 6000m and reaching a fall speed of 7.0m/s at 1000m AGL, an average fall speed of 5.5m/s is calculated. Using this terminal velocity and solving Equation 5 gives a time of 860 seconds for the droplet to fall through the saturated 5000m layer. Also, assuming that the air in the first 1000m is nearly saturated and little evaporation will occur, then a droplet of 1mm in size will fall at 7.0m/s for 1000m in approximately 143 seconds. Adding the two times gives a value of around 1000 seconds for the smaller drops to fall from the top of the cloud to the ground. This value will be used to help determine the final shape of the cone.

The procedure for determining the cone starts with locating the rainfall station point on the grid. The horizontal wind speed and direction from WOCSS are then used for that particular grid point to calculate the cone. The wind components are calculated, and using these components the two lines are defined to make up the edges of the cone. For example, if the cone angle is determined to be 20 degrees and the wind direction is 270 degrees, then the two lines would be calculated by simply finding the slope and y intercept of both lines extending out from the center of the cone. The x and y variables, the rainfall station grid point, would be the same for the lines on each side of the cone. The slope of one line is determined by taking the tangent of the addition of the wind direction and half the cone angle. In this example the wind direction is 270 degrees and half of the cone angle would be 10 degrees. This means that cone angle would extend from 260 to 280 degrees. The second line is calculated by taking the tangent of the difference of the wind direction and half the cone angle. Once the slope of the lines is determined, then the y intercept points to be calculated using the x and y coordinates of the rainfall station grid point.

Just as two lines are used to define the cone width, two circles will be used as a measure of its extent upstream. The outer circle is centered at the rainfall station grid point and intercepts two points along the lines of the cone. Solving Equation 5 above gives a calculated value of 1000 seconds for the longest time the raindrops will take to fall to the ground. This value, along with the wind speed at the rainfall point, determines the radius of the circle. For example if the wind speed is 5m/s and the fall time of the raindrop is 1000 seconds, then the radius of the circle is 5km. This linear calculation holds true for any wind speed used in this study.

The larger raindrops will also take some time to fall from the cloud base. A second (inner) circle is defined closer to the rainfall station to eliminate the closest points. These points provide rainfall to areas downwind of the station and should not be included in the correlation calculations. The inner circle is tested with a variable radius to see how much the correlations are affected. Only a small number of vertical velocity points are eliminated from the cone region, especially if the cone angle is small. If the wind speed is less than the radius of the inner and outer circle, then only the vertical velocity points closest to the rainfall station are used for correlation calculations.

After the cone is defined, all the grid points around the rainfall station point are tested to determine if they fall within the cone. Once all the points are tested, the vertical velocities of all the included points are averaged (equally weighted) and used in the correlation calculation for that hour. Each hour will have a different sized cone if the wind speed and direction vary throughout the time period.

E. Outline of WOCSS Runs

Four model runs were performed to test the accuracy of the analysis and to determine if WOCSS could diagnose enhancement of rainfall across the Santa Cruz Mountains. The WOCSS model runs are performed for the time period from Feb. 1st at 0100Z through Feb. 7th at 2300Z. Correlation calculations for the first two runs were performed at only 4 of the 18 rainfall stations. The identifiers of the four stations used are 1085, 1973, 1975, and 2096 (Table 9). Only these stations were used because they have the most complete rainfall records for the time period, and because their locations cover the northern, central and southern regions of the Santa Cruz Mountains. Many of the other stations were not used in the correlation study due to the lack of a complete rainfall record or the fact that they were located in the same region as one of the 4 representative stations.

The first analysis run used all 28 surface meteorological stations as input for wind and temperature information. There were many hours when data was missing. If data were missing from a station, WOCSS skips it and only uses the available wind data for that hour. Many of the RAWS stations did not report during the overnight hours. Also it was apparent from the first analysis run that poor wind data was affecting the results of the study. The Corralitos station, in particular, reported very light winds throughout the study period and was not representative of the wind field around it. This continuous light wind may be the result of a sheltered or damaged wind sensor. Rainfall station 1 is mainly affected, due to its close proximity to Corralitos.

To eliminate this error, the second run kept all the input parameters the same as the first run except to remove the Corralitos station. Although this eliminates the error from the Corralitos station, it also removes a station from a portion of the domain that has few wind stations. Correlation results of the first two analysis runs will be made at both the surface and along the other five (upper level) flow-following surfaces.

Analysis run three used all the same parameters as the second run except to exclude much of the Chalks wind data (see Fig. 25 for location) and replace it with data from a coastal station at Pigeon Point. Chalks is located along the western slopes of the Santa Cruz Mountains. Looking at the winds from the Chalks station, it was apparent that there were some times when Chalks had much different wind directions from other stations across the region. These winds may be the result of localized mountain breezes that do not extend very far away from the station. The coastal Pigeon Point station would not have these localized effects and should more accurately represent the wind flow across this portion of the domain. The Pigeon Point station was not used initially because the data were only available from February 1st through February 5th and the Chalks station had a more complete record. For times when the Pigeon Point data are not available, Chalks wind is substituted in its place. Results of this model run were to test the differences in correlations at rainfall station 9 (1975) and are only calculated for surface winds.

The fourth analysis run uses the same input data as the second analysis run except to adjust the sounding data to be neutral with respect to the dry adiabatic lapse rate. Because WOCSS does not contain moisture parameters, a neutral sounding using the moist adiabatic lapse rate will be stable with respect to the dry adiabatic lapse rate. All stability calculations in WOCSS are made using the dry adiabatic lapse rate so WOCSS model runs one and two may be too stable during the storm period tested. This model run will allow any stability error of the model to be assessed. The fourth analysis run will be tested on the above-surface flow levels only.

5.0 WOCSS Analysis Results

A. Test Runs

This section describes the correlation results from the test run using the 18 rainfall stations. The test run calculated vertical velocity values using surface winds at each rainfall station without the use of the cone method. Table 10 gives the results of the first correlation test. These results show that 13 of the 18 correlations were negative in value. Using Equation 1 to calculate the vertical velocities, positive (or upward) vertical winds will be found strictly along the windward side of the terrain with negative vertical velocities along the leeward side of the mountains. Winds with a southerly component during the test period would place many of the rainfall stations in a region of downward (or negative) vertical velocity region of the Santa Cruz Mountains. This may explain the negative vertical velocities calculated at most of the rainfall stations. Highly negative correlation values are found at a few of the stations, including stations 2, 4, 13 and especially 18, where a value of -0.73 was calculated

Stations on the windward side showed mixed results. Station 8 has the highest correlation with a value of 0.43. Station 8 was also the farthest north where the wind field seemed to be represented more accurately. Windward stations across the southern portion of the domain showed very low correlations, generally under 0.20, with values both positive and negative. This may also be due to the lack of wind representation across the southern portion of the domain caused primarily by the light winds at Corralitos.

Another possible cause of the low correlations is that the precipitation may take longer to reach San Jose, which is to the east of the Santa Cruz Mountains. This is important because the rain enhancement is determined by comparing the rainfall at San Jose and the stations across the Santa Cruz Mountains. To account for this, a second test is performed in which the rainfall difference is calculated by taking the rainfall at the mountain locations each hour and at San Jose one hour later. Correlation results from this are given in Table 11. Almost all 18 rain stations showed a diminished correlation in both positive and negative values.

Table 12 shows the results from both tests and the net change in correlation from each analysis. Station 18 fell from a value of -0.73 in the first test to -0.62, station 4 from a -0.61 to -0.43, station 13 from -0.31 to -0.10 and station 2 changed from -0.48 to -0.42. Three out of the four stations with positive correlations from test one showed a minor decrease in value while station 1 remained nearly constant. Station 8, with the highest positive correlation in test one, only dropped from 0.43 to 0.40. Of the 12 stations with correlations between -0.2 and +0.2 in the first test, 11 remained between that range. Station 12 is the exception with correlations rising from -0.18 to -0.27.

A decrease in positive correlations or any negative correlations indicates a decrease in the accuracy of the analysis. From the results above there is not enough evidence to show that one method works better than another. Future tests will all be run with the time of the rainfall occurring at the same time as the vertical velocity calculations.

Obviously the negative correlations in the two test runs showed the limitations of the WOCSS analysis when dealing with the diagnosing of enhanced rainfall. The lack of a moisture transport regime caused many stations with enhanced rainfall to report negative correlations. Thus the cone method, described in the previous chapter, was devised and used to calculate the vertical velocities at our four rainfall stations. These four stations were chosen so each represents a particular region of the Santa Cruz Mountains (See Fig. 26). Station 1 is located near the southeast corner of the range, station 8 represents the central portion, and 18 near the northern edge of the mountains. Station 9, on an offshoot from the main range, is located farthest west across the central portion of the Santa Cruz Mountains.

When the cone method was developed, some initial tests were made using data from rainfall station 9 to see how the correlations would vary with more simplified cone specifications. Instead of allowing the cone angle to vary depending on the wind speed, this test kept the cone angle the same for all wind speeds. The angles tested were 20, 30, and 40 degrees. For each cone angle, the inner and outer radius of the circles were allowed to vary. Variance of the outer radius is by a factor ranging from 0.9 to 1.2 during the calculation of the vertical velocity. The radius of inner circle varies from 2-6km while the outer circle remains proportional to the speed. Table 13 shows the results from these tests. The 40 degree set of correlation values gave the best results with the 20 degree angle the lowest. The highest correlation is 0.44 for all wind direction angles and 0.47 for only the southeast component. Overall, there is little difference between the first analysis run and the results from this simplified cone analysis.

B. First Analysis Run

Results from the first analysis run, using surface winds and the cone technique, show a large improvement in correlations for a few of stations, with little to no improvement for the others. Four sets of results are given for each station (Tables 14-17). Each set of correlations test the results at different wind speed thresholds for cone angle. The cone angle is allowed to decrease as the wind speed increases. For example, in the first set of correlation results, the cone angle is 40 degrees when the wind speed is between 0 and 3m/s, 30 degrees for winds of 4-7m/s and 20 degrees for winds over 8m/s. The four sets of wind speed thresholds to adjust the cone angles are (0, 4, 8), (0, 5, 10), (0, 6, 12) and (0, 7, 14). These wind speed thresholds are also independent of wind direction and can be applied for all compass angles.

Within each set of wind speed thresholds, the inner circle radius is tested with variable distances between 2 and 6 kilometers. The outer radius always remains proportional to the wind speed. A correlation will be calculated for each inner radius distance between 2 to 6 kilometers. For example, if the wind speed is 6m/s, then the radius of the outer circle will be 6km. The cone angle is 30 degrees in the first three sets of thresholds and 40 degrees for the fourth. In cases where the value of the outer radius is less than the inner radius, then only the outer radius is used. For wind speed less than

2m/s, only the vertical velocity at the rainfall station is used (no cone). Each set of correlation results are also broken down into southerly wind direction components. The first column in each set of tables will represent correlations which include all 360 degrees of wind directions. Since most of the winds during our study period are from a southerly direction, correlations are also broken down into their individual southerly components. The next two columns in each set of tables include correlations with wind directions between 90-180 degrees and 181-270 degrees respectively to see if the analysis does a better job when only certain ranges of wind directions are used.

The results from rainfall station 1 are shown in Table 14. Correlations are slightly negative for each set except when the inner radius is 2km. For all compass angles, the greatest negative correlation is -0.23, with the highest positive value of only 0.05. Comparing these values with the first test run of 0.19 shows that the cone method at this station does not improve the correlation results. Negative correlations are much higher with southwest wind directions while southeast winds produced nearly zero values in each case. As the inner radius is increased, the trend is to increase the negative correlations with the peak occurring at a 5km value. There is very little change in correlation values by varying the wind speed threshold at this rainfall station. Overall, the results are disappointing for this station. These low correlation values can be attributed to the light winds at the Corralitos weather station, and not the use of the cone technique. In the second analysis run we will remove the questionable winds at the Corralitos meteorological station and recalculate the correlations.

The results from station 8 are given in Table 15. This windward station showed promising results in the initial test runs, with correlations as high as 0.43. The results in Table 14 show that for all 360 degree wind directions, the correlation range is from 0.15-0.19. There is little variation when the winds are broken down into southerly components, with the highest southwest value of 0.24. There is also almost no difference in values when the inner radius is adjusted. This is another station where the results are disappointing. The reason for the lower correlation numbers may be that vertical velocities upstream will be zero in the WOCSS analysis because the flow surfaces will be flat. If the cone extends into this region, then this would significantly lower the vertical velocity average. This effect would tend to lower correlation values during times of higher rainfall.

Table 16 shows the correlation results from rainfall station 9. While the test runs calculated a -0.11 value for this station, the cone technique improved these correlations, with values as high as 0.47 when winds are southerly. The best overall inner radius values are at 3km and 5km while only very minor differences are seen between the four sets of cone angle thresholds. This station did show major improvement over the test runs.

The last station examined in the first analysis run is station 18. This station had the highest negative correlation of -0.73 during the test runs. Table 17 lists this station's results using the cone technique. This station showed the greatest improvement in results with the best all wind direction correlation value of 0.36. The most impressive correlations are seen with only the southeast wind component examined and correlations as high as 0.78 are measured. Unfortunately the southwest wind directions have much lower correlations ranging between 0.20 and 0.31. The improved correlations at these stations are likely from its close proximity to the La Honda meteorological station. The good southeast correlations could be attributed to a greater concentration of meteorological stations on the lee side of the Santa Cruz Mountains, giving a more accurate representation of the winds to the east.

The first analysis run gives valuable information on the way WOCSS calculates the vertical velocity field. The lack of any moisture parameters to account for the development and transport of enhanced precipitation downwind of regions of upward vertical velocity lower the correlations. The cone method was devised to try to track this enhanced precipitation by taking into account the upwind vertical velocity points in the correlation calculations. This cone technique greatly improves the results for leeward stations, when compared to the initial test runs which used only the vertical velocity at the station as input for the correlation calculations. Station 18 showed the greatest improvement, while locations across the southern domain and windward stations showed the least improvement (and in certain cases a decrease in correlations). The diminished results at station 1 are looked at in more detail in the second analysis run.

C. Second Analysis Run

After examining the data from the first analysis run it was discovered that the winds at the Correlitos station were very light throughout the study and did not represent the wind field in the region around it. The second analysis run incorporates the same input data as the first run but excludes the Corralitos station. Results from the surface flow level results from the second analysis run compared to the first run are given below for rainfall stations 1, 8, 9, and 18.

The results from station 1 are shown in Table 18. Correlations range between 0.07 and 0.15 for all wind directions. This is slightly lower than the 0.19 value attained during the test runs, but higher than the maximum positive correlation of 0.05 from the first analysis run. Examining correlations from only southerly wind components show improvement, with southeast wind correlations as high as 0.34. The southwest correlations are as high as 0.19, just equaling the results from the test run. The small minority of winds with a northerly component lowered the overall correlation values. There is very little change in correlations between the different cone angle thresholds at this station. Improvement is seen by removing Corralitos, showing the importance of having accurate wind measurements near the rainfall stations. However, the scarce number of meteorological stations across the southern part of the domain could account for the continued low correlation values found at this rainfall station.

Removing the Corralitos wind data should also have an effect on the other three rainfall stations but to a lesser degree because of the inverse weighting scheme of WOCSS. The results from station 8, given in Table 19, show that the correlations improved slightly over the first analysis run. Correlation values using all wind directions are as high as 0.21 versus 0.19 from the first run. The best correlations come from the first set cone angle threshold numbers, and there were only very minor differences when the inner circle radius was adjusted. The most improvement is in the southeast winds component where values of 0.36 and 0.37 are measured. Southwest wind correlations fell from the first run with a maximum value of 0.17. This is the second station that has shown improvement in all wind direction correlations from the removal of Corralitos. Stations 1 and 8 are also the closest to the removed station and were expected to show some improvement.

Rainfall station 9 is mainly affected by the winds from the Chalks station. Chalks is located about 10km to the west of rainfall station 9 and has the most influence on it. Because of this, very little change in the correlation results for station 9 is expected in the second analysis run. Table 20 shows that this is true for southwest winds, where correlations as high as 0.43 are reported. This is compared to 0.44 from the first run. Southeast winds, and the overall correlations, are lower with values only as high as 0.37 compared to 0.47 in the first run. For all wind directions, the maximum correlation values for both runs is 0.38, but some values were substantially lower. This is especially true for values when the inner radius is 2-3km. The reason that only certain inner radius values were significantly affected is unknown.

Table 21 shows the second analysis run results for station 18. Large changes in correlations are not expected in this run because of the distance between station 18 and Corralitos. Comparison of Table 21 and Table 17 (from the first run) shows that there are some major differences between the runs. There are once again only small differences between the four sets of speed thresholds, while the largest changes take place when only southeast wind directions are examined and when the inner radius has a higher value of 5 to 6km. At an inner radius of 5km the maximum correlation dropped from 0.78 in the first run to 0.43 for the second and from 0.65 to 0.14 at a 6km inner radius. While the values drop for the upper range of inner radius values, the 2 to 4 km values show almost no drop in correlation when the overall wind direction are tested.

The second analysis run shows the importance of having an accurate wind field defined across the domain. By removing one station, the correlation values are affected at all four rainfall stations covering most of the Santa Cruz Mountains. There is improvement at the two stations closest to the removed Corralitos station, while stations 9 and 18 show no improvement and values for certain chosen inner radius values were significantly lower. Station 9 was the least affected by the removal of Corralitos, and this is likely due to its close proximity to the Chalks meteorological station. Results of both analysis runs do not show the level of accuracy necessary to be used as a diagnostic tool for precipitation enhancement across the region.

D. Third Analysis Run

The goal of the third analysis run is to see if using the coastal wind station Pigeon Point, as opposed to using the mountain station Chalks in the first two runs, has any affect on the surface flow level correlations at rainfall station 9. Located at UTM coordinates 4115km north and 553km east, this station is only 4km north and 9km west of Chalks. The coastal Pigeon Point station was not used before because of its incomplete data record during the time period and its close proximity to the Chalks station. With Corralitos already removed, not having Chalks or Pigeon Point data for a given time period would leave most of the western Santa Cruz Mountains without wind representation. For this reason, during this analysis run, Chalks will be substituted into the analysis when Pigeon Point is not available.

Pigeon Point is located directly on the coast and should record unobstructed south to southwest winds coming onshore. The mountain station Chalks may be susceptible to small-scale localized wind patterns that may not be representative of the region around it. By replacing the Chalks station with Pigeon Point, this possible effect may be removed. Unfortunately without a complete data record, this effect cannot be applied throughout the entire time period of the study. In addition to some missing data overnight, Pigeon Point's winds are not available after the 5th of February.

The results from the third analysis are shown in Table 22. The results show some improvement in the southeast wind component, while southwest and overall angle results show mixed results. Southeast correlations as high as 0.58 are calculated, showing an improvement over both of the first runs where values of 0.47 and 0.37 were recorded. Extracted southwest wind direction correlation recorded maximums of 0.42, and all wind direction values reached 0.41. This was very similar to the maximum values from the first runs although the 2-3km inner radius values dropped slightly in the third run. There is little variation between the four sets of wind speed thresholds for cone angle, giving high confidence that the cone angle is not as important as the radius of the inner circle. This is reflected in most of the results from the three analysis runs.

E. Upper Flow Surface Results

Although our study set out to look at surface winds, it is important to also consider the vertical velocity along the above ground flow surfaces. The vertical velocity values produced by WOCSS along the upper flow surfaces may better represent the region where precipitation is developing. A series of tests were conducted examining each of the five above ground flow surfaces. Vertical velocities were calculated along flow surfaces 2-6 using the same four rainfall stations as the surface flow level correlations. The results for each test are focused on overall wind direction correlations, because sounding winds were mainly from the southwest, leaving very few occasions where winds are from the southeast.

The first test used input data from the first analysis run. Above ground correlation results from this run are given in Tables 23-42. Results generally show lower correlations compared to the surface flow level. Rainfall station 1 showed correlations between -0.20 and 0.20 which is not much different from surface values. Rainfall station 8 showed slight improvement over surface values with peak correlations of 0.28 (Table 32) along flow surface level 4. This represents about a 10% improvement over the surface level (Table 14). Rainfall station 9 showed positive correlations decreasing with height, with 10-30% decreases compared to surface values (Table 33 vs. Table 15). Comparing Table 33 (flow level 4) and Table 41 (flow level 2) show this decrease as well. Interestingly, the correlations increase slightly by flow level 6 (Table 24). Station 18 showed rapidly decreasing positive correlations from the surface (Table 16) with values as high as 0.36 changing to -0.29 for flow surface level 2 (Table 42). Some recovery is seen in levels 3 and 4 (Tables 34 and 38) but become negative again by level 6 (Table 26). Overall the correlations along the flow surfaces 2-6 for analysis run one is disappointing.

The second test used input data from the second analysis run. Correlation results from this run are given in Tables 43-62. Results show very similar correlations to the first test run. This is because the only change between the two test runs is the removal of the surface Correlitos station. This change affected rainfall station 1 the most, with an increase in positive correlations along flow surface level 2 (Table 59) of up to 25% compared to the first analysis run results (Table 39). This should be expected due to its close proximity to the Correlitos station. Differences in correlations between the two runs decrease along the upper flow surfaces, indicating that surface winds have less influence at these levels. The other three rainfall stations showed mainly minor differences of 5-10% between the two runs at flow surface levels 3-6, with differences of almost 20% for flow level 2. Overall, the differences between analysis runs one and two along the upper flow surfaces are minor (under 10%) except for station 1 and 18 along flow surface levels 2-3.

One possible reason that may explain the decreasing positive correlations, and increasing negative correlations in most cases along the above-ground flow surfaces, is that the soundings are only taken once every 12 hours while surface observations are every hour. The impact of surface winds interpolated to higher flow surfaces decreases with altitude. This means that the higher flow surfaces are mainly influenced by sounding winds. The lower resolution time scale of the sounding wind data is a likely cause of the diminishing positive correlations with height.

One concern during the calculations along flow levels 2-6 is the WOCSS-determined stability. The WOCSS model only uses the dry adiabatic lapse rate to determine stability. The Oakland soundings used in this study indicate that there are saturated layers in the first 3000m during most of the study period. Saturated layers within the sounding should be determined via the moist adiabatic lapse rate. Thus the

WOCSS scheme is overestimating the stability during much of the time period, and likely underpredicting vertical velocities across the Santa Cruz Mountains.

It is important to determine the extent of any error produced when the WOCSS analysis is too stable. To test this error, the Oakland soundings were adjusted to produce neutral conditions for saturated layers in the vertical domain. Surface wind data was used from analysis run two. Results of this test are given in Tables 63-82 as analysis run four. Comparing the correlations of the neutral flow surface levels and the second analysis run for the four rainfall stations shows mixed results. Station 1 has the least change, with differences in correlations within 10%. In most cases the correlations from run 4 are lower or have increased negative values over the second analysis run. Comparing Tables 43 and 63 shows an example of the differences for station 1. Correlation differences were mainly within 10% for rainfall station 8 as well. Only along flow level 2 is there greater correlation. Comparing Tables 60 and 80 show the increased difference, with results dropping from as high as 0.19 from the second analysis run to -0.04 to -0.07 for run 4. Correlations also diminish in value or become more highly negative for rainfall station 9. These differences are relatively small along flow surface level 2 (under 10% difference) and are shown by comparing Tables 61 and 81. Differences in correlations from the two runs increase up to flow level 6, with the second analysis run results reaching as high as 0.28 (Table 45), while negative correlations for the fourth analysis run values as large as -0.25 (Table 65). While station 9 results showed lower positive correlations along the higher flow surfaces, station 18 showed the opposite. Comparing flow levels 5-6 from the two runs (Tables 46 to 66 and 50 to 70) shows increasing positive correlation improvement of 20-30%. These improvements are not seen on the lower flow surface levels, and differences between the two runs are generally within 10-15%.

A possible reason for the diminished results (for leeward rainfall stations) during the fourth analysis run is that WOCSS seems to produce greater negative vertical velocity values during neutral conditions. When captured with the cone method, the higher negative values overwhelm the positive vertical velocities reducing positive correlation. This is likely why leeward stations 9 and 18 showed the highest differences in correlations between the two analysis runs because these stations may capture more negative vertical velocities during southwest winds.

F. Summary of Results

The results of the study show there may be some promise to the use of the WOCSS analysis as a diagnostic tool for determining rainfall enhancement across complex terrain. Correlations between vertical velocity and rainfall enhancement are as high as 0.41 at rainfall station 9 during the third analysis run of the study, while individual southerly component correlation values as high as 0.78 are seen at station 18 during the first analysis run.

The study also showed the importance of the accuracy and placement of meteorological stations for the input of surface wind and sounding data into the WOCSS model. The highest correlations are found at rainfall stations that have accurate wind data nearby, and across the portion of the domain where the highest concentration of surface wind data is available. The accuracy of the model decreased across the southern portion of the domain. Rainfall station 1 showed the lowest correlation values in the first analysis run, due to the poor wind representation from the Correlitos station. Once this station was removed in the second analysis run, the correlations increased but were still well below the correlations at rainfall stations 9 and 18. This is likely due to the lack of meteorological stations in that portion of the domain. Careful placement of accurate meteorological stations in this region could improve correlations at both rainfall stations 1 and 8.

Overall correlations at rainfall station 9 did not change much between the first and second analysis runs due to the station's close proximity to the Chalks meteorological station. The maximum overall correlation during each run was 0.36, while correlations during southwest winds were 0.45 for analysis run one and 0.43 for the second run. Southeast component correlations fell between the two analysis runs, with a maximum value of 0.47 from the first run and 0.37 for the second. An attempt was made to improve the correlations at rainfall station 9 by replacing the Chalks winds with a partial wind dataset from Pigeon Point. Results from this run are discussed below.

Results from analysis run three show that correlations based on surface winds improved for both overall wind direction values and for the individual southeast wind component. Overall, maximum wind correlations improved from 0.36 to 0.41, while southeast component values improved from a maximum of 0.47 in the first analysis to 0.58 in the third run. Southwest component correlations are only slightly lower with a maximum value of 0.42.

Analysis run 4 (using winds on upper surfaces to generate correlations) showed mainly lower positive correlation values. In some cases there is a 30% reduction in positive correlations compared to those made with surface winds. Adjusting the sounding to reflect near neutral conditions compared to the dry adiabatic lapse rate also produced lower positive correlations in most cases.

While no one inner radius distance proved optimal in the cone method, sufficiently high correlation values were found during this study to promote further research into using the WOCSS model as a rainfall diagnostic tool across complex terrain.

6.0 CONCLUSIONS

A. Overview

The difficult task of diagnosing precipitation patterns across areas of complex terrain was the focus of this study. One problem associated with diagnosing precipitation across complex terrain is that regional and mesoscale prognostic models do not typically use the horizontal resolution necessary to resolve terrain features because of the time limitations to run the model. This can lead to an underprediction of model rainfall compared to observations. Higher resolution prognostic models such as the MM5 and Eta tend to overpredict rainfall along the windward slopes of a terrain barrier, while underpredicting precipitation along the lee side.

This study used the WOCSS model (Ludwig 1988) to diagnose wind patterns across the Santa Cruz Mountains during the time period of February 1st-7th 1998. The WOCSS analysis used a simple mass consistent procedure to generate horizontal and vertical winds at high resolutions across the terrain of the Santa Cruz Mountains. In our study the vertical velocity values were correlated with enhanced rainfall to see if values similar to Rhea (1996) could be achieved. High correlations would indicate that WOCSS has the capability to diagnose rainfall enhancement patterns across the complex terrain of the Santa Cruz Mountains. This would be useful because a quick and accurate assessment of rainfall across mountain regions is an advantage over slower prognostic models.

Wind data from 28 NWS and RAWS meteorological stations were used as input into WOCSS, along with upper level data from the Oakland sounding. The study also used precipitation data to compare to the vertical velocity fields produced by WOCSS. Rainfall data was provided by the SCVWD for 18 remote rainfall gauges across the Santa Cruz Mountains. Enhanced rainfall was found by taking the difference in rainfall between reference valley station and adjacent mountain location. San Jose was used as the reference valley station for all the calculations.

Correlation values between vertical velocities and the associated rainfall enhancement were calculated for the first week of February 1998 at the 18 rainfall stations. The initial test correlation values were mainly negative. It was determined that the cause of the negative values was related to the fact that WOCSS has no moisture parameters to track the production and transport of raindrops from the windward to leeward side of the terrain. A method for tracking this droplet motion was developed and employed into the correlation procedure. The resulting cone method captures information from a given number of upstream vertical velocity grid points. The number of grid points captured depends on the wind speed, with a narrower cone at higher wind speeds. Variations of the cone method were tested to try to find an optimal value of cone angle and radius to produce the highest correlation values.

B. Results

Correlations were calculated along both the surface and above-ground flow surfaces during the first two analysis runs. The surface correlation results are discussed in the following paragraphs.

The first analysis run was made implementing the cone technique at four rainfall stations across the terrain. Correlations were broken down by southerly wind direction components, along with an overall value containing all wind directions. Unlike the test run, correlations were mainly positive, with rainfall stations 9 and 18 showing maximum overall values above 0.40 while stations 1 and 8 had very low to slightly negative correlation values. During southeast wind conditions at station 18, correlations were as high as 0.78. It was determined that the main possibility the latter stations had poor results may be due to inaccurate wind data from the RAWS Correlitos station.

Analysis run two removed the Correlitos station but kept other parameters the same. Results showed that correlations improved at station 1, with overall results improving from slightly negative to slightly positive. Results stayed nearly the same at station 9 which is likely due to the station's close proximity to the Chalks meteorological station. Station 18 had little change in overall correlation values, but southeast correlations decreased, especially as the inner radius of the cone increased. Overall correlation values at station 8 also changed little, remaining around 0.20 for each model run. Interestingly, the reason the overall results changed very little is because correlations with a southeast component increased while southwest correlations decreased. Analysis run two showed that removing a station with poor wind data can increase correlations, especially for nearby stations.

Analysis run three used the coastal wind station Pigeon Point to replace the mountain station Chalks. Otherwise, the parameters were the same as the second run. Rainfall station 9 was used because of its close proximity to both meteorological stations. Mountain stations tend to have local wind effects that are not representative of the larger-scale winds, while the unobstructed coastal station will represent the correct direction of the flow coming into the terrain from the Pacific. Results showed that some improvement occurred in the overall and southwest correlations, with maximum overall results improving from 0.38 to 0.41 and maximum southwest values improving from 0.37 to 0.58. There was little change in the maximum southeast component correlations, with values dropping from 0.43 to 0.42.

Correlations for above ground-flow surfaces showed mainly lower positive correlations compared to those obtained using surface winds. These differences were over 30% in some cases, with generally 10-20% reductions recorded. The WOCSS model has no moisture parameters and determines stability using only the dry adiabatic lapse rate. In saturated layers, the atmosphere determined by WOCSS would be too stable, tending to reduce vertical velocity values. By adjusting the soundings to be neutral with respect to the dry adiabatic lapse rate for saturated layers, these errors can be examined. Correlations were generally about 10-20% lower, indicating that this error is not much of a factor in the low positive correlations for the above-ground surfaces in the first two analysis runs.

Overall, results show correlations between the WOCSS-produced vertical velocity values captured using the cone technique and the rainfall enhancement produced at the four rainfall stations tested to be mainly less than 0.40. Without correlation values approaching those achieved by Rhea (1978, 1996), the WOCSS analysis does not have the accuracy to be used as a diagnostic tool for determining rainfall enhancement across terrain. Also, the variations to the cone angle and inner radius produced no obvious optimal value, although smaller inner radius values of 2km produced the most stable, if not the highest, correlations between the model runs. The four wind speed-dependent cone angle thresholds produced little differences, indicating that this will not be a factor in future tests, and any of the four thresholds can be used.

C. Summary

There are a number of ways that the WOCSS analysis scheme can be improved for future tests. As discussed above, the placement and accuracy of the meteorological wind and temperature input stations are extremely important in the results of the study. This was also demonstrated by Becker (1992) when winds from different directions were tested under stable conditions. The need for more meteorological stations in the southern part of the domain and across the Santa Cruz Mountains is apparent from the study.

A second possible way to improve the analysis is to include hourly profiler wind and temperature data along with the twice-per-day upper level sounding from Oakland. This should improve the accuracy of the wind analysis (especially the above ground flow surfaces) and distinguish wind shifts during frontal passages more readily.

Because the large-scale precipitation field is not usually uniform across a given region, there may be non-orographic differences in the amount of precipitation between the reference valley station and the mountain rainfall station. This will increase the error in the rainfall enhancement and correlation calculation. Although the cone technique worked well to analyze droplet enhancement and transport downwind, it does not have the capability to distinguish spatial differences in large-scale precipitation rates. One way to account for this is to incorporate a procedure similar to Rhea (1978) using parcel theory to keep track of moisture across the domain. This would also be a way to calculate Reference Basin Average (RBA) precipitation instead of determining rainfall enhancement at a point in the domain. Correlation calculations between the two models could then be compared to see which analysis produce the most accurate RBA precipitation values.

Another way to increase the accuracy of the WOCSS analysis is to include the use of high frequency radar sampling of ocean waves to estimate the offshore winds. A paper by Vesecky and associates (Vesecky et. al. 1998) showed that preliminary results using high frequency radar from offshore ships or coastal locations can provide an accurate assessment of wind speed and direction. This would allow winds to be input into the analysis along the entire coastal domain. This would increase the accuracy of the analysis, especially along the windward slopes of the coastal terrain.

Lastly the WOCSS analysis should be used on other mountain basins to further test the accuracy of the analysis. WOCSS could be run for an entire season to smooth out errors from frontal passages and convection, which were likely the cause of the correlation decrease seen in the RBA correlations of the Rhea model when 13 year seasonal values dropped from 0.75-0.94 to 0.56-0.87 for 24 hour periods (Rhea 1978).

Results from this study were encouraging, and further study is needed to decide if the WOCSS analysis can eventually be used as a diagnostic tool for determining rainfall enhancement across areas of complex terrain. Outlined above are some simple techniques that can be applied to the analysis to attempt to increase the correlation values between vertical velocity and rainfall enhancement.

REFERENCES

Archer, Scott., 1998: Model Verification of Quantitative Precipitation Forecasts over California. Masters Thesis, University of San Jose, California, 103 pp.

Becker, Allen Jacob., 1992: Implementation of a Mesoscale Boundary Layer Wind Model in the San Francisco Bay Area. Masters Thesis, University of San Jose, California, 167 pp.

Bhumralkar, C. M., R. L. Mancuso, F. L. Ludwig and D. S. Renne, 1980: A practical and economic method for estimating wind characteristics at potential wind energy conversion sites. *Sol. Energy.*, **25**, 55-65.

Blier, Warren, Marty Ralph, Brad Coleman, and Wendell Nuss., 1999: PACJET Planning Workshop., Monterey, CA. Aug./Sept. 1999.

Bond, Nicholas A., Clifford F. Mass, Bradley F. Smull, Robert A. Houze, Ming-Jen Yang, Brian A. Colle, Scott A. Braun, M.A. Shapiro, Bradley R. Colman, Paul J. Neiman, James E. Overland, William D. Neff, and James D. Doyle, 1997: The Coastal Observation and Simulation with Topography (COAST) Experiment. *Bull. Amer. Meteor. Soc.*, **78**, No 9, 1941-1955.

Bridger, Alison F.C., Allen J. Becker, Francis L. Ludwig, and Roy M. Endlich, 1994: Evaluation of the WOCSS Wind Analysis Scheme for the San Francisco Bay Area. *J. Appl. Meteor.*, **33**, 1210-1218.

Chong, M., J.-F. Georgis, O. Bousquet, S.R. Brodzik, C. Burghart, S. Cosma, U. Germann, V. Gouget, R. A. Houze Jr., C. N. James, S. Prieur, R. Rotunno, F. Roux, J. Vivekanandan, and Z.-X. Zeng., 2000: Real-Time Wind Synthesis from Doppler Radar Observations during the Mesoscale Alpine Programme. *Bull.Amer. Meteor. Soc.*, **81**, No 12, 2953-2962.

Colle, Brian A., and Clifford F. Mass, 1996: An Observational and Modeling Study of the Interaction of Low-Level Southwesterly Flow with the Olympic Mountains during COAST IOP 4. *Mon. Wea. Rev.*, **124**, 2152-2175.

Colle, Brian A., Clifford F. Mass, Kenneth J. Westrick., 2000: MM5 Precipitation Verification over the Pacific Northwest during the 1997-99 Cool Seasons. *Weather and Forecasting.*, **15**, 730-744.

Colle, Brian A., Kenneth J. Westrick, and Clifford F. Mass., 1999: Evaluation of MM5 and Eta-10 Precipitation Forecasts over the Pacific Northwest during the Cool Season. *Weather and Forecasting.*, **14**, 137-154.

Dudhia, J., 1993: A nonhydrostatic version of the Penn State-NCAR mesoscale model: Validation tests and simulations of an Atlantic cyclone and cold front. *Mon. Wea. Rev.*, **121**, 1493-1513.

Dyson, L.L., and J. Van Heerden., 2001: The Heavy Rainfall and Floods over the Northeastern Interior of South Africa during February 2000. *South African Journal of Science.*, **97**, Issue3 / 4 , 80-87.

Edlinger, J. G., and R. A. Helvey, 1961: The San Fernando convergence zone. *Bull. Amer. Meteor. Soc.*, **42**, 626-635.

Elliott, Robert D., and Russell W. Shaffer., 1962: The Development of Quantitative Relationships between Orographic Precipitation and Air-Mass Parameters for Use in Forecasting and Cloud Seeding Evaluation. *J. Appl. Meteor.*, **1**, 218-228.

Endlich, R. M., 1967: An iterative method for altering the kinematic properties of wind fields. *J. Appl. Meteor.*, **6**, 837-844.

Endlich, R. M., 1984: Wind energy estimates by use of a diagnostic model. *Bound.-Layer Meteor.*, **30**. 375-386.

Fleagle, Robert G., and Joost A. Businger., 1980: An Introduction to Atmospheric Physics, 2nd ed. Academic Press Inc., London, Vol. 25., 432 pp.

Grell, G. A., J. Dudhia, and D. R. Stauffer, 1994: A description of the fifth-generation Penn State/NCAR Mesoscale Model (MM5). NCAR Tech. Note NCAR/TN-398+STR. 138 pp.

Ishikawa, Hirohiko, 1994: Mass-Consistent Wind Model as a Meteorological Preprocessor for Tracer Transport Models. *J. Appl. Meteor.*, **33**, 733-743.

Ludwig, F. L., 1988: Users' guide for the winds on critical streamline surfaces (WOCSS) code. SRI International Project No. 4354, Menlo Park, CA., 94025.

Ludwig, F.L., 1998: Using a Dense network of Meteorological Observations to Evaluate Objective Wind Analyses Suitable for Real-Time and Retrospective Air Pollution Applications. Preprints, *10th Conf. on the Applications of Air Pollution.*, AMS and Air and Waste Management Association, Phoenix, AZ. Jan, 1998.

Ludwig, F.L., J.M. Livingston, and R.M. Endlich, 1991: Use of Mass Conservation and Critical Dividing Streamline Concepts for Efficient Objective Analysis of Winds in Complex Terrain. *J. Appl. Meteor.*, **30**, 1490-1499.

Mao, Qi, and Stephen F. Mueller., 2000: Quantitative Precipitation Forecasting for the Tennessee and Cumberland River Watersheds Using the NCEP Regional Spectral Model. *Weather and Forecasting.*, **15**, 29-45.

Mass, Clifford, 1981: Topographically Forced Convergence in Western Washington State. *Mon. Wea. Rev.*, **109**, 1335-1347.

Mass, Clifford F., and Garth K. Ferber, 1990: Surface Pressure Perturbations Produced by an Isolated Mesoscale Topographic Barrier. Part I: General Characteristics and Dynamics. *Mon. Wea. Rev.*, **118**, 2579-2596.

McPherson, Ronald D., 1986: Operational Objective Analysis Techniques and Potential Applications for Mesoscale Meteorology. American Meteorological Society, Boston., 151-172 pp.

National Center for Environmental Prediction (NCEP) home page, cited 2001: *http://www.ncep.noaa.gov*

Ralph, F. M., 1997: The California Land-Falling Jets Experiment. WR-Technical Attachment 97-14.

Rhea, J.O., 1978: Orographic precipitation model for hydrometeorological use. Colorado St. Univ., Dept. of Atmospheric Science, Atmospheric Science Paper No 287, 221p.

Rhea, J.O., 1996: An objective orographically-based QPF aid for California. WR-Technical Attachment 96-02.

Rhea, J.O., 1997: Use and Expansion of an Objective Orographic QPF Aid. WR-Technical Attachment 97-04.

Sherman, C. A., 1978: A Mass-Consistent Model for Wind Fields over Complex Terrain. *J. Appl. Meteor.*, **17**, 312-319.

Slade, David H., ed., 1968: Diffusion in the Lower Layers of the Atmosphere. *Meteorology and Atomic Energy 1968.*, §3-2.3, 92-103.

Smith, Ronald, Jan Paegle, Terry Clark, William Cotton, Dale Durran, Gregory Forbes, John Marwitz, Cliff Mass, John McGinley, Hua-lu Pan, and Martin Ralph., 1997: Local and Remote Effects of Mountains on Weather: Research Needs and Opportunities. *Bull. Amer. Meteor. Soc.*, **78**, No 5, 877-892.

Steenburgh, W. James, and Clifford F. Mass, 1996: Interaction of an Intense Extratropical Cyclone with Coastal Orography. *Mon. Wea. Rev.*, **124**, 1329-1352.

Thuiller, Richard H., 1987: Real-Time Analysis of Local Wind Patterns for Application to Nuclear-Emergency Response. *Bull. Amer. Meteor. Soc.*, **68**, No 9, 1111-1115.

Thykier-Nielsen, S. T. Mikkelsen, R. Kamada and S. A. Drake, 1990: Wind flow model study for complex terrain. Preprints, *Ninth Symp. on Turbulence and Diffusion*, Copenhagen, Amer. Meteor. Soc., 421-424.

Vesecky, John F., F.L. Ludwig, Calvin C. Teague, Wendell Nuss, Robert G. Onstott, Peter Hansen, Dan Fernandez, Jason Daida, and Ken Fischer., 1998: Estimating the Surface Wind Field Over Coastal Oceans using Multifrequency , High Frequency Radar and in SITU Observations. Preprints, *2nd Conf. on the Coastal Atmos. & Ocean.*, AMS, Phoenix, AZ. Jan. 1998.

Westrick, Kenneth J., Clifford F. Mass, and Brian A. Colle., 1999: The Limitations of the WSR-88D Radar Network for Quantitative Precipitation Measurement over the Coastal Western United States. *Bulletin of the American Meteorological Society.*, **80**, No 11, 2289-2298.

Table 1a. Oakland Sounding for 0000Z Feb. 1st. Missing Values Given by 999.0

OAK - 0000Z February 1st

Pressure mb	Height Meters	Temp Deg C	Dew Pt. Deg C	Wind Speed (m/s)	Wind Dir (Deg)
1010	6	16.2	10.2	1.0	240.0
1000	92	14.2	7.2	2.1	240.0
985	218	12.4	6.4	999.0	999.0
975	304	999.0	999.0	4.6	235.0
940	609	999.0	999.0	6.7	220.0
925	742	8.0	3.8	7.2	215.0
906	914	999.0	999.0	7.2	210.0
873	1219	999.0	999.0	6.2	195.0
850	1434	2.4	-2.0	5.7	185.0
841	1524	999.0	999.0	5.7	185.0
809	1828	999.0	999.0	5.7	195.0
795	1968	-1.5	-8.5	999.0	999.0
786	2058	-1.5	-14.5	999.0	999.0
779	2133	999.0	999.0	6.7	225.0
749	2438	999.0	999.0	7.7	235.0
729	2651	-4.9	-22.9	999.0	999.0
721	2743	999.0	999.0	9.3	235.0
700	2974	-7.1	-22.1	10.3	230.0

Table 1b. Oakland Sounding for 1200Z Feb. 1st.
Missing Values Given by 999.0

OAK - 1200Z February 1st

Pressure mb	Height Meters	Temp Deg C	Dew Pt. Deg C	Wind Speed (m/s)	Wind Dir (Deg)
1008	6	12.2	9.9	6.2	140.0
1000	76	12.4	9.2	7.2	145.0
973	304	999.0	999.0	10.3	155.0
938	609	999.0	999.0	10.8	170.0
925	724	8.4	3.9	10.8	175.0
913	831	7.8	-0.2	999.0	999.0
904	914	999.0	999.0	11.3	175.0
871	1219	999.0	999.0	13.4	185.0
850	1417	3.4	-4.6	15.9	185.0
807	1828	999.0	999.0	19.5	190.0
777	2133	999.0	999.0	20.6	195.0
749	2423	-4.9	-7.1	999.0	999.0
748	2438	999.0	999.0	22.6	210.0
723	2699	-5.5	-5.8	999.0	999.0
719	2743	999.0	999.0	21.1	220.0
700	2960	-2.9	-3.3	18.5	240.0

**Table 2a. Oakland Sounding for 0000Z Feb. 2nd.
Missing Values Given by 999.0**

OAK - 0000Z February 2nd

Pressure mb	Height Meters	Temp Deg C	Dew Pt. Deg C	Wind Speed (m/s)	Wind Dir (Deg)
1005	6	14.2	13.6	2.1	250.0
1000	49	14.0	12.2	2.6	250.0
990	133	13.6	9.9	999.0	999.0
970	304	999.0	999.0	6.2	250.0
935	609	999.0	999.0	6.7	240.0
925	701	8.2	7.6	7.2	235.0
901	914	999.0	999.0	7.7	235.0
877	1137	5.4	1.1	999.0	999.0
868	1219	999.0	999.0	10.3	235.0
850	1395	3.8	0.1	10.8	230.0
805	1828	999.0	999.0	12.9	230.0
796	1922	0.0	-0.9	999.0	999.0
775	2133	999.0	999.0	14.9	230.0
746	2438	999.0	999.0	13.4	230.0
718	2743	999.0	999.0	12.9	235.0
700	2944	-5.7	-6.5	13.4	235.0

Table 2b. Oakland Sounding for 1200Z Feb. 2nd. Missing Values Given by 999.0

OAK - 1200Z February 2nd

Pressure mb	Height Meters	Temp Deg C	Dew Pt. Deg C	Wind Speed (m/s)	Wind Dir (Deg)
1007	6	12.2	11.2	5.1	135.0
1000	67	12.4	10.7	5.7	140.0
972	304	999.0	999.0	7.7	150.0
966	355	11.8	8.1	999.0	999.0
937	609	999.0	999.0	8.2	180.0
925	719	8.8	6.7	8.2	185.0
903	914	999.0	999.0	9.3	195.0
900	944	7.8	0.8	999.0	999.0
883	1100	6.6	0.6	999.0	999.0
877	1156	6.6	-4.4	999.0	999.0
870	1219	999.0	999.0	10.8	205.0
858	1335	5.4	-5.6	999.0	999.0
850	1414	4.6	-1.4	10.3	205.0
837	1539	3.8	1.2	999.0	999.0
816	1744	2.4	1.4	999.0	999.0
808	1828	999.0	999.0	10.8	210.0
795	1953	1.6	-2.1	999.0	999.0
777	2133	999.0	999.0	10.3	210.0
749	2428	-2.1	-3.1	999.0	999.0
748	2438	999.0	999.0	11.3	205.0
720	2743	999.0	999.0	12.3	205.0
700	2969	-5.3	-6.8	12.9	205.0

Table 3a. Oakland Sounding for 0000Z Feb. 3rd.
Missing Values Given by 999.0

OAK - 0000Z February 3rd

Pressure mb	Height Meters	Temp Deg C	Dew Pt. Deg C	Wind Speed (m/s)	Wind Dir (Deg)
994	6	13.0	12.7	10.3	160.0
991	31	15.2	13.8	999.0	999.0
931	609	999.0	999.0	20.1	170.0
925	615	12.0	11.0	20.1	170.0
892	914	999.0	999.0	23.1	175.0
860	1219	999.0	999.0	32.4	175.0
850	1319	7.6	7.1	33.4	175.0
829	1524	999.0	999.0	34.0	180.0
798	1828	999.0	999.0	30.9	180.0
769	2133	999.0	999.0	34.0	190.0
740	2438	999.0	999.0	35.5	195.0
731	2539	0.0	-0.5	999.0	999.0
713	2743	999.0	999.0	35.0	195.0
700	2893	-2.3	-5.7	33.4	195.0

Table 3b. Oakland Sounding for 1200Z Feb. 3rd.
Missing Values Given by 999.0

OAK - 1200Z February 3rd

Pressure mb	Height Meters	Temp Deg C	Dew Pt. Deg C	Wind Speed (m/s)	Wind Dir (Deg)
989	6	11.4	9.8	6.2	140.0
963	226	9.0	6.2	999.0	999.0
925	564	7.2	5.0	999.0	999.0
923	914	999.0	999.0	10.8	200.0
858	1219	999.0	999.0	10.3	205.0
850	1256	3.4	1.6	10.3	205.0
792	1828	999.0	999.0	11.3	205.0
790	1844	0.0	-1.6	999.0	999.0
762	2133	999.0	999.0	12.9	205.0
739	2376	-1.5	-3.9	999.0	999.0
733	2438	999.0	999.0	14.4	210.0
706	2743	999.0	999.0	13.9	210.0
700	2809	-4.7	-7.8	13.4	210.0

**Table 4a. Oakland Sounding for 0000Z Feb. 4th.
Missing Values Given by 999.0**

OAK - 0000Z February 4th

Pressure mb	Height Meters	Temp Deg C	Dew Pt. Deg C	Wind Speed (m/s)	Wind Dir (Deg)
994	6	13.4	10.9	3.1	240.0
990	40	12.6	5.6	6.2	230.0
982	108	12.0	4.0	999.0	999.0
925	603	7.4	2.8	6.7	225.0
924	609	999.0	999.0	6.7	225.0
890	914	999.0	999.0	7.2	230.0
884	972	3.8	2.6	999.0	999.0
850	1291	1.0	-1.4	7.2	230.0
848	1310	0.8	-1.7	999.0	999.0
845	1338	0.8	-4.2	999.0	999.0
833	1452	0.0	-6.0	999.0	999.0
819	1587	-1.3	-5.7	999.0	999.0
811	1665	-1.9	-9.9	999.0	999.0
796	1813	-1.9	-16.9	999.0	999.0
795	1828	999.0	999.0	7.7	215.0
764	2133	999.0	999.0	9.3	220.0
835	2438	999.0	999.0	9.8	220.0
829	2506	-4.7	-21.7	999.0	999.0
708	2743	999.0	999.0	9.8	220.0
700	2828	-6.7	-21.7	9.8	220.0

Table 4b. Oakland Sounding for 1200Z Feb. 4th.
Missing Values Given by 999.0

OAK - 1200Z February 4th

Pressure mb	Height Meters	Temp Deg C	Dew Pt. Deg C	Wind Speed (m/s)	Wind Dir (Deg)
1000	6	10.2	9.3	1.5	330.0
996	39	8.4	6.3	999.0	999.0
925	652	5.8	2.2	10.3	275.0
850	1337	0.4	-3.6	12.9	275.0
811	1711	-1.9	-7.9	999.0	999.0
725	2592	-6.3	-9.4	999.0	999.0
700	2870	-8.5	-12.1	8.7	230.0

Table 5a. Oakland Sounding for 0000Z Feb. 5th.
Missing Values Given by 999.0

OAK - 0000Z February 5th

Pressure mb	Height Meters	Temp Deg C	Dew Pt. Deg C	Wind Speed (m/s)	Wind Dir (Deg)
1008	6	15.0	11.0	2.6	180.0
1000	76	11.4	7.3	999.0	999.0
938	609	999.0	999.0	7.2	215.0
925	721	6.4	3.5	6.7	205.0
903	914	999.0	999.0	6.2	190.0
870	1219	999.0	999.0	6.7	175.0
850	1409	1.2	0.1	6.7	180.0
834	1561	0.0	-0.7	999.0	999.0
806	1828	999.0	999.0	8.7	190.0
776	2133	999.0	999.0	10.3	195.0
746	2438	999.0	999.0	10.8	195.0
724	2676	-6.3	-7.0	999.0	999.0
718	2743	999.0	999.0	11.3	200.0
717	2752	-7.7	-11.7	999.0	999.0
700	2944	-9.1	-16.1	11.8	210.0

Table 5b. Oakland Sounding for 1200Z Feb. 5th.
Missing Values Given by 999.0

OAK - 1200Z February 5th

Pressure mb	Height Meters	Temp Deg C	Dew Pt. Deg C	Wind Speed (m/s)	Wind Dir (Deg)
1011	6	12.0	8.5	6.2	135.0
1000	93	11.4	6.4	8.7	140.0
975	304	999.0	999.0	13.9	145.0
951	508	8.6	2.6	999.0	999.0
940	609	999.0	999.0	14.4	160.0
925	740	6.8	3.0	14.9	165.0
905	914	999.0	999.0	15.4	170.0
872	1219	999.0	999.0	16.5	175.0
850	1428	1.6	1.0	18.0	180.0
840	1524	999.0	999.0	19.0	180.0
808	1828	999.0	999.0	18.5	190.0
778	2133	999.0	999.0	17.5	200.0
749	2438	999.0	999.0	17.0	210.0
721	2743	999.0	999.0	15.4	220.0
700	2976	-4.5	-5.1	13.9	230.0

Table 6a. Oakland Sounding for 0000Z Feb. 6th.
Missing Values Given by 999.0

OAK - 0000Z February 6th

Pressure mb	Height Meters	Temp Deg C	Dew Pt. Deg C	Wind Speed (m/s)	Wind Dir (Deg)
1009	6	13.8	11.7	10.3	150.0
1007	23	14.0	8.0	999.0	999.0
1000	82	13.8	7.8	12.9	150.0
974	304	999.0	999.0	18.0	155.0
939	609	999.0	999.0	18.5	165.0
925	734	8.2	5.9	19.0	170.0
905	914	999.0	999.0	20.1	170.0
885	1095	4.8	4.3	999.0	999.0
872	1219	999.0	999.0	24.7	175.0
850	1426	3.0	2.4	24.7	180.0
808	1828	999.0	999.0	25.7	185.0
778	2133	999.0	999.0	25.2	195.0
749	2438	999.0	999.0	23.7	200.0
721	2743	999.0	999.0	23.7	200.0
700	2980	-4.1	-4.7	22.6	195.0

Table 6b. Oakland Sounding for 1200Z Feb. 6th. Missing Values Given by 999.0

OAK - 1200Z February 6th

Pressure mb	Height Meters	Temp Deg C	Dew Pt. Deg C	Wind Speed (m/s)	Wind Dir (Deg)
997	6	16.0	9.0	17.0	150.0
982	134	14.0	3.0	999.0	999.0
962	304	12.2	1.2	28.8	145.0
940	609	999.0	999.0	27.8	145.0
925	631	9.8	1.8	27.8	145.0
894	914	999.0	999.0	26.2	150.0
878	1059	5.8	1.8	999.0	999.0
861	1219	999.0	999.0	27.3	160.0
850	1326	4.4	2.5	27.3	160.0
800	1816	2.8	2.1	999.0	999.0
799	1828	999.0	999.0	40.6	175.0
769	2133	999.0	999.0	44.8	175.0
740	2438	999.0	999.0	45.8	180.0
713	2743	999.0	999.0	47.8	185.0
707	2701	999.0	999.0	999.0	999.0
700	2889	-2.9	-3.6	999.0	999.0

Table 7a. Oakland Sounding for 0000Z Feb. 7th.
Missing Values Given by 999.0

OAK - 0000Z February 7th

Pressure mb	Height Meters	Temp Deg C	Dew Pt. Deg C	Wind Speed (m/s)	Wind Dir (Deg)
1000	6	11.0	10.5	7.2	140.0
998	23	10.8	8.5	999.0	999.0
965	304	999.0	999.0	11.8	180.0
948	448	8.8	6.1	999.0	999.0
930	609	999.0	999.0	13.9	205.0
925	651	7.2	6.4	14.9	205.0
896	914	999.0	999.0	17.0	210.0
863	1219	999.0	999.0	18.0	210.0
850	1341	2.0	0.3	17.5	210.0
818	1648	0.0	-1.0	999.0	999.0
800	1828	999.0	999.0	15.9	210.0
769	2133	999.0	999.0	16.5	210.0
740	2438	999.0	999.0	17.5	210.0
712	2743	999.0	999.0	18.0	210.0
700	2882	-6.9	-7.5	18.0	210.0

Table 7b. Oakland Sounding for 1200Z Feb. 7th.
Missing Values Given by 999.0

OAK -1200Z February 7th

Pressure mb	Height Meters	Temp Deg C	Dew Pt. Deg C	Wind Speed (m/s)	Wind Dir (Deg)
1009	6	10.4	9.5	7.7	140.0
1000	81	10.2	9.5	9.3	145.0
980	248	10.4	9.1	999.0	999.0
973	304	999.0	999.0	12.9	160.0
938	609	999.0	999.0	13.9	170.0
925	728	6.6	6.0	14.4	175.0
904	914	999.0	999.0	15.4	180.0
871	1219	999.0	999.0	16.5	185.0
850	1416	10.0	0.7	15.9	185.0
815	1751	-1.7	-1.9	999.0	999.0
807	1828	999.0	999.0	15.4	195.0
776	2133	999.0	999.0	16.5	200.0
754	2363	-5.5	-7.1	999.0	999.0
747	2438	999.0	999.0	16.5	205.0
745	2457	-5.7	-11.7	999.0	999.0
735	2563	-5.7	-14.7	999.0	999.0
719	2743	999.0	999.0	17.5	215.0
700	2949	-7.1	-15.1	17.5	220.0

Table 7c. Oakland Sounding for 0000Z Feb. 8th.
Missing Values Given by 999.0

OAK -0000Z February 8th

Pressure mb	Height Meters	Temp Deg C	Dew Pt. Deg C	Wind Speed (m/s)	Wind Dir (Deg)
1003	6	12.6	11.3	5.1	140.0
1000	35	12.4	10.2	5.7	145.0
968	304	999.0	999.0	10.3	180.0
934	609	999.0	999.0	11.8	205.0
925	686	8.8	7.5	12.9	210.0
912	802	7.8	6.7	999.0	999.0
900	914	999.0	999.0	15.4	220.0
884	1057	6.2	0.2	999.0	999.0
867	1219	999.0	999.0	17.0	225.0
850	1380	3.4	-1.4	17.5	225.0
804	1828	999.0	999.0	19.0	220.0
773	2133	999.0	999.0	19.0	220.0
751	2365	-5.1	-6.4	999.0	999.0
741	2470	-5.3	-5.9	999.0	999.0
726	2630	-6.3	-13.3	999.0	999.0
720	2695	-6.5	-13.5	999.0	999.0
700	2919	-8.5	-13.5	22.1	230.0

Table 8. 28 RAWS and NWS Meteorological Stations. Identification, UTM and Grid Location.

Station #	Station Identifier	Station Name	UTM North	UTM East	X km	Y km
1	CA013	Barnaby	4218	551	124	232
2	CA022	Black Diamond	4201	598	171	215
3	CA032	Briones	4198	577	150	212
4	CA042	Chalks	4113	562	135	127
5	CA053	Corralitos	4093	608	181	107
6	CA104	La Honda	4128	566	139	142
7	CA0108	Las Trampas	4187	582	155	201
8	CA119	Los Banos	4102	675	248	116
9	CA174	Rose Peak	4151	612	185	165
10	CA181	Santa Rosa	4259	525	98	273
11	CA204	Sweetwater	4139	635	208	153
12	SFO	San Fran.	4163	555	128	177
13	SAC	Sacramento	4265	631	204	279
14	SNS	Salinas	4058	625	198	72
15	SJC	San Jose	4135	595	168	149
16	CCR	Concord	4203	583	156	217
17	SUU	Travis AFB.	4236	594	167	250
18	HWD	Hayward	4168	578	151	182
19	LVK	Livermore	4173	604	177	187
20	NUQ	Moffet AFB.	4141	584	157	155
21	MRY	Monterey	4049	603	176	63
22	APC	Napa	4230	563	136	244
23	OAK	Oakland	4175	569	142	189
24	PAO	Palo Alto	4147	578	151	161
25	SQL	San Carlos	4153	566	139	167
26	RHV	Reed Hillview	4132	605	178	146
27	SCK	Stockton	4196	654	227	210
28	46026	Offshore Buoy	4173	518	91	187

Table 9. 18 Rainfall Stations Identification and UTM Location.

Station #	Station Identifier	UTM North	UTM East
1	1085	4097	615
2	1509	4122	583
3	1530	4105	607
4	1879	4132	570
5	1965	4108	597
6	1969	4102	596
7	1971	4107	582
8	1973	4118	583
9	1975	4111	574
10	1987	4110	592
11	1995	4098	609
12	1997	4100	606
13	2066	4120	595
14	2068	4116	590
15	2072	4108	603
16	2080	4113	603
17	2081	4114	597
18	2096	4133	573

Table 10. Test Run Station Correlations w(t) vs. rain(t).

Station #	Correlation w(t) vs. rain(t)
1	0.19
2	-0.48
3	-0.19
4	-0.61
5	-0.19
6	0.00
7	-0.17
8	0.43
9	-0.11
10	0.08
11	-0.15
12	-0.18
13	-0.31
14	-0.29
15	-0.13
16	0.15
17	-0.07
18	-0.73

Table 11. Test Run Station Correlations w(t) vs. rain(t+1).

Station #	Correlation w(t) vs. rain(t+1)
1	0.18
2	-0.42
3	0.10
4	-0.43
5	-0.14
6	0.00
7	-0.06
8	0.40
9	-0.10
10	-0.09
11	-0.14
12	-0.27
13	-0.10
14	-0.24
15	-0.18
16	0.06
17	-0.12
18	-0.64

Table 12. Test Run Correlation Difference.

Station #	Correlation w(t) vs. rain(t)	Correlation w(t) vs. rain(t+1)	Net Change
1	0.19	0.18	-0.01
2	-0.48	-0.42	0.06
3	-0.19	0.10	0.29
4	-0.61	-0.43	0.18
5	-0.19	-0.14	0.05
6	0.00	0.00	0.00
7	-0.17	-0.06	0.11
8	0.43	0.40	-0.03
9	-0.11	-0.10	0.01
10	0.08	-0.09	-0.17
11	-0.15	-0.14	0.01
12	-0.18	-0.27	-0.09
13	-0.31	-0.10	0.21
14	-0.29	-0.24	0.05
15	-0.13	-0.18	-0.05
16	0.15	0.06	-0.09
17	-0.07	-0.12	-0.05
18	-0.73	-0.64	0.09

Table 13. Correlation Test Results From Analysis Run 1 (Rainfall Station 9).

Cone Angle Degrees	r1=Outer Radius r2=Inner Radius Units (km) (SPD Proportional To Wind Speed)	All 360 Degree Wind Directions	Southwest Winds 181-270 Degrees	Southeast Winds 90-180 Degrees
Angle = 40 Degrees	r1=SPD, r2=0	0.37	0.38	0.41
	r1=1.1*SPD, r2 = 0	0.33	0.27	0.43
	r1=0.9*SPD, r2 = 0	0.26	0.19	0.35
	r1=1.2*SPD, r2 = 0	0.30	0.24	0.40
	r1=SPD, r2 = 2km	0.35	0.37	0.43
	r1=SPD, r2 = 3km	0.36	0.40	0.45
	r1=SPD, r2 = 4km	0.35	0.32	0.44
	r1=SPD, r2 = 5km	0.44	0.47	0.44
	r1= SPD, r2 = 6km	0.44	0.42	0.48
Angle = 30 Degrees	r1=SPD, r2=0	0.37	0.37	0.32
	r1=1.1*SPD, r2 = 0	0.33	0.27	0.34
	r1=0.9*SPD, r2 = 0	0.24	0.14	0.28
	r1=1.2*SPD, r2 = 0	0.28	0.22	0.31
	r1=SPD, r2 = 2km	0.37	0.46	0.30
	r1=SPD, r2 = 3km	0.37	0.47	0.32
	r1=SPD, r2 = 4km	0.38	0.37	0.31
	r1=SPD, r2 = 5km	0.43	0.44	0.33
	r1= SPD, r2 = 6km	0.43	0.41	0.36
Angle = 20 Degrees	r1=SPD, r2=0	0.31	0.38	0.41
	r1=1.1*SPD, r2 = 0	0.28	0.27	0.44
	r1=0.9*SPD, r2 = 0	0.20	0.14	0.46
	r1=1.2*SPD, r2 = 0	0.24	0.23	0.39
	r1=SPD, r2 = 2km	0.35	0.38	0.45
	r1=SPD, r2 = 3km	0.36	0.40	0.46
	r1=SPD, r2 = 4km	0.24	0.35	0.45
	r1=SPD, r2 = 5km	0.28	0.46	0.43
	r1= SPD, r2 = 6km	0.29	0.42	0.45

Table 14. Correlation Results From Analysis Run 1 (Rainfall Station 1).

Wind Speed Thresholds to Determine the Cone Angle	Inner Radius (r2) (Outer Radius (r1) Proportional To Wind Speed)	All 360 Degree Wind Directions	Southeast Winds 90-180 Degrees	Southwest Winds 181-270 Degrees
0-3m/s = 40° 4-7m/s = 30° > 8m/s = 20°	r2 = 2km	0.05	0.05	0.11
	r2 = 3km	-0.04	-0.02	-0.02
	r2 = 4km	-0.12	-0.02	-0.20
	r2 = 5km	-0.22	-0.08	-0.34
	r2 = 6km	-0.20	-0.09	-0.27
0-4m/s = 40° 5-9m/s = 30° > 10m/s = 20°	r2 = 2km	0.03	0.03	0.09
	r2 = 3km	-0.05	-0.03	-0.04
	r2 = 4km	-0.14	-0.06	-0.20
	r2 = 5km	-0.23	-0.10	-0.34
	r2 = 6km	-0.22	-0.10	-0.27
0-5m/s = 40° 6-11m/s = 30° > 12m/s = 20°	r2 = 2km	0.03	0.03	0.09
	r2 = 3km	-0.04	-0.03	-0.04
	r2 = 4km	-0.14	-0.07	-0.20
	r2 = 5km	-0.23	-0.11	-0.32
	r2 = 6km	-0.21	-0.12	-0.26
0-6m/s = 40° 7-13m/s = 30° > 14m/s = 20°	r2 = 2km	0.03	0.03	0.09
	r2 = 3km	-0.04	-0.03	-0.04
	r2 = 4km	-0.14	-0.07	-0.20
	r2 = 5km	-0.22	-0.11	-0.32
	r2 = 6km	-0.21	-0.11	-0.25

Table 15. Correlation Results From Analysis Run 1 (Rainfall Station 8).

Wind Speed Thresholds to Determine the Cone Angle	Inner Radius (r2) (Outer Radius (r1) Proportional To Wind Speed)	All 360 Degree Wind Directions	Southeast Winds 90-180 Degrees	Southwest Winds 181-270 Degrees
0-3m/s = 40° 4-7m/s = 30° > 8m/s = 20°	r2 = 2km r2 = 3km r2 = 4km r2 = 5km r2 = 6km	0.18 0.18 0.19 0.19 0.19	0.17 0.17 0.17 0.17 0.17	0.22 0.23 0.23 0.24 0.24
0-4m/s = 40° 5-9m/s = 30° > 10m/s = 20°	r2 = 2km r2 = 3km r2 = 4km r2 = 5km r2 = 6km	0.16 0.16 0.17 0.17 0.17	0.17 0.17 0.17 0.17 0.17	0.17 0.17 0.18 0.19 0.18
0-5m/s = 40° 6-11m/s = 30° > 12m/s = 20°	r2 = 2km r2 = 3km r2 = 4km r2 = 5km r2 = 6km	0.16 0.16 0.16 0.16 0.16	0.14 0.14 0.14 0.14 0.14	0.19 0.19 0.20 0.20 0.20
0-6m/s = 40° 7-13m/s = 30° > 14m/s = 20°	r2 = 2km r2 = 3km r2 = 4km r2 = 5km r2 = 6km	0.15 0.16 0.16 0.16 0.16	0.14 0.14 0.14 0.14 0.13	0.19 0.19 0.20 0.20 0.20

Table 16. Correlation Results From Analysis Run 1 (Rainfall Station 9).

Wind Speed Thresholds to Determine the Cone Angle	Inner Radius (r2) (Outer Radius (r1) Proportional To Wind Speed)	All 360 Degree Wind Directions	Southeast Winds 90-180 Degrees	Southwest Winds 181-270 Degrees
0-3m/s = 40° 4-7m/s = 30° > 8m/s = 20°	r2 = 2km r2 = 3km r2 = 4km r2 = 5km r2 = 6km	0.36 0.35 0.32 0.35 0.34	0.41 0.41 0.30 0.32 0.31	0.40 0.42 0.43 0.40 0.42
0-4m/s = 40° 5-9m/s = 30° > 10m/s = 20°	r2 = 2km r2 = 3km r2 = 4km r2 = 5km r2 = 6km	0.34 0.37 0.33 0.36 0.34	0.37 0.46 0.30 0.32 0.30	0.40 0.43 0.44 0.41 0.42
0-5m/s = 40° 6-11m/s = 30° > 12m/s = 20°	r2 = 2km r2 = 3km r2 = 4km r2 = 5km r2 = 6km	0.35 0.38 0.34 0.38 0.36	0.39 0.47 0.31 0.38 0.34	0.40 0.42 0.44 0.40 0.41
0-6m/s = 40° 7-13m/s = 30° > 14m/s = 20°	r2 = 2km r2 = 3km r2 = 4km r2 = 5km r2 = 6km	0.35 0.38 0.34 0.40 0.36	0.39 0.47 0.31 0.38 0.33	0.40 0.43 0.45 0.43 0.42

Table 17. Correlation Results From Analysis Run 1 (Rainfall Station 18).

Wind Speed Thresholds to Determine the Cone Angle	Inner Radius (r2) (Outer Radius (r1) Proportional To Wind Speed)	All 360 Degree Wind Directions	Southeast Winds 90-180 Degrees	Southwest Winds 181-270 Degrees
0-3m/s = 40° 4-7m/s = 30° > 8m/s = 20°	r2 = 2km r2 = 3km r2 = 4km r2 = 5km r2 = 6km	0.36 0.27 0.25 0.30 0.28	0.59 0.48 0.53 0.77 0.63	0.31 0.26 0.22 0.24 0.27
0-4m/s = 40° 5-9m/s = 30° > 10m/s = 20°	r2 = 2km r2 = 3km r2 = 4km r2 = 5km r2 = 6km	0.34 0.26 0.23 0.29 0.30	0.58 0.52 0.54 0.78 0.65	0.29 0.23 0.20 0.23 0.30
0-5m/s = 40° 6-11m/s = 30° > 12m/s = 20°	r2 = 2km r2 = 3km r2 = 4km r2 = 5km r2 = 6km	0.34 0.28 0.25 0.31 0.32	0.56 0.49 0.52 0.73 0.54	0.31 0.26 0.24 0.26 0.33
0-6m/s = 40° 7-13m/s = 30° > 14m/s = 20°	r2 = 2km r2 = 3km r2 = 4km r2 = 5km r2 = 6km	0.34 0.29 0.27 0.32 0.32	0.51 0.51 0.53 0.76 0.50	0.31 0.26 0.25 0.27 0.33

Table 18. Correlation Results From Analysis Run 2 (Rainfall Station 1).

Wind Speed Thresholds to Determine the Cone Angle	Inner Radius (r2) (Outer Radius (r1) Proportional To Wind Speed)	All 360 Degree Wind Directions	Southeast Winds 90-180 Degrees	Southwest Winds 181-270 Degrees
	r2 = 2km	0.09	0.25	0.18
0-3m/s = 40°	r2 = 3km	0.10	0.25	0.17
4-7m/s = 30°	r2 = 4km	0.10	0.27	0.15
> 8m/s = 20°	r2 = 5km	0.15	0.34	0.18
	r2 = 6km	0.12	0.26	0.13
	r2 = 2km	0.07	0.22	0.18
0-4m/s = 40°	r2 = 3km	0.10	0.24	0.18
5-9m/s = 30°	r2 = 4km	0.09	0.23	0.16
> 10m/s = 20°	r2 = 5km	0.15	0.31	0.18
	r2 = 6km	0.13	0.26	0.14
	r2 = 2km	0.08	0.22	0.18
0-5m/s = 40°	r2 = 3km	0.11	0.26	0.19
6-11m/s = 30°	r2 = 4km	0.11	0.30	0.17
> 12m/s = 20°	r2 = 5km	0.15	0.32	0.18
	r2 = 6km	0.12	0.29	0.13
	r2 = 2km	0.07	0.22	0.16
0-6m/s = 40°	r2 = 3km	0.09	0.25	0.17
7-13m/s = 30°	r2 = 4km	0.09	0.29	0.15
> 14m/s = 20°	r2 = 5km	0.14	0.30	0.17
	r2 = 6km	0.11	0.29	0.12

Table 19. Correlation Results From Analysis Run 2 (Rainfall Station 8).

Wind Speed Thresholds to Determine the Cone Angle	Inner Radius (r2) (Outer Radius (r1) Proportional To Wind Speed)	All 360 Degree Wind Directions	Southeast Winds 90-180 Degrees	Southwest Winds 181-270 Degrees
0-3m/s = 40° 4-7m/s = 30° > 8m/s = 20°	r2 = 2km r2 = 3km r2 = 4km r2 = 5km r2 = 6km	0.20 0.20 0.21 0.21 0.21	0.37 0.37 0.37 0.37 0.37	0.12 0.12 0.17 0.14 0.13
0-4m/s = 40° 5-9m/s = 30° > 10m/s = 20°	r2 = 2km r2 = 3km r2 = 4km r2 = 5km r2 = 6km	0.19 0.19 0.20 0.20 0.19	0.37 0.37 0.37 0.37 0.37	0.11 0.11 0.12 0.11 0.08
0-5m/s = 40° 6-11m/s = 30° > 12m/s = 20°	r2 = 2km r2 = 3km r2 = 4km r2 = 5km r2 = 6km	0.17 0.17 0.17 0.18 0.17	0.36 0.36 0.36 0.36 0.36	0.08 0.09 0.09 0.09 0.09
0-6m/s = 40° 7-13m/s = 30° > 14m/s = 20°	r2 = 2km r2 = 3km r2 = 4km r2 = 5km r2 = 6km	0.17 0.17 0.17 0.17 0.17	0.36 0.36 0.36 0.36 0.36	0.09 0.09 0.09 0.09 0.09

Table 20. Correlation Results From Analysis Run 2 (Rainfall Station 9).

Wind Speed Thresholds to Determine the Cone Angle	Inner Radius (r2) (Outer Radius (r1) Proportional To Wind Speed)	All 360 Degree Wind Directions	Southeast Winds 90-180 Degrees	Southwest Winds 181-270 Degrees
0-3m/s = 40° 4-7m/s = 30° > 8m/s = 20°	r2 = 2km r2 = 3km r2 = 4km r2 = 5km r2 = 6km	0.26 0.21 0.33 0.34 0.32	0.22 0.16 0.35 0.30 0.27	0.33 0.33 0.36 0.39 0.38
0-4m/s = 40° 5-9m/s = 30° > 10m/s = 20°	r2 = 2km r2 = 3km r2 = 4km r2 = 5km r2 = 6km	0.28 0.28 0.35 0.35 0.32	0.23 0.23 0.36 0.31 0.28	0.37 0.38 0.37 0.40 0.39
0-5m/s = 40° 6-11m/s = 30° > 12m/s = 20°	r2 = 2km r2 = 3km r2 = 4km r2 = 5km r2 = 6km	0.30 0.30 0.38 0.36 0.33	0.23 0.23 0.37 0.32 0.29	0.39 0.42 0.42 0.41 0.38
0-6m/s = 40° 7-13m/s = 30° > 14m/s = 20°	r2 = 2km r2 = 3km r2 = 4km r2 = 5km r2 = 6km	0.30 0.30 0.38 0.37 0.33	0.23 0.23 0.36 0.32 0.29	0.41 0.43 0.43 0.42 0.39

Table 21. Correlation Results From Analysis Run 2 (Rainfall Station 18).

Wind Speed Thresholds to Determine the Cone Angle	Inner Radius (r2) (Outer Radius (r1) Proportional To Wind Speed)	All 360 Degree Wind Directions	Southeast Winds 90-180 Degrees	Southwest Winds 181-270 Degrees
0-3m/s = 40° 4-7m/s = 30° > 8m/s = 20°	r2 = 2km r2 = 3km r2 = 4km r2 = 5km r2 = 6km	0.33 0.26 0.25 0.22 0.20	0.55 0.46 0.43 0.42 0.12	0.26 0.20 0.19 0.17 0.21
0-4m/s = 40° 5-9m/s = 30° > 10m/s = 20°	r2 = 2km r2 = 3km r2 = 4km r2 = 5km r2 = 6km	0.35 0.25 0.28 0.24 0.22	0.53 0.46 0.45 0.43 0.14	0.31 0.18 0.24 0.19 0.23
0-5m/s = 40° 6-11m/s = 30° > 12m/s = 20°	r2 = 2km r2 = 3km r2 = 4km r2 = 5km r2 = 6km	0.36 0.25 0.30 0.25 0.24	0.53 0.46 0.45 0.43 0.14	0.31 0.18 0.26 0.20 0.26
0-6m/s = 40° 7-13m/s = 30° > 14m/s = 20°	r2 = 2km r2 = 3km r2 = 4km r2 = 5km r2 = 6km	0.34 0.24 0.30 0.24 0.23	0.48 0.45 0.43 0.33 0.07	0.31 0.18 0.27 0.22 0.26

Table 22. Correlation Results From Analysis Run 3 (Rainfall Station 9).

Wind Speed Thresholds to Determine the Cone Angle	Inner Radius (r2) (Outer Radius (r1) Proportional To Wind Speed)	All 360 Degree Wind Directions	Southeast Winds 90-180 Degrees	Southwest Winds 181-270 Degrees
0-3m/s = 40° 4-7m/s = 30° > 8m/s = 20°	r2 = 2km r2 = 3km r2 = 4km r2 = 5km r2 = 6km	0.20 0.22 0.31 0.39 0.34	0.37 0.40 0.53 0.39 0.30	0.18 0.20 0.28 0.40 0.38
0-4m/s = 40° 5-9m/s = 30° > 10m/s = 20°	r2 = 2km r2 = 3km r2 = 4km r2 = 5km r2 = 6km	0.21 0.24 0.34 0.41 0.36	0.36 0.41 0.58 0.46 0.35	0.20 0.23 0.31 0.42 0.40
0-5m/s = 40° 6-11m/s = 30° > 12m/s = 20°	r2 = 2km r2 = 3km r2 = 4km r2 = 5km r2 = 6km	0.20 0.23 0.32 0.41 0.36	0.34 0.40 0.56 0.45 0.36	0.20 0.22 0.30 0.42 0.39
0-6m/s = 40° 7-13m/s = 30° > 14m/s = 20°	r2 = 2km r2 = 3km r2 = 4km r2 = 5km r2 = 6km	0.20 0.21 0.30 0.40 0.35	0.34 0.38 0.52 0.43 0.33	0.20 0.20 0.30 0.41 0.39

Table 23. Correlation Results From Analysis Run 1. Upper Flow Surface Level 6 (Rainfall Station 1).

Wind Speed Thresholds to Determine the Cone Angle	Inner Radius (r2) (Outer Radius (r1) Proportional To Wind Speed)	All 360 Degree Wind Directions	Southeast Winds 90-180 Degrees	Southwest Winds 181-270 Degrees
0-3m/s = 40° 4-7m/s = 30° > 8m/s = 20°	r2 = 2km	0.14	0.06	0.19
	r2 = 3km	0.15	0.04	0.20
	r2 = 4km	0.13	0.11	0.17
	r2 = 5km	0.09	0.21	0.14
	r2 = 6km	0.12	0.24	0.20
0-4m/s = 40° 5-9m/s = 30° > 10m/s = 20°	r2 = 2km	0.15	0.06	0.21
	r2 = 3km	0.16	0.04	0.22
	r2 = 4km	0.13	0.11	0.18
	r2 = 5km	0.09	0.21	0.15
	r2 = 6km	0.11	0.24	0.21
0-5m/s = 40° 6-11m/s = 30° > 12m/s = 20°	r2 = 2km	0.15	-0.03	0.22
	r2 = 3km	0.16	-0.04	0.23
	r2 = 4km	0.14	0.02	0.20
	r2 = 5km	0.08	0.13	0.15
	r2 = 6km	0.10	0.15	0.20
0-6m/s = 40° 7-13m/s = 30° > 14m/s = 20°	r2 = 2km	0.18	0.05	0.24
	r2 = 3km	0.18	-1.00	0.25
	r2 = 4km	0.17	-1.00	0.23
	r2 = 5km	0.12	-1.00	0.20
	r2 = 6km	0.12	-1.00	0.21

Table 24. Correlation Results From Analysis Run 1. Upper Flow Surface Level 6 (Rainfall Station 8).

Wind Speed Thresholds to Determine the Cone Angle	Inner Radius (r2) (Outer Radius (r1) Proportional To Wind Speed)	All 360 Degree Wind Directions	Southeast Winds 90-180 Degrees	Southwest Winds 181-270 Degrees
0-3m/s = 40° 4-7m/s = 30° > 8m/s = 20°	r2 = 2km	0.11	0.05	0.20
	r2 = 3km	0.11	0.05	0.20
	r2 = 4km	0.11	0.05	0.20
	r2 = 5km	0.11	0.05	0.20
	r2 = 6km	0.11	0.05	0.20
0-4m/s = 40° 5-9m/s = 30° > 10m/s = 20°	r2 = 2km	0.15	0.08	0.25
	r2 = 3km	0.15	0.08	0.25
	r2 = 4km	0.15	0.08	0.25
	r2 = 5km	0.15	0.08	0.25
	r2 = 6km	0.15	0.08	0.25
0-5m/s = 40° 6-11m/s = 30° > 12m/s = 20°	r2 = 2km	0.15	0.05	0.26
	r2 = 3km	0.15	0.05	0.26
	r2 = 4km	0.15	0.05	0.26
	r2 = 5km	0.15	0.05	0.26
	r2 = 6km	0.15	0.05	0.26
0-6m/s = 40° 7-13m/s = 30° > 14m/s = 20°	r2 = 2km	0.11	0.00	0.23
	r2 = 3km	0.11	0.00	0.23
	r2 = 4km	0.11	0.00	0.23
	r2 = 5km	0.11	0.55	0.23
	r2 = 6km	0.11	0.55	0.23

Table 25. Correlation Results From Analysis Run 1. Upper Flow Surface Level 6 (Rainfall Station 9).

Wind Speed Thresholds to Determine the Cone Angle	Inner Radius (r2) (Outer Radius (r1) Proportional To Wind Speed)	All 360 Degree Wind Directions	Southeast Winds 90-180 Degrees	Southwest Winds 181-270 Degrees
0-3m/s = 40° 4-7m/s = 30° > 8m/s = 20°	r2 = 2km	0.24	0.29	0.29
	r2 = 3km	0.24	0.28	0.28
	r2 = 4km	0.24	0.29	0.27
	r2 = 5km	0.27	0.31	0.29
	r2 = 6km	0.23	0.26	0.26
0-4m/s = 40° 5-9m/s = 30° > 10m/s = 20°	r2 = 2km	0.25	0.29	0.29
	r2 = 3km	0.24	0.30	0.28
	r2 = 4km	0.25	0.30	0.28
	r2 = 5km	0.27	0.31	0.29
	r2 = 6km	0.24	0.26	0.27
0-5m/s = 40° 6-11m/s = 30° > 12m/s = 20°	r2 = 2km	0.24	0.30	0.28
	r2 = 3km	0.24	0.30	0.27
	r2 = 4km	0.25	0.30	0.27
	r2 = 5km	0.27	0.31	0.29
	r2 = 6km	0.24	0.26	0.27
0-6m/s = 40° 7-13m/s = 30° > 14m/s = 20°	r2 = 2km	0.24	0.30	0.27
	r2 = 3km	0.23	0.30	0.26
	r2 = 4km	0.24	0.29	0.27
	r2 = 5km	0.26	0.30	0.28
	r2 = 6km	0.24	0.26	0.26

Table 26. Correlation Results From Analysis Run 1. Upper Flow Surface Level 6 (Rainfall Station 18).

Wind Speed Thresholds to Determine the Cone Angle	Inner Radius (r2) (Outer Radius (r1) Proportional To Wind Speed)	All 360 Degree Wind Directions	Southeast Winds 90-180 Degrees	Southwest Winds 181-270 Degrees
0-3m/s = 40° 4-7m/s = 30° > 8m/s = 20°	r2 = 2km	-0.08	0.08	0.04
	r2 = 3km	-0.13	0.07	0.00
	r2 = 4km	-0.17	0.06	-0.06
	r2 = 5km	-0.17	0.05	-0.07
	r2 = 6km	-0.16	0.02	-0.11
0-4m/s = 40° 5-9m/s = 30° > 10m/s = 20°	r2 = 2km	-0.08	0.08	0.03
	r2 = 3km	-0.13	0.07	-0.01
	r2 = 4km	-0.17	0.05	-0.05
	r2 = 5km	-0.17	0.05	-0.06
	r2 = 6km	-0.16	0.02	-0.10
0-5m/s = 40° 6-11m/s = 30° > 12m/s = 20°	r2 = 2km	-0.10	0.08	0.01
	r2 = 3km	-0.15	0.07	-0.02
	r2 = 4km	-0.18	0.05	-0.04
	r2 = 5km	-0.17	0.05	-0.06
	r2 = 6km	-0.17	0.01	-0.09
0-6m/s = 40° 7-13m/s = 30° > 14m/s = 20°	r2 = 2km	-0.09	0.10	0.00
	r2 = 3km	-0.14	0.09	-0.02
	r2 = 4km	-0.17	0.07	-0.05
	r2 = 5km	-0.17	0.08	-0.06
	r2 = 6km	-0.16	0.04	-0.10

Table 27. Correlation Results From Analysis Run 1.
Upper Flow Surface Level 5 (Rainfall Station 1).

Wind Speed Thresholds to Determine the Cone Angle	Inner Radius (r2) (Outer Radius (r1) Proportional To Wind Speed)	All 360 Degree Wind Directions	Southeast Winds 90-180 Degrees	Southwest Winds 181-270 Degrees
0-3m/s = 40° 4-7m/s = 30° > 8m/s = 20°	r2 = 2km	0.00	-0.34	0.07
	r2 = 3km	0.03	-0.33	0.11
	r2 = 4km	0.04	-0.33	0.13
	r2 = 5km	0.01	-0.32	0.09
	r2 = 6km	0.02	-0.30	0.10
0-4m/s = 40° 5-9m/s = 30° > 10m/s = 20°	r2 = 2km	0.01	-0.29	0.07
	r2 = 3km	0.03	-0.30	0.11
	r2 = 4km	0.05	-0.29	0.13
	r2 = 5km	0.01	-0.29	0.09
	r2 = 6km	0.01	-0.29	0.09
0-5m/s = 40° 6-11m/s = 30° > 12m/s = 20°	r2 = 2km	-0.01	-0.29	0.04
	r2 = 3km	0.00	-0.31	0.08
	r2 = 4km	0.01	-0.30	0.09
	r2 = 5km	-0.02	-0.27	0.04
	r2 = 6km	-0.01	-0.27	0.06
0-6m/s = 40° 7-13m/s = 30° > 14m/s = 20°	r2 = 2km	-0.01	-0.29	0.05
	r2 = 3km	0.01	-0.32	0.09
	r2 = 4km	0.01	-0.30	0.09
	r2 = 5km	-0.04	-0.32	0.02
	r2 = 6km	-0.01	-0.32	0.07

Table 28. Correlation Results From Analysis Run 1. Upper Flow Surface Level 5 (Rainfall Station 8).

Wind Speed Thresholds to Determine the Cone Angle	Inner Radius (r2) (Outer Radius (r1) Proportional To Wind Speed)	All 360 Degree Wind Directions	Southeast Winds 90-180 Degrees	Southwest Winds 181-270 Degrees
0-3m/s = 40° 4-7m/s = 30° > 8m/s = 20°	r2 = 2km	0.14	0.14	0.18
	r2 = 3km	0.14	0.14	0.18
	r2 = 4km	0.14	0.14	0.18
	r2 = 5km	0.14	0.14	0.18
	r2 = 6km	0.14	0.14	0.18
0-4m/s = 40° 5-9m/s = 30° > 10m/s = 20°	r2 = 2km	0.15	0.19	0.17
	r2 = 3km	0.15	0.19	0.17
	r2 = 4km	0.15	0.19	0.17
	r2 = 5km	0.15	0.19	0.17
	r2 = 6km	0.15	0.19	0.17
0-5m/s = 40° 6-11m/s = 30° > 12m/s = 20°	r2 = 2km	0.13	0.14	0.17
	r2 = 3km	0.13	0.14	0.17
	r2 = 4km	0.13	0.14	0.17
	r2 = 5km	0.13	0.14	0.17
	r2 = 6km	0.13	0.14	0.17
0-6m/s = 40° 7-13m/s = 30° > 14m/s = 20°	r2 = 2km	0.13	0.14	0.17
	r2 = 3km	0.13	0.14	0.17
	r2 = 4km	0.13	0.14	0.17
	r2 = 5km	0.13	0.14	0.17
	r2 = 6km	0.13	0.14	0.17

Table 29. **Correlation Results From Analysis Run 1. Upper Flow Surface Level 5 (Rainfall Station 9).**

Wind Speed Thresholds to Determine the Cone Angle	Inner Radius (r2) (Outer Radius (r1) Proportional To Wind Speed)	All 360 Degree Wind Directions	Southeast Winds 90-180 Degrees	Southwest Winds 181-270 Degrees
0-3m/s = 40° 4-7m/s = 30° > 8m/s = 20°	r2 = 2km	0.15	0.14	0.32
	r2 = 3km	0.14	0.14	0.30
	r2 = 4km	0.11	0.12	0.27
	r2 = 5km	0.13	0.11	0.28
	r2 = 6km	0.13	0.08	0.30
0-4m/s = 40° 5-9m/s = 30° > 10m/s = 20°	r2 = 2km	0.17	0.17	0.33
	r2 = 3km	0.15	0.15	0.31
	r2 = 4km	0.12	0.14	0.27
	r2 = 5km	0.13	0.13	0.28
	r2 = 6km	0.13	0.10	0.30
0-5m/s = 40° 6-11m/s = 30° > 12m/s = 20°	r2 = 2km	0.16	0.17	0.32
	r2 = 3km	0.14	0.15	0.30
	r2 = 4km	0.13	0.15	0.27
	r2 = 5km	0.14	0.13	0.29
	r2 = 6km	0.14	0.10	0.30
0-6m/s = 40° 7-13m/s = 30° > 14m/s = 20°	r2 = 2km	0.17	0.18	0.32
	r2 = 3km	0.14	0.16	0.30
	r2 = 4km	0.13	0.15	0.27
	r2 = 5km	0.14	0.14	0.29
	r2 = 6km	0.14	0.11	0.30

Table 30. Correlation Results From Analysis Run 1.
Upper Flow Surface Level 5 (Rainfall Station 18).

Wind Speed Thresholds to Determine the Cone Angle	Inner Radius (r2) (Outer Radius (r1) Proportional To Wind Speed)	All 360 Degree Wind Directions	Southeast Winds 90-180 Degrees	Southwest Winds 181-270 Degrees
0-3m/s = 40° 4-7m/s = 30° > 8m/s = 20°	r2 = 2km	0.07	0.24	0.16
	r2 = 3km	0.04	0.21	0.16
	r2 = 4km	-0.01	0.18	0.14
	r2 = 5km	0.01	0.13	0.17
	r2 = 6km	0.04	0.15	0.18
0-4m/s = 40° 5-9m/s = 30° > 10m/s = 20°	r2 = 2km	0.10	0.28	0.22
	r2 = 3km	0.05	0.26	0.19
	r2 = 4km	0.00	0.22	0.16
	r2 = 5km	0.04	0.16	0.21
	r2 = 6km	0.04	0.17	0.17
0-5m/s = 40° 6-11m/s = 30° > 12m/s = 20°	r2 = 2km	0.08	0.22	0.22
	r2 = 3km	0.03	0.20	0.20
	r2 = 4km	-0.02	0.17	0.16
	r2 = 5km	0.03	0.11	0.23
	r2 = 6km	0.03	0.13	0.20
0-6m/s = 40° 7-13m/s = 30° > 14m/s = 20°	r2 = 2km	0.10	0.26	0.22
	r2 = 3km	0.04	0.23	0.20
	r2 = 4km	-0.01	0.20	0.15
	r2 = 5km	0.04	0.14	0.23
	r2 = 6km	0.05	0.17	0.20

Table 31. Correlation Results From Analysis Run 1. Upper Flow Surface Level 4 (Rainfall Station 1).

Wind Speed Thresholds to Determine the Cone Angle	Inner Radius (r2) (Outer Radius (r1) Proportional To Wind Speed)	All 360 Degree Wind Directions	Southeast Winds 90-180 Degrees	Southwest Winds 181-270 Degrees
0-3m/s = 40° 4-7m/s = 30° > 8m/s = 20°	r2 = 2km	0.03	0.03	0.02
	r2 = 3km	-0.06	0.03	-0.06
	r2 = 4km	-0.12	0.03	-0.12
	r2 = 5km	-0.16	0.04	-0.16
	r2 = 6km	-0.10	0.03	-0.09
0-4m/s = 40° 5-9m/s = 30° > 10m/s = 20°	r2 = 2km	0.04	0.03	0.03
	r2 = 3km	-0.05	0.03	-0.05
	r2 = 4km	-0.12	0.03	-0.12
	r2 = 5km	-0.15	0.04	-0.16
	r2 = 6km	-0.11	0.03	-0.11
0-5m/s = 40° 6-11m/s = 30° > 12m/s = 20°	r2 = 2km	0.05	0.03	0.04
	r2 = 3km	-0.05	0.03	-0.05
	r2 = 4km	-0.14	0.03	-0.14
	r2 = 5km	-0.17	0.04	-0.17
	r2 = 6km	-0.10	0.03	-0.10
0-6m/s = 40° 7-13m/s = 30° > 14m/s = 20°	r2 = 2km	0.07	0.03	0.06
	r2 = 3km	0.03	0.03	0.03
	r2 = 4km	-0.12	0.03	-0.12
	r2 = 5km	-0.16	0.04	-0.17
	r2 = 6km	-0.12	0.03	-0.12

Table 32. Correlation Results From Analysis Run 1. Upper Flow Surface Level 4 (Rainfall Station 8).

Wind Speed Thresholds to Determine the Cone Angle	Inner Radius (r2) (Outer Radius (r1) Proportional To Wind Speed)	All 360 Degree Wind Directions	Southeast Winds 90-180 Degrees	Southwest Winds 181-270 Degrees
0-3m/s = 40° 4-7m/s = 30° > 8m/s = 20°	r2 = 2km	0.28	0.41	0.24
	r2 = 3km	0.28	0.41	0.24
	r2 = 4km	0.28	0.41	0.24
	r2 = 5km	0.28	0.41	0.24
	r2 = 6km	0.28	0.41	0.24
0-4m/s = 40° 5-9m/s = 30° > 10m/s = 20°	r2 = 2km	0.28	0.41	0.24
	r2 = 3km	0.28	0.41	0.24
	r2 = 4km	0.28	0.41	0.24
	r2 = 5km	0.28	0.41	0.24
	r2 = 6km	0.28	0.41	0.24
0-5m/s = 40° 6-11m/s = 30° > 12m/s = 20°	r2 = 2km	0.28	0.41	0.24
	r2 = 3km	0.28	0.41	0.24
	r2 = 4km	0.28	0.41	0.24
	r2 = 5km	0.28	0.41	0.24
	r2 = 6km	0.28	0.41	0.24
0-6m/s = 40° 7-13m/s = 30° > 14m/s = 20°	r2 = 2km	0.27	0.41	0.23
	r2 = 3km	0.27	0.41	0.23
	r2 = 4km	0.27	0.41	0.23
	r2 = 5km	0.27	0.41	0.23
	r2 = 6km	0.27	0.41	0.23

Table 33. Correlation Results From Analysis Run 1. Upper Flow Surface Level 4 (Rainfall Station 9).

Wind Speed Thresholds to Determine the Cone Angle	Inner Radius (r2) (Outer Radius (r1) Proportional To Wind Speed)	All 360 Degree Wind Directions	Southeast Winds 90-180 Degrees	Southwest Winds 181-270 Degrees
0-3m/s = 40° 4-7m/s = 30° > 8m/s = 20°	r2 = 2km	0.10	-0.07	0.08
	r2 = 3km	0.09	-0.07	0.07
	r2 = 4km	0.10	-0.08	0.07
	r2 = 5km	0.09	-0.09	0.06
	r2 = 6km	0.04	-0.07	0.02
0-4m/s = 40° 5-9m/s = 30° > 10m/s = 20°	r2 = 2km	0.10	-0.07	0.08
	r2 = 3km	0.09	-0.07	0.07
	r2 = 4km	0.09	-0.08	0.07
	r2 = 5km	0.09	-0.09	0.05
	r2 = 6km	0.05	-0.07	0.02
0-5m/s = 40° 6-11m/s = 30° > 12m/s = 20°	r2 = 2km	0.09	-0.07	0.07
	r2 = 3km	0.08	-0.07	0.06
	r2 = 4km	0.09	-0.08	0.06
	r2 = 5km	0.09	-0.09	0.05
	r2 = 6km	0.05	-0.07	0.02
0-6m/s = 40° 7-13m/s = 30° > 14m/s = 20°	r2 = 2km	0.10	-0.07	0.08
	r2 = 3km	0.09	-0.07	0.07
	r2 = 4km	0.09	-0.08	0.07
	r2 = 5km	0.09	-0.09	0.05
	r2 = 6km	0.05	-0.07	0.02

Table 34. Correlation Results From Analysis Run 1. Upper Flow Surface Level 4 (Rainfall Station 18).

Wind Speed Thresholds to Determine the Cone Angle	Inner Radius (r2) (Outer Radius (r1) Proportional To Wind Speed)	All 360 Degree Wind Directions	Southeast Winds 90-180 Degrees	Southwest Winds 181-270 Degrees
0-3m/s = 40° 4-7m/s = 30° > 8m/s = 20°	r2 = 2km	0.17	0.50	0.07
	r2 = 3km	0.14	0.50	0.04
	r2 = 4km	0.13	0.48	0.03
	r2 = 5km	0.15	0.48	0.05
	r2 = 6km	0.15	0.48	0.05
0-4m/s = 40° 5-9m/s = 30° > 10m/s = 20°	r2 = 2km	0.17	0.50	0.07
	r2 = 3km	0.14	0.50	0.04
	r2 = 4km	0.13	0.48	0.03
	r2 = 5km	0.15	0.48	0.05
	r2 = 6km	0.15	0.48	0.05
0-5m/s = 40° 6-11m/s = 30° > 12m/s = 20°	r2 = 2km	0.17	0.50	0.08
	r2 = 3km	0.14	0.50	0.04
	r2 = 4km	0.13	0.48	0.03
	r2 = 5km	0.15	0.48	0.05
	r2 = 6km	0.15	0.48	0.05
0-6m/s = 40° 7-13m/s = 30° > 14m/s = 20°	r2 = 2km	0.15	0.50	0.05
	r2 = 3km	0.12	0.50	0.02
	r2 = 4km	0.11	0.48	0.01
	r2 = 5km	0.13	0.48	0.03
	r2 = 6km	0.13	0.48	0.04

Table 35. Correlation Results From Analysis Run 1. Upper Flow Surface Level 3 (Rainfall Station 1).

Wind Speed Thresholds to Determine the Cone Angle	Inner Radius (r2) (Outer Radius (r1) Proportional To Wind Speed)	All 360 Degree Wind Directions	Southeast Winds 90-180 Degrees	Southwest Winds 181-270 Degrees
0-3m/s = 40° 4-7m/s = 30° > 8m/s = 20°	r2 = 2km	0.00	0.36	-0.01
	r2 = 3km	-0.05	0.36	-0.06
	r2 = 4km	-0.02	0.35	-0.03
	r2 = 5km	-0.10	0.34	-0.11
	r2 = 6km	-0.12	0.32	-0.13
0-4m/s = 40° 5-9m/s = 30° > 10m/s = 20°	r2 = 2km	-0.02	0.36	-0.03
	r2 = 3km	-0.08	0.36	-0.09
	r2 = 4km	-0.05	0.35	-0.05
	r2 = 5km	-0.14	0.34	-0.15
	r2 = 6km	-0.13	0.32	-0.14
0-5m/s = 40° 6-11m/s = 30° > 12m/s = 20°	r2 = 2km	0.04	0.36	0.03
	r2 = 3km	0.04	0.36	0.03
	r2 = 4km	-0.07	0.35	-0.08
	r2 = 5km	-0.12	0.34	-0.13
	r2 = 6km	-0.14	0.32	-0.15
0-6m/s = 40° 7-13m/s = 30° > 14m/s = 20°	r2 = 2km	0.05	0.36	0.04
	r2 = 3km	0.04	0.36	0.04
	r2 = 4km	-0.06	0.35	-0.06
	r2 = 5km	-0.12	0.34	-0.12
	r2 = 6km	-0.13	0.32	-0.14

Table 36. Correlation Results From Analysis Run 1. Upper Flow Surface Level 3 (Rainfall Station 8).

Wind Speed Thresholds to Determine the Cone Angle	Inner Radius (r2) (Outer Radius (r1) Proportional To Wind Speed)	All 360 Degree Wind Directions	Southeast Winds 90-180 Degrees	Southwest Winds 181-270 Degrees
0-3m/s = 40° 4-7m/s = 30° > 8m/s = 20°	r2 = 2km	0.26	0.11	0.22
	r2 = 3km	0.26	0.11	0.22
	r2 = 4km	0.26	0.11	0.22
	r2 = 5km	0.26	0.11	0.22
	r2 = 6km	0.26	0.11	0.22
0-4m/s = 40° 5-9m/s = 30° > 10m/s = 20°	r2 = 2km	0.26	0.11	0.22
	r2 = 3km	0.26	0.11	0.22
	r2 = 4km	0.26	0.11	0.22
	r2 = 5km	0.26	0.11	0.22
	r2 = 6km	0.26	0.11	0.22
0-5m/s = 40° 6-11m/s = 30° > 12m/s = 20°	r2 = 2km	0.26	0.11	0.22
	r2 = 3km	0.26	0.11	0.22
	r2 = 4km	0.26	0.11	0.22
	r2 = 5km	0.26	0.11	0.22
	r2 = 6km	0.26	0.11	0.22
0-6m/s = 40° 7-13m/s = 30° > 14m/s = 20°	r2 = 2km	0.26	0.11	0.22
	r2 = 3km	0.26	0.11	0.22
	r2 = 4km	0.26	0.11	0.22
	r2 = 5km	0.26	0.11	0.22
	r2 = 6km	0.26	0.11	0.22

Table 37. Correlation Results From Analysis Run 1. Upper Flow Surface Level 3 (Rainfall Station 9).

Wind Speed Thresholds to Determine the Cone Angle	Inner Radius (r2) (Outer Radius (r1) Proportional To Wind Speed)	All 360 Degree Wind Directions	Southeast Winds 90-180 Degrees	Southwest Winds 181-270 Degrees
0-3m/s = 40° 4-7m/s = 30° > 8m/s = 20°	r2 = 2km	0.16	-0.32	0.08
	r2 = 3km	0.16	-0.32	0.07
	r2 = 4km	0.19	-0.25	0.08
	r2 = 5km	0.20	-0.22	0.08
	r2 = 6km	0.17	-0.22	0.05
0-4m/s = 40° 5-9m/s = 30° > 10m/s = 20°	r2 = 2km	0.17	-0.32	0.08
	r2 = 3km	0.16	-0.32	0.08
	r2 = 4km	0.19	-0.25	0.08
	r2 = 5km	0.20	-0.22	0.08
	r2 = 6km	0.17	-0.22	0.05
0-5m/s = 40° 6-11m/s = 30° > 12m/s = 20°	r2 = 2km	0.17	-0.32	0.08
	r2 = 3km	0.16	-0.32	0.08
	r2 = 4km	0.19	-0.25	0.08
	r2 = 5km	0.20	-0.22	0.09
	r2 = 6km	0.17	-0.22	0.05
0-6m/s = 40° 7-13m/s = 30° > 14m/s = 20°	r2 = 2km	0.17	-0.32	0.09
	r2 = 3km	0.17	-0.32	0.08
	r2 = 4km	0.20	-0.25	0.09
	r2 = 5km	0.21	-0.22	0.09
	r2 = 6km	0.18	-0.22	0.06

Table 38. Correlation Results From Analysis Run 1. Upper Flow Surface Level 3 (Rainfall Station 18).

Wind Speed Thresholds to Determine the Cone Angle	Inner Radius (r2) (Outer Radius (r1) Proportional To Wind Speed)	All 360 Degree Wind Directions	Southeast Winds 90-180 Degrees	Southwest Winds 181-270 Degrees
0-3m/s = 40° 4-7m/s = 30° > 8m/s = 20°	r2 = 2km	-0.16	-0.50	-0.16
	r2 = 3km	-0.19	-0.50	-0.17
	r2 = 4km	-0.19	-0.50	-0.17
	r2 = 5km	-0.16	-0.50	-0.16
	r2 = 6km	-0.13	-0.50	-0.15
0-4m/s = 40° 5-9m/s = 30° > 10m/s = 20°	r2 = 2km	-0.16	-0.50	-0.16
	r2 = 3km	-0.18	-0.50	-0.17
	r2 = 4km	-0.19	-0.50	-0.17
	r2 = 5km	-0.16	-0.50	-0.16
	r2 = 6km	-0.13	-0.50	-0.15
0-5m/s = 40° 6-11m/s = 30° > 12m/s = 20°	r2 = 2km	-0.17	-0.50	-0.17
	r2 = 3km	-0.19	-0.50	-0.18
	r2 = 4km	-0.20	-0.50	-0.18
	r2 = 5km	-0.16	-0.50	-0.16
	r2 = 6km	-0.14	-0.50	-0.15
0-6m/s = 40° 7-13m/s = 30° > 14m/s = 20°	r2 = 2km	-0.18	-0.50	-0.17
	r2 = 3km	-0.20	-0.50	-0.18
	r2 = 4km	-0.20	-0.50	-0.18
	r2 = 5km	-0.17	-0.50	-0.17
	r2 = 6km	-0.14	-0.50	-0.16

Table 39. Correlation Results From Analysis Run 1. Upper Flow Surface Level 2 (Rainfall Station 1).

Wind Speed Thresholds to Determine the Cone Angle	Inner Radius (r2) (Outer Radius (r1) Proportional To Wind Speed)	All 360 Degree Wind Directions	Southeast Winds 90-180 Degrees	Southwest Winds 181-270 Degrees
0-3m/s = 40°	r2 = 2km	0.12	0.45	0.06
4-7m/s = 30°	r2 = 3km	0.07	0.45	0.00
> 8m/s = 20°	r2 = 4km	0.00	0.44	-0.05
	r2 = 5km	-0.10	0.47	-0.14
	r2 = 6km	-0.12	0.47	-0.14
0-4m/s = 40°	r2 = 2km	0.12	0.45	0.06
5-9m/s = 30°	r2 = 3km	0.06	0.45	-0.01
> 10m/s = 20°	r2 = 4km	0.00	0.44	-0.06
	r2 = 5km	-0.14	0.47	-0.18
	r2 = 6km	-0.15	0.47	-0.18
0-5m/s = 40°	r2 = 2km	0.09	0.45	0.03
6-11m/s = 30°	r2 = 3km	0.05	0.45	-0.02
> 12m/s = 20°	r2 = 4km	-0.02	0.44	-0.08
	r2 = 5km	-0.14	0.47	-0.19
	r2 = 6km	-0.15	0.47	-0.18
0-6m/s = 40°	r2 = 2km	0.07	0.43	0.00
7-13m/s = 30°	r2 = 3km	0.03	0.42	-0.04
> 14m/s = 20°	r2 = 4km	-0.05	0.42	-0.12
	r2 = 5km	-0.16	0.43	-0.21
	r2 = 6km	-0.16	0.41	-0.20

Table 40. Correlation Results From Analysis Run 1. Upper Flow Surface Level 2 (Rainfall Station 8).

Wind Speed Thresholds to Determine the Cone Angle	Inner Radius (r2) (Outer Radius (r1) Proportional To Wind Speed)	All 360 Degree Wind Directions	Southeast Winds 90-180 Degrees	Southwest Winds 181-270 Degrees
0-3m/s = 40° 4-7m/s = 30° > 8m/s = 20°	r2 = 2km	0.22	0.63	0.11
	r2 = 3km	0.22	0.63	0.11
	r2 = 4km	0.22	0.63	0.11
	r2 = 5km	0.22	0.63	0.11
	r2 = 6km	0.22	0.63	0.11
0-4m/s = 40° 5-9m/s = 30° > 10m/s = 20°	r2 = 2km	0.22	0.63	0.11
	r2 = 3km	0.22	0.63	0.11
	r2 = 4km	0.22	0.63	0.11
	r2 = 5km	0.22	0.63	0.11
	r2 = 6km	0.22	0.63	0.11
0-5m/s = 40° 6-11m/s = 30° > 12m/s = 20°	r2 = 2km	0.21	0.63	0.10
	r2 = 3km	0.21	0.63	0.10
	r2 = 4km	0.21	0.63	0.10
	r2 = 5km	0.21	0.63	0.10
	r2 = 6km	0.21	0.63	0.10
0-6m/s = 40° 7-13m/s = 30° > 14m/s = 20°	r2 = 2km	0.22	0.63	0.11
	r2 = 3km	0.22	0.63	0.11
	r2 = 4km	0.22	0.63	0.11
	r2 = 5km	0.22	0.63	0.11
	r2 = 6km	0.22	0.63	0.11

Table 41. Correlation Results From Analysis Run 1.
Upper Flow Surface Level 2 (Rainfall Station 9).

Wind Speed Thresholds to Determine the Cone Angle	Inner Radius (r2) (Outer Radius (r1) Proportional To Wind Speed)	All 360 Degree Wind Directions	Southeast Winds 90-180 Degrees	Southwest Winds 181-270 Degrees
0-3m/s = 40° 4-7m/s = 30° > 8m/s = 20°	r2 = 2km	0.27	0.40	0.12
	r2 = 3km	0.28	0.41	0.11
	r2 = 4km	0.32	0.42	0.14
	r2 = 5km	0.33	0.41	0.15
	r2 = 6km	0.27	0.41	0.06
0-4m/s = 40° 5-9m/s = 30° > 10m/s = 20°	r2 = 2km	0.26	0.40	0.11
	r2 = 3km	0.27	0.41	0.10
	r2 = 4km	0.32	0.41	0.13
	r2 = 5km	0.32	0.40	0.13
	r2 = 6km	0.26	0.39	0.05
0-5m/s = 40° 6-11m/s = 30° > 12m/s = 20°	r2 = 2km	0.26	0.41	0.10
	r2 = 3km	0.27	0.42	0.09
	r2 = 4km	0.31	0.43	0.12
	r2 = 5km	0.32	0.41	0.12
	r2 = 6km	0.26	0.39	0.04
0-6m/s = 40° 7-13m/s = 30° > 14m/s = 20°	r2 = 2km	0.26	0.41	0.10
	r2 = 3km	0.26	0.42	0.09
	r2 = 4km	0.31	0.43	0.11
	r2 = 5km	0.32	0.41	0.13
	r2 = 6km	0.27	0.39	0.06

Table 42. Correlation Results From Analysis Run 1. Upper Flow Surface Level 2 (Rainfall Station 18).

Wind Speed Thresholds to Determine the Cone Angle	Inner Radius (r2) (Outer Radius (r1) Proportional To Wind Speed)	All 360 Degree Wind Directions	Southeast Winds 90-180 Degrees	Southwest Winds 181-270 Degrees
0-3m/s = 40° 4-7m/s = 30° > 8m/s = 20°	r2 = 2km	-0.23	-0.63	-0.24
	r2 = 3km	-0.26	-0.63	-0.24
	r2 = 4km	-0.26	-0.63	-0.22
	r2 = 5km	-0.22	-0.63	-0.21
	r2 = 6km	-0.19	-0.64	-0.25
0-4m/s = 40° 5-9m/s = 30° > 10m/s = 20°	r2 = 2km	-0.23	-0.63	-0.24
	r2 = 3km	-0.26	-0.63	-0.25
	r2 = 4km	-0.27	-0.63	-0.23
	r2 = 5km	-0.22	-0.63	-0.22
	r2 = 6km	-0.19	-0.64	-0.25
0-5m/s = 40° 6-11m/s = 30° > 12m/s = 20°	r2 = 2km	-0.23	-0.63	-0.25
	r2 = 3km	-0.27	-0.63	-0.25
	r2 = 4km	-0.27	-0.63	-0.24
	r2 = 5km	-0.23	-0.63	-0.23
	r2 = 6km	-0.20	-0.64	-0.25
0-6m/s = 40° 7-13m/s = 30° > 14m/s = 20°	r2 = 2km	-0.25	-0.63	-0.26
	r2 = 3km	-0.29	-0.63	-0.26
	r2 = 4km	-0.29	-0.63	-0.25
	r2 = 5km	-0.24	-0.63	-0.24
	r2 = 6km	-0.21	-0.63	-0.26

Table 43. Correlation Results From Analysis Run 2. Upper Flow Surface Level 6 (Rainfall Station 1).

Wind Speed Thresholds to Determine the Cone Angle	Inner Radius (r2) (Outer Radius (r1) Proportional To Wind Speed)	All 360 Degree Wind Directions	Southeast Winds 90-180 Degrees	Southwest Winds 181-270 Degrees
0-3m/s = 40° 4-7m/s = 30° > 8m/s = 20°	r2 = 2km	0.03	0.00	0.06
	r2 = 3km	0.04	0.00	0.09
	r2 = 4km	0.06	-0.01	0.13
	r2 = 5km	0.06	-0.02	0.17
	r2 = 6km	-0.01	0.00	0.11
0-4m/s = 40° 5-9m/s = 30° > 10m/s = 20°	r2 = 2km	0.03	0.01	0.06
	r2 = 3km	0.05	0.00	0.09
	r2 = 4km	0.09	-0.01	0.17
	r2 = 5km	0.08	-0.01	0.20
	r2 = 6km	0.00	0.01	0.14
0-5m/s = 40° 6-11m/s = 30° > 12m/s = 20°	r2 = 2km	0.02	-0.03	0.06
	r2 = 3km	0.04	-0.03	0.09
	r2 = 4km	0.07	-0.04	0.15
	r2 = 5km	0.05	-0.05	0.18
	r2 = 6km	-0.01	-0.04	0.13
0-6m/s = 40° 7-13m/s = 30° > 14m/s = 20°	r2 = 2km	0.01	-0.05	0.05
	r2 = 3km	0.03	-0.05	0.09
	r2 = 4km	0.06	-0.06	0.15
	r2 = 5km	0.04	-0.08	0.16
	r2 = 6km	-0.02	-0.06	0.12

Table 44. Correlation Results From Analysis Run 2. Upper Flow Surface Level 6 (Rainfall Station 8).

Wind Speed Thresholds to Determine the Cone Angle	Inner Radius (r2) (Outer Radius (r1) Proportional To Wind Speed)	All 360 Degree Wind Directions	Southeast Winds 90-180 Degrees	Southwest Winds 181-270 Degrees
0-3m/s = 40° 4-7m/s = 30° > 8m/s = 20°	r2 = 2km	0.17	0.16	0.21
	r2 = 3km	0.17	0.16	0.21
	r2 = 4km	0.17	0.16	0.21
	r2 = 5km	0.17	0.16	0.21
	r2 = 6km	0.17	0.16	0.21
0-4m/s = 40° 5-9m/s = 30° > 10m/s = 20°	r2 = 2km	0.19	0.18	0.26
	r2 = 3km	0.19	0.18	0.26
	r2 = 4km	0.19	0.18	0.26
	r2 = 5km	0.19	0.18	0.26
	r2 = 6km	0.19	0.18	0.26
0-5m/s = 40° 6-11m/s = 30° > 12m/s = 20°	r2 = 2km	0.17	0.15	0.26
	r2 = 3km	0.17	0.15	0.26
	r2 = 4km	0.17	0.15	0.26
	r2 = 5km	0.17	0.15	0.26
	r2 = 6km	0.17	0.15	0.26
0-6m/s = 40° 7-13m/s = 30° > 14m/s = 20°	r2 = 2km	0.15	0.12	0.24
	r2 = 3km	0.15	0.12	0.24
	r2 = 4km	0.15	0.12	0.24
	r2 = 5km	0.15	0.12	0.24
	r2 = 6km	0.15	0.12	0.24

Table 45. Correlation Results From Analysis Run 2. Upper Flow Surface Level 6 (Rainfall Station 9).

Wind Speed Thresholds to Determine the Cone Angle	Inner Radius (r2) (Outer Radius (r1) Proportional To Wind Speed)	All 360 Degree Wind Directions	Southeast Winds 90-180 Degrees	Southwest Winds 181-270 Degrees
0-3m/s = 40° 4-7m/s = 30° > 8m/s = 20°	r2 = 2km	0.19	0.14	0.33
	r2 = 3km	0.20	0.17	0.32
	r2 = 4km	0.23	0.18	0.34
	r2 = 5km	0.28	0.23	0.36
	r2 = 6km	0.25	0.20	0.35
0-4m/s = 40° 5-9m/s = 30° > 10m/s = 20°	r2 = 2km	0.19	0.13	0.33
	r2 = 3km	0.20	0.18	0.32
	r2 = 4km	0.22	0.18	0.33
	r2 = 5km	0.28	0.23	0.36
	r2 = 6km	0.25	0.20	0.36
0-5m/s = 40° 6-11m/s = 30° > 12m/s = 20°	r2 = 2km	0.19	0.13	0.33
	r2 = 3km	0.20	0.18	0.32
	r2 = 4km	0.22	0.18	0.33
	r2 = 5km	0.28	0.22	0.36
	r2 = 6km	0.25	0.19	0.36
0-6m/s = 40° 7-13m/s = 30° > 14m/s = 20°	r2 = 2km	0.20	0.15	0.34
	r2 = 3km	0.20	0.18	0.33
	r2 = 4km	0.23	0.18	0.34
	r2 = 5km	0.28	0.22	0.37
	r2 = 6km	0.26	0.19	0.37

Table 46. Correlation Results From Analysis Run 2. Upper Flow Surface Level 6 (Rainfall Station 18).

Wind Speed Thresholds to Determine the Cone Angle	Inner Radius (r2) (Outer Radius (r1) Proportional To Wind Speed)	All 360 Degree Wind Directions	Southeast Winds 90-180 Degrees	Southwest Winds 181-270 Degrees
0-3m/s = 40° 4-7m/s = 30° > 8m/s = 20°	r2 = 2km	-0.06	0.10	0.05
	r2 = 3km	-0.10	0.08	0.04
	r2 = 4km	-0.13	0.08	0.03
	r2 = 5km	-0.13	0.08	-0.01
	r2 = 6km	-0.11	0.05	-0.03
0-4m/s = 40° 5-9m/s = 30° > 10m/s = 20°	r2 = 2km	-0.07	0.10	0.06
	r2 = 3km	-0.10	0.09	0.05
	r2 = 4km	-0.13	0.07	0.04
	r2 = 5km	-0.13	0.07	-0.01
	r2 = 6km	-0.12	0.05	-0.04
0-5m/s = 40° 6-11m/s = 30° > 12m/s = 20°	r2 = 2km	-0.06	0.10	0.08
	r2 = 3km	-0.09	0.09	0.08
	r2 = 4km	-0.12	0.07	0.07
	r2 = 5km	-0.13	0.07	0.01
	r2 = 6km	-0.12	0.04	-0.02
0-6m/s = 40° 7-13m/s = 30° > 14m/s = 20°	r2 = 2km	-0.05	0.11	0.09
	r2 = 3km	-0.09	0.09	0.07
	r2 = 4km	-0.12	0.08	0.07
	r2 = 5km	-0.13	0.07	0.03
	r2 = 6km	-0.11	0.07	-0.01

Table 47. Correlation Results From Analysis Run 2. Upper Flow Surface Level 5 (Rainfall Station 1).

Wind Speed Thresholds to Determine the Cone Angle	Inner Radius (r2) (Outer Radius (r1) Proportional To Wind Speed)	All 360 Degree Wind Directions	Southeast Winds 90-180 Degrees	Southwest Winds 181-270 Degrees
0-3m/s = 40° 4-7m/s = 30° > 8m/s = 20°	r2 = 2km	-0.03	0.11	-0.34
	r2 = 3km	-0.02	0.11	-0.33
	r2 = 4km	-0.02	0.11	-0.29
	r2 = 5km	-0.03	0.10	-0.31
	r2 = 6km	0.00	0.09	-0.23
0-4m/s = 40° 5-9m/s = 30° > 10m/s = 20°	r2 = 2km	0.02	0.17	-0.31
	r2 = 3km	0.03	0.17	-0.29
	r2 = 4km	0.01	0.16	-0.28
	r2 = 5km	0.03	0.17	-0.29
	r2 = 6km	0.04	0.15	-0.25
0-5m/s = 40° 6-11m/s = 30° > 12m/s = 20°	r2 = 2km	0.02	0.18	-0.31
	r2 = 3km	0.02	0.17	-0.30
	r2 = 4km	0.02	0.16	-0.28
	r2 = 5km	0.04	0.18	-0.30
	r2 = 6km	0.04	0.15	-0.26
0-6m/s = 40° 7-13m/s = 30° > 14m/s = 20°	r2 = 2km	0.00	0.15	-0.31
	r2 = 3km	0.00	0.14	-0.30
	r2 = 4km	0.00	0.14	-0.29
	r2 = 5km	0.01	0.13	-0.30
	r2 = 6km	0.02	0.13	-0.27

Table 48. Correlation Results From Analysis Run 2. Upper Flow Surface Level 5 (Rainfall Station 8).

Wind Speed Thresholds to Determine the Cone Angle	Inner Radius (r2) (Outer Radius (r1) Proportional To Wind Speed)	All 360 Degree Wind Directions	Southeast Winds 90-180 Degrees	Southwest Winds 181-270 Degrees
0-3m/s = 40° 4-7m/s = 30° > 8m/s = 20°	r2 = 2km	0.16	0.12	0.25
	r2 = 3km	0.16	0.12	0.25
	r2 = 4km	0.16	0.12	0.25
	r2 = 5km	0.16	0.12	0.25
	r2 = 6km	0.16	0.12	0.25
0-4m/s = 40° 5-9m/s = 30° > 10m/s = 20°	r2 = 2km	0.17	0.13	0.28
	r2 = 3km	0.17	0.13	0.28
	r2 = 4km	0.17	0.13	0.28
	r2 = 5km	0.17	0.13	0.28
	r2 = 6km	0.17	0.13	0.28
0-5m/s = 40° 6-11m/s = 30° > 12m/s = 20°	r2 = 2km	0.16	0.09	0.34
	r2 = 3km	0.16	0.09	0.34
	r2 = 4km	0.16	0.09	0.34
	r2 = 5km	0.16	0.09	0.34
	r2 = 6km	0.16	0.09	0.34
0-6m/s = 40° 7-13m/s = 30° > 14m/s = 20°	r2 = 2km	0.16	0.09	0.34
	r2 = 3km	0.16	0.09	0.34
	r2 = 4km	0.16	0.09	0.34
	r2 = 5km	0.16	0.09	0.34
	r2 = 6km	0.16	0.09	0.34

Table 49. Correlation Results From Analysis Run 2. Upper Flow Surface Level 5 (Rainfall Station 9).

Wind Speed Thresholds to Determine the Cone Angle	Inner Radius (r2) (Outer Radius (r1) Proportional To Wind Speed)	All 360 Degree Wind Directions	Southeast Winds 90-180 Degrees	Southwest Winds 181-270 Degrees
0-3m/s = 40° 4-7m/s = 30° > 8m/s = 20°	r2 = 2km	0.14	0.16	0.26
	r2 = 3km	0.12	0.14	0.25
	r2 = 4km	0.11	0.15	0.23
	r2 = 5km	0.14	0.18	0.25
	r2 = 6km	0.13	0.12	0.29
0-4m/s = 40° 5-9m/s = 30° > 10m/s = 20°	r2 = 2km	0.13	0.15	0.26
	r2 = 3km	0.12	0.14	0.25
	r2 = 4km	0.10	0.14	0.23
	r2 = 5km	0.13	0.17	0.25
	r2 = 6km	0.12	0.10	0.28
0-5m/s = 40° 6-11m/s = 30° > 12m/s = 20°	r2 = 2km	0.13	0.15	0.26
	r2 = 3km	0.12	0.15	0.26
	r2 = 4km	0.11	0.14	0.24
	r2 = 5km	0.14	0.17	0.26
	r2 = 6km	0.12	0.09	0.29
0-6m/s = 40° 7-13m/s = 30° > 14m/s = 20°	r2 = 2km	0.14	0.18	0.26
	r2 = 3km	0.13	0.17	0.26
	r2 = 4km	0.12	0.17	0.24
	r2 = 5km	0.15	0.19	0.26
	r2 = 6km	0.13	0.11	0.29

Table 50. Correlation Results From Analysis Run 2. Upper Flow Surface Level 5 (Rainfall Station 18).

Wind Speed Thresholds to Determine the Cone Angle	Inner Radius (r2) (Outer Radius (r1) Proportional To Wind Speed)	All 360 Degree Wind Directions	Southeast Winds 90-180 Degrees	Southwest Winds 181-270 Degrees
0-3m/s = 40° 4-7m/s = 30° > 8m/s = 20°	r2 = 2km	0.04	0.18	0.16
	r2 = 3km	-0.01	0.17	0.13
	r2 = 4km	-0.07	0.15	0.09
	r2 = 5km	-0.03	0.12	0.15
	r2 = 6km	-0.02	0.13	0.11
0-4m/s = 40° 5-9m/s = 30° > 10m/s = 20°	r2 = 2km	0.07	0.21	0.20
	r2 = 3km	0.02	0.20	0.19
	r2 = 4km	-0.05	0.17	0.14
	r2 = 5km	0.00	0.14	0.23
	r2 = 6km	0.02	0.14	0.22
0-5m/s = 40° 6-11m/s = 30° > 12m/s = 20°	r2 = 2km	0.05	0.17	0.20
	r2 = 3km	0.00	0.16	0.19
	r2 = 4km	-0.07	0.14	0.14
	r2 = 5km	0.00	0.10	0.25
	r2 = 6km	0.01	0.12	0.24
0-6m/s = 40° 7-13m/s = 30° > 14m/s = 20°	r2 = 2km	0.06	0.20	0.20
	r2 = 3km	0.00	0.19	0.19
	r2 = 4km	-0.06	0.17	0.14
	r2 = 5km	0.01	0.13	0.25
	r2 = 6km	0.03	0.14	0.23

Table 51. Correlation Results From Analysis Run 2.
Upper Flow Surface Level 4 (Rainfall Station 1).

Wind Speed Thresholds to Determine the Cone Angle	Inner Radius (r2) (Outer Radius (r1) Proportional To Wind Speed)	All 360 Degree Wind Directions	Southeast Winds 90-180 Degrees	Southwest Winds 181-270 Degrees
0-3m/s = 40° 4-7m/s = 30° > 8m/s = 20°	r2 = 2km	0.03	-0.33	0.04
	r2 = 3km	-0.04	-0.37	-0.03
	r2 = 4km	-0.06	-0.31	-0.04
	r2 = 5km	-0.13	-0.38	-0.14
	r2 = 6km	-0.07	-0.36	-0.05
0-4m/s = 40° 5-9m/s = 30° > 10m/s = 20°	r2 = 2km	0.03	-0.33	0.04
	r2 = 3km	-0.05	-0.37	-0.03
	r2 = 4km	-0.07	-0.31	-0.06
	r2 = 5km	-0.13	-0.38	-0.13
	r2 = 6km	-0.08	-0.36	-0.07
0-5m/s = 40° 6-11m/s = 30° > 12m/s = 20°	r2 = 2km	0.00	-0.33	0.01
	r2 = 3km	-0.07	-0.37	-0.06
	r2 = 4km	-0.07	-0.31	-0.05
	r2 = 5km	-0.15	-0.38	-0.16
	r2 = 6km	-0.10	-0.36	-0.09
0-6m/s = 40° 7-13m/s = 30° > 14m/s = 20°	r2 = 2km	0.07	-0.33	0.08
	r2 = 3km	0.03	-0.37	0.04
	r2 = 4km	-0.09	-0.31	-0.07
	r2 = 5km	-0.14	-0.38	-0.14
	r2 = 6km	-0.12	-0.36	-0.12

Table 52. Correlation Results From Analysis Run 2.
Upper Flow Surface Level 4 (Rainfall Station 8).

Wind Speed Thresholds to Determine the Cone Angle	Inner Radius (r2) (Outer Radius (r1) Proportional To Wind Speed)	All 360 Degree Wind Directions	Southeast Winds 90-180 Degrees	Southwest Winds 181-270 Degrees
0-3m/s = 40° 4-7m/s = 30° > 8m/s = 20°	r2 = 2km	0.28	0.46	0.24
	r2 = 3km	0.28	0.46	0.24
	r2 = 4km	0.28	0.46	0.24
	r2 = 5km	0.28	0.46	0.24
	r2 = 6km	0.28	0.46	0.24
0-4m/s = 40° 5-9m/s = 30° > 10m/s = 20°	r2 = 2km	0.28	0.46	0.24
	r2 = 3km	0.28	0.46	0.24
	r2 = 4km	0.28	0.46	0.24
	r2 = 5km	0.28	0.46	0.24
	r2 = 6km	0.28	0.46	0.24
0-5m/s = 40° 6-11m/s = 30° > 12m/s = 20°	r2 = 2km	0.28	0.46	0.24
	r2 = 3km	0.28	0.46	0.24
	r2 = 4km	0.28	0.46	0.24
	r2 = 5km	0.28	0.46	0.24
	r2 = 6km	0.28	0.46	0.24
0-6m/s = 40° 7-13m/s = 30° > 14m/s = 20°	r2 = 2km	0.28	0.46	0.24
	r2 = 3km	0.28	0.46	0.24
	r2 = 4km	0.28	0.46	0.24
	r2 = 5km	0.28	0.46	0.24
	r2 = 6km	0.28	0.46	0.24

Table 53. Correlation Results From Analysis Run 2. Upper Flow Surface Level 4 (Rainfall Station 9).

Wind Speed Thresholds to Determine the Cone Angle	Inner Radius (r2) (Outer Radius (r1) Proportional To Wind Speed)	All 360 Degree Wind Directions	Southeast Winds 90-180 Degrees	Southwest Winds 181-270 Degrees
0-3m/s = 40° 4-7m/s = 30° > 8m/s = 20°	r2 = 2km	0.11	-0.22	0.11
	r2 = 3km	0.10	-0.25	0.09
	r2 = 4km	0.11	-0.27	0.10
	r2 = 5km	0.11	-0.27	0.08
	r2 = 6km	0.05	-0.30	0.04
0-4m/s = 40° 5-9m/s = 30° > 10m/s = 20°	r2 = 2km	0.11	-0.22	0.11
	r2 = 3km	0.10	-0.25	0.09
	r2 = 4km	0.11	-0.27	0.10
	r2 = 5km	0.10	-0.27	0.08
	r2 = 6km	0.06	-0.30	0.05
0-5m/s = 40° 6-11m/s = 30° > 12m/s = 20°	r2 = 2km	0.11	-0.22	0.10
	r2 = 3km	0.09	-0.25	0.09
	r2 = 4km	0.10	-0.27	0.09
	r2 = 5km	0.10	-0.27	0.08
	r2 = 6km	0.05	-0.30	0.04
0-6m/s = 40° 7-13m/s = 30° > 14m/s = 20°	r2 = 2km	0.12	-0.22	0.11
	r2 = 3km	0.10	-0.25	0.10
	r2 = 4km	0.11	-0.27	0.10
	r2 = 5km	0.10	-0.27	0.08
	r2 = 6km	0.06	-0.30	0.05

Table 54. Correlation Results From Analysis Run 2. Upper Flow Surface Level 4 (Rainfall Station 18).

Wind Speed Thresholds to Determine the Cone Angle	Inner Radius (r2) (Outer Radius (r1) Proportional To Wind Speed)	All 360 Degree Wind Directions	Southeast Winds 90-180 Degrees	Southwest Winds 181-270 Degrees
0-3m/s = 40° 4-7m/s = 30° > 8m/s = 20°	r2 = 2km	0.17	0.48	0.07
	r2 = 3km	0.14	0.50	0.04
	r2 = 4km	0.13	0.48	0.03
	r2 = 5km	0.15	0.49	0.05
	r2 = 6km	0.15	0.48	0.05
0-4m/s = 40° 5-9m/s = 30° > 10m/s = 20°	r2 = 2km	0.17	0.48	0.07
	r2 = 3km	0.14	0.50	0.04
	r2 = 4km	0.13	0.48	0.03
	r2 = 5km	0.15	0.49	0.05
	r2 = 6km	0.15	0.48	0.05
0-5m/s = 40° 6-11m/s = 30° > 12m/s = 20°	r2 = 2km	0.17	0.48	0.08
	r2 = 3km	0.14	0.50	0.04
	r2 = 4km	0.13	0.48	0.04
	r2 = 5km	0.15	0.49	0.05
	r2 = 6km	0.15	0.48	0.05
0-6m/s = 40° 7-13m/s = 30° > 14m/s = 20°	r2 = 2km	0.15	0.48	0.05
	r2 = 3km	0.13	0.50	0.02
	r2 = 4km	0.12	0.48	0.01
	r2 = 5km	0.13	0.49	0.04
	r2 = 6km	0.14	0.48	0.04

Table 55. Correlation Results From Analysis Run 2.
Upper Flow Surface Level 3 (Rainfall Station 1).

Wind Speed Thresholds to Determine the Cone Angle	Inner Radius (r2) (Outer Radius (r1) Proportional To Wind Speed)	All 360 Degree Wind Directions	Southeast Winds 90-180 Degrees	Southwest Winds 181-270 Degrees
0-3m/s = 40° 4-7m/s = 30° > 8m/s = 20°	r2 = 2km	0.16	0.37	0.14
	r2 = 3km	0.12	0.32	0.10
	r2 = 4km	0.04	0.30	0.02
	r2 = 5km	-0.02	0.27	-0.02
	r2 = 6km	-0.08	0.17	-0.07
0-4m/s = 40° 5-9m/s = 30° > 10m/s = 20°	r2 = 2km	0.16	0.37	0.13
	r2 = 3km	0.13	0.32	0.11
	r2 = 4km	0.05	0.30	0.03
	r2 = 5km	-0.01	0.27	0.00
	r2 = 6km	-0.08	0.17	-0.08
0-5m/s = 40° 6-11m/s = 30° > 12m/s = 20°	r2 = 2km	0.16	0.37	0.13
	r2 = 3km	0.12	0.32	0.10
	r2 = 4km	0.08	0.30	0.06
	r2 = 5km	0.00	0.27	0.01
	r2 = 6km	-0.08	0.17	-0.07
0-6m/s = 40° 7-13m/s = 30° > 14m/s = 20°	r2 = 2km	0.17	0.37	0.14
	r2 = 3km	0.14	0.32	0.12
	r2 = 4km	0.11	0.30	0.10
	r2 = 5km	0.02	0.27	0.03
	r2 = 6km	-0.06	0.17	-0.05

Table 56. Correlation Results From Analysis Run 2. Upper Flow Surface Level 3 (Rainfall Station 8).

Wind Speed Thresholds to Determine the Cone Angle	Inner Radius (r2) (Outer Radius (r1) Proportional To Wind Speed)	All 360 Degree Wind Directions	Southeast Winds 90-180 Degrees	Southwest Winds 181-270 Degrees
0-3m/s = 40° 4-7m/s = 30° > 8m/s = 20°	r2 = 2km	0.26	0.05	0.22
	r2 = 3km	0.26	0.05	0.22
	r2 = 4km	0.26	0.05	0.22
	r2 = 5km	0.26	0.05	0.22
	r2 = 6km	0.26	0.05	0.22
0-4m/s = 40° 5-9m/s = 30° > 10m/s = 20°	r2 = 2km	0.26	0.05	0.22
	r2 = 3km	0.26	0.05	0.22
	r2 = 4km	0.26	0.05	0.22
	r2 = 5km	0.26	0.05	0.22
	r2 = 6km	0.26	0.05	0.22
0-5m/s = 40° 6-11m/s = 30° > 12m/s = 20°	r2 = 2km	0.26	0.05	0.22
	r2 = 3km	0.26	0.05	0.22
	r2 = 4km	0.26	0.05	0.22
	r2 = 5km	0.26	0.05	0.22
	r2 = 6km	0.26	0.05	0.22
0-6m/s = 40° 7-13m/s = 30° > 14m/s = 20°	r2 = 2km	0.27	0.05	0.23
	r2 = 3km	0.27	0.05	0.23
	r2 = 4km	0.27	0.05	0.23
	r2 = 5km	0.27	0.05	0.23
	r2 = 6km	0.27	0.05	0.23

Table 57. Correlation Results From Analysis Run 2. Upper Flow Surface Level 3 (Rainfall Station 9).

Wind Speed Thresholds to Determine the Cone Angle	Inner Radius (r2) (Outer Radius (r1) Proportional To Wind Speed)	All 360 Degree Wind Directions	Southeast Winds 90-180 Degrees	Southwest Winds 181-270 Degrees
0-3m/s = 40° 4-7m/s = 30° > 8m/s = 20°	r2 = 2km	0.18	-0.32	0.11
	r2 = 3km	0.17	-0.31	0.10
	r2 = 4km	0.19	-0.25	0.10
	r2 = 5km	0.21	-0.23	0.10
	r2 = 6km	0.17	-0.22	0.07
0-4m/s = 40° 5-9m/s = 30° > 10m/s = 20°	r2 = 2km	0.18	-0.32	0.11
	r2 = 3km	0.17	-0.31	0.10
	r2 = 4km	0.20	-0.25	0.11
	r2 = 5km	0.21	-0.23	0.11
	r2 = 6km	0.18	-0.22	0.08
0-5m/s = 40° 6-11m/s = 30° > 12m/s = 20°	r2 = 2km	0.18	-0.32	0.11
	r2 = 3km	0.17	-0.31	0.10
	r2 = 4km	0.20	-0.25	0.11
	r2 = 5km	0.21	-0.23	0.11
	r2 = 6km	0.18	-0.22	0.08
0-6m/s = 40° 7-13m/s = 30° > 14m/s = 20°	r2 = 2km	0.17	-0.32	0.10
	r2 = 3km	0.17	-0.31	0.09
	r2 = 4km	0.20	-0.25	0.10
	r2 = 5km	0.21	-0.23	0.10
	r2 = 6km	0.18	-0.22	0.08

Table 58. Correlation Results From Analysis Run 2. Upper Flow Surface Level 3 (Rainfall Station 18).

Wind Speed Thresholds to Determine the Cone Angle	Inner Radius (r2) (Outer Radius (r1) Proportional To Wind Speed)	All 360 Degree Wind Directions	Southeast Winds 90-180 Degrees	Southwest Winds 181-270 Degrees
0-3m/s = 40° 4-7m/s = 30° > 8m/s = 20°	r2 = 2km	-0.17	-0.54	-0.18
	r2 = 3km	-0.19	-0.55	-0.19
	r2 = 4km	-0.19	-0.54	-0.18
	r2 = 5km	-0.16	-0.54	-0.17
	r2 = 6km	-0.13	-0.54	-0.16
0-4m/s = 40° 5-9m/s = 30° > 10m/s = 20°	r2 = 2km	-0.17	-0.54	-0.18
	r2 = 3km	-0.19	-0.55	-0.19
	r2 = 4km	-0.19	-0.54	-0.18
	r2 = 5km	-0.16	-0.54	-0.17
	r2 = 6km	-0.13	-0.54	-0.16
0-5m/s = 40° 6-11m/s = 30° > 12m/s = 20°	r2 = 2km	-0.17	-0.54	-0.18
	r2 = 3km	-0.19	-0.55	-0.19
	r2 = 4km	-0.19	-0.54	-0.19
	r2 = 5km	-0.16	-0.54	-0.17
	r2 = 6km	-0.14	-0.54	-0.16
0-6m/s = 40° 7-13m/s = 30° > 14m/s = 20°	r2 = 2km	-0.18	-0.54	-0.20
	r2 = 3km	-0.20	-0.55	-0.20
	r2 = 4km	-0.20	-0.54	-0.20
	r2 = 5km	-0.17	-0.54	-0.18
	r2 = 6km	-0.15	-0.54	-0.17

Table 59. Correlation Results From Analysis Run 2. Upper Flow Surface Level 2 (Rainfall Station 1).

Wind Speed Thresholds to Determine the Cone Angle	Inner Radius (r2) (Outer Radius (r1) Proportional To Wind Speed)	All 360 Degree Wind Directions	Southeast Winds 90-180 Degrees	Southwest Winds 181-270 Degrees
0-3m/s = 40° 4-7m/s = 30° > 8m/s = 20°	r2 = 2km	0.19	0.33	0.14
	r2 = 3km	0.20	0.32	0.17
	r2 = 4km	0.24	0.30	0.25
	r2 = 5km	0.19	0.28	0.23
	r2 = 6km	0.12	0.23	0.18
0-4m/s = 40° 5-9m/s = 30° > 10m/s = 20°	r2 = 2km	0.18	0.34	0.13
	r2 = 3km	0.20	0.33	0.16
	r2 = 4km	0.23	0.31	0.24
	r2 = 5km	0.20	0.30	0.24
	r2 = 6km	0.12	0.23	0.18
0-5m/s = 40° 6-11m/s = 30° > 12m/s = 20°	r2 = 2km	0.18	0.35	0.13
	r2 = 3km	0.20	0.34	0.17
	r2 = 4km	0.23	0.33	0.22
	r2 = 5km	0.20	0.33	0.21
	r2 = 6km	0.16	0.28	0.23
0-6m/s = 40° 7-13m/s = 30° > 14m/s = 20°	r2 = 2km	0.16	0.27	0.13
	r2 = 3km	0.19	0.26	0.17
	r2 = 4km	0.21	0.25	0.22
	r2 = 5km	0.19	0.26	0.22
	r2 = 6km	0.14	0.21	0.22

Table 60. Correlation Results From Analysis Run 2. Upper Flow Surface Level 2 (Rainfall Station 8).

Wind Speed Thresholds to Determine the Cone Angle	Inner Radius (r2) (Outer Radius (r1) Proportional To Wind Speed)	All 360 Degree Wind Directions	Southeast Winds 90-180 Degrees	Southwest Winds 181-270 Degrees
0-3m/s = 40° 4-7m/s = 30° > 8m/s = 20°	r2 = 2km	0.19	0.38	0.16
	r2 = 3km	0.19	0.38	0.16
	r2 = 4km	0.19	0.38	0.16
	r2 = 5km	0.19	0.38	0.16
	r2 = 6km	0.19	0.38	0.16
0-4m/s = 40° 5-9m/s = 30° > 10m/s = 20°	r2 = 2km	0.18	0.38	0.15
	r2 = 3km	0.18	0.38	0.15
	r2 = 4km	0.18	0.38	0.15
	r2 = 5km	0.18	0.38	0.15
	r2 = 6km	0.18	0.38	0.15
0-5m/s = 40° 6-11m/s = 30° > 12m/s = 20°	r2 = 2km	0.18	0.38	0.14
	r2 = 3km	0.18	0.38	0.14
	r2 = 4km	0.18	0.38	0.14
	r2 = 5km	0.18	0.38	0.14
	r2 = 6km	0.18	0.38	0.14
0-6m/s = 40° 7-13m/s = 30° > 14m/s = 20°	r2 = 2km	0.17	0.38	0.14
	r2 = 3km	0.17	0.38	0.14
	r2 = 4km	0.17	0.38	0.14
	r2 = 5km	0.17	0.38	0.14
	r2 = 6km	0.17	0.38	0.14

Table 61. Correlation Results From Analysis Run 2. Upper Flow Surface Level 2 (Rainfall Station 9).

Wind Speed Thresholds to Determine the Cone Angle	Inner Radius (r2) (Outer Radius (r1) Proportional To Wind Speed)	All 360 Degree Wind Directions	Southeast Winds 90-180 Degrees	Southwest Winds 181-270 Degrees
0-3m/s = 40° 4-7m/s = 30° > 8m/s = 20°	r2 = 2km	0.17	-0.08	0.22
	r2 = 3km	0.18	-0.02	0.21
	r2 = 4km	0.20	0.08	0.19
	r2 = 5km	0.23	0.10	0.19
	r2 = 6km	0.21	0.14	0.17
0-4m/s = 40° 5-9m/s = 30° > 10m/s = 20°	r2 = 2km	0.16	-0.04	0.21
	r2 = 3km	0.18	0.04	0.20
	r2 = 4km	0.22	0.12	0.20
	r2 = 5km	0.25	0.15	0.20
	r2 = 6km	0.23	0.17	0.19
0-5m/s = 40° 6-11m/s = 30° > 12m/s = 20°	r2 = 2km	0.16	-0.03	0.22
	r2 = 3km	0.17	0.02	0.20
	r2 = 4km	0.22	0.12	0.20
	r2 = 5km	0.24	0.12	0.20
	r2 = 6km	0.23	0.17	0.19
0-6m/s = 40° 7-13m/s = 30° > 14m/s = 20°	r2 = 2km	0.16	0.02	0.20
	r2 = 3km	0.16	0.07	0.19
	r2 = 4km	0.21	0.12	0.19
	r2 = 5km	0.25	0.15	0.21
	r2 = 6km	0.23	0.17	0.19

Table 62. Correlation Results From Analysis Run 2. Upper Flow Surface Level 2 (Rainfall Station 18).

Wind Speed Thresholds to Determine the Cone Angle	Inner Radius (r2) (Outer Radius (r1) Proportional To Wind Speed)	All 360 Degree Wind Directions	Southeast Winds 90-180 Degrees	Southwest Winds 181-270 Degrees
0-3m/s = 40° 4-7m/s = 30° > 8m/s = 20°	r2 = 2km	-0.38	-0.48	-0.42
	r2 = 3km	-0.44	-0.49	-0.47
	r2 = 4km	-0.44	-0.48	-0.47
	r2 = 5km	-0.39	-0.48	-0.42
	r2 = 6km	-0.37	-0.47	-0.43
0-4m/s = 40° 5-9m/s = 30° > 10m/s = 20°	r2 = 2km	-0.37	-0.48	-0.41
	r2 = 3km	-0.43	-0.49	-0.46
	r2 = 4km	-0.43	-0.48	-0.46
	r2 = 5km	-0.38	-0.48	-0.41
	r2 = 6km	-0.36	-0.47	-0.42
0-5m/s = 40° 6-11m/s = 30° > 12m/s = 20°	r2 = 2km	-0.37	-0.48	-0.42
	r2 = 3km	-0.43	-0.49	-0.46
	r2 = 4km	-0.44	-0.48	-0.46
	r2 = 5km	-0.39	-0.48	-0.42
	r2 = 6km	-0.37	-0.47	-0.42
0-6m/s = 40° 7-13m/s = 30° > 14m/s = 20°	r2 = 2km	-0.39	-0.48	-0.44
	r2 = 3km	-0.45	-0.49	-0.48
	r2 = 4km	-0.46	-0.49	-0.48
	r2 = 5km	-0.41	-0.49	-0.44
	r2 = 6km	-0.39	-0.47	-0.45

Table 63. Correlation Results From Analysis Run 4 (Neutral Conditions). Upper Flow Surface Level 6 (Rainfall Station 1).

Wind Speed Thresholds to Determine the Cone Angle	Inner Radius (r2) (Outer Radius (r1) Proportional To Wind Speed)	All 360 Degree Wind Directions	Southeast Winds 90-180 Degrees	Southwest Winds 181-270 Degrees
0-3m/s = 40° 4-7m/s = 30° > 8m/s = 20°	r2 = 2km	-0.06	0.00	-0.09
	r2 = 3km	-0.11	0.00	-0.13
	r2 = 4km	-0.15	0.00	-0.17
	r2 = 5km	-0.20	0.00	-0.20
	r2 = 6km	-0.18	0.00	-0.19
0-4m/s = 40° 5-9m/s = 30° > 10m/s = 20°	r2 = 2km	-0.06	0.00	-0.08
	r2 = 3km	-0.10	0.00	-0.13
	r2 = 4km	-0.15	0.00	-0.17
	r2 = 5km	-0.20	0.00	-0.20
	r2 = 6km	-0.20	0.00	-0.20
0-5m/s = 40° 6-11m/s = 30° > 12m/s = 20°	r2 = 2km	-0.04	0.00	-0.06
	r2 = 3km	-0.09	0.00	-0.12
	r2 = 4km	-0.15	0.00	-0.16
	r2 = 5km	-0.19	0.00	-0.19
	r2 = 6km	-0.17	0.00	-0.17
0-6m/s = 40° 7-13m/s = 30° > 14m/s = 20°	r2 = 2km	-0.02	0.00	-0.04
	r2 = 3km	-0.08	0.00	-0.09
	r2 = 4km	-0.13	0.00	-0.15
	r2 = 5km	-0.18	0.00	-0.18
	r2 = 6km	-0.18	0.00	-0.18

Table 64. Correlation Results From Analysis Run 4 (Neutral Conditions). Upper Flow Surface Level 6 (Rainfall Station 8).

Wind Speed Thresholds to Determine the Cone Angle	Inner Radius (r2) (Outer Radius (r1) Proportional To Wind Speed)	All 360 Degree Wind Directions	Southeast Winds 90-180 Degrees	Southwest Winds 181-270 Degrees
0-3m/s = 40° 4-7m/s = 30° > 8m/s = 20°	r2 = 2km	0.21	0.00	0.18
	r2 = 3km	0.21	0.00	0.18
	r2 = 4km	0.21	0.00	0.18
	r2 = 5km	0.21	0.00	0.18
	r2 = 6km	0.21	0.00	0.18
0-4m/s = 40° 5-9m/s = 30° > 10m/s = 20°	r2 = 2km	0.21	0.00	0.18
	r2 = 3km	0.21	0.00	0.18
	r2 = 4km	0.21	0.00	0.18
	r2 = 5km	0.21	0.00	0.18
	r2 = 6km	0.21	0.00	0.18
0-5m/s = 40° 6-11m/s = 30° > 12m/s = 20°	r2 = 2km	0.21	0.00	0.18
	r2 = 3km	0.21	0.00	0.18
	r2 = 4km	0.21	0.00	0.18
	r2 = 5km	0.21	0.00	0.18
	r2 = 6km	0.21	0.00	0.18
0-6m/s = 40° 7-13m/s = 30° > 14m/s = 20°	r2 = 2km	0.20	0.00	0.17
	r2 = 3km	0.20	0.00	0.17
	r2 = 4km	0.20	0.00	0.17
	r2 = 5km	0.20	0.00	0.17
	r2 = 6km	0.20	0.00	0.17

Table 65. Correlation Results From Analysis Run 4 (Neutral Conditions). Upper Flow Surface Level 6 (Rainfall Station 9).

Wind Speed Thresholds to Determine the Cone Angle	Inner Radius (r2) (Outer Radius (r1) Proportional To Wind Speed)	All 360 Degree Wind Directions	Southeast Winds 90-180 Degrees	Southwest Winds 181-270 Degrees
0-3m/s = 40° 4-7m/s = 30° > 8m/s = 20°	r2 = 2km	-0.26	0.00	-0.17
	r2 = 3km	-0.27	0.00	-0.18
	r2 = 4km	-0.26	0.00	-0.18
	r2 = 5km	-0.25	0.00	-0.18
	r2 = 6km	-0.27	0.00	-0.20
0-4m/s = 40° 5-9m/s = 30° > 10m/s = 20°	r2 = 2km	-0.26	0.00	-0.17
	r2 = 3km	-0.27	0.00	-0.18
	r2 = 4km	-0.26	0.00	-0.18
	r2 = 5km	-0.26	0.00	-0.19
	r2 = 6km	-0.27	0.00	-0.20
0-5m/s = 40° 6-11m/s = 30° > 12m/s = 20°	r2 = 2km	-0.26	0.00	-0.17
	r2 = 3km	-0.27	0.00	-0.18
	r2 = 4km	-0.25	0.00	-0.17
	r2 = 5km	-0.25	0.00	-0.18
	r2 = 6km	-0.26	0.00	-0.19
0-6m/s = 40° 7-13m/s = 30° > 14m/s = 20°	r2 = 2km	-0.24	0.00	-0.15
	r2 = 3km	-0.25	0.00	-0.16
	r2 = 4km	-0.24	0.00	-0.16
	r2 = 5km	-0.24	0.00	-0.17
	r2 = 6km	-0.26	0.00	-0.19

Table 66. Correlation Results From Analysis Run 4 (Neutral Conditions). Upper Flow Surface Level 6 (Rainfall Station 18).

Wind Speed Thresholds to Determine the Cone Angle	Inner Radius (r2) (Outer Radius (r1) Proportional To Wind Speed)	All 360 Degree Wind Directions	Southeast Winds 90-180 Degrees	Southwest Winds 181-270 Degrees
0-3m/s = 40° 4-7m/s = 30° > 8m/s = 20°	r2 = 2km	0.22	0.00	0.16
	r2 = 3km	0.19	0.00	0.13
	r2 = 4km	0.19	0.00	0.13
	r2 = 5km	0.19	0.00	0.13
	r2 = 6km	0.19	0.00	0.13
0-4m/s = 40° 5-9m/s = 30° > 10m/s = 20°	r2 = 2km	0.22	0.00	0.17
	r2 = 3km	0.19	0.00	0.13
	r2 = 4km	0.18	0.00	0.12
	r2 = 5km	0.19	0.00	0.13
	r2 = 6km	0.19	0.00	0.13
0-5m/s = 40° 6-11m/s = 30° > 12m/s = 20°	r2 = 2km	0.23	0.00	0.17
	r2 = 3km	0.19	0.00	0.13
	r2 = 4km	0.18	0.00	0.12
	r2 = 5km	0.19	0.00	0.13
	r2 = 6km	0.19	0.00	0.13
0-6m/s = 40° 7-13m/s = 30° > 14m/s = 20°	r2 = 2km	0.20	0.00	0.14
	r2 = 3km	0.17	0.00	0.11
	r2 = 4km	0.16	0.00	0.10
	r2 = 5km	0.17	0.00	0.11
	r2 = 6km	0.17	0.00	0.11

Table 67. Correlation Results From Analysis Run 4 (Neutral Conditions). Upper Flow Surface Level 5 (Rainfall Station 1).

Wind Speed Thresholds to Determine the Cone Angle	Inner Radius (r2) (Outer Radius (r1) Proportional To Wind Speed)	All 360 Degree Wind Directions	Southeast Winds 90-180 Degrees	Southwest Winds 181-270 Degrees
0-3m/s = 40° 4-7m/s = 30° > 8m/s = 20°	r2 = 2km	-0.05	0.68	-0.07
	r2 = 3km	-0.09	0.54	-0.11
	r2 = 4km	-0.15	0.54	-0.16
	r2 = 5km	-0.19	0.68	-0.19
	r2 = 6km	-0.16	0.58	-0.15
0-4m/s = 40° 5-9m/s = 30° > 10m/s = 20°	r2 = 2km	-0.05	0.68	-0.07
	r2 = 3km	-0.09	0.54	-0.11
	r2 = 4km	-0.15	0.54	-0.16
	r2 = 5km	-0.18	0.68	-0.18
	r2 = 6km	-0.16	0.58	-0.17
0-5m/s = 40° 6-11m/s = 30° > 12m/s = 20°	r2 = 2km	-0.03	0.68	-0.05
	r2 = 3km	-0.07	0.54	-0.09
	r2 = 4km	-0.14	0.54	-0.15
	r2 = 5km	-0.17	0.68	-0.18
	r2 = 6km	-0.14	0.58	-0.13
0-6m/s = 40° 7-13m/s = 30° > 14m/s = 20°	r2 = 2km	-0.01	0.68	-0.03
	r2 = 3km	-0.05	0.54	-0.07
	r2 = 4km	-0.11	0.54	-0.12
	r2 = 5km	-0.16	0.68	-0.17
	r2 = 6km	-0.15	0.58	-0.15

Table 68. Correlation Results From Analysis Run 4 (Neutral Conditions). Upper Flow Surface Level 5 (Rainfall Station 8).

Wind Speed Thresholds to Determine the Cone Angle	Inner Radius (r2) (Outer Radius (r1) Proportional To Wind Speed)	All 360 Degree Wind Directions	Southeast Winds 90-180 Degrees	Southwest Winds 181-270 Degrees
0-3m/s = 40° 4-7m/s = 30° > 8m/s = 20°	r2 = 2km	0.21	0.44	0.17
	r2 = 3km	0.21	0.44	0.17
	r2 = 4km	0.21	0.44	0.17
	r2 = 5km	0.21	0.44	0.17
	r2 = 6km	0.21	0.44	0.17
0-4m/s = 40° 5-9m/s = 30° > 10m/s = 20°	r2 = 2km	0.21	0.44	0.18
	r2 = 3km	0.21	0.44	0.18
	r2 = 4km	0.21	0.44	0.18
	r2 = 5km	0.21	0.44	0.18
	r2 = 6km	0.21	0.44	0.18
0-5m/s = 40° 6-11m/s = 30° > 12m/s = 20°	r2 = 2km	0.21	0.44	0.17
	r2 = 3km	0.21	0.44	0.17
	r2 = 4km	0.21	0.44	0.17
	r2 = 5km	0.21	0.44	0.17
	r2 = 6km	0.21	0.44	0.17
0-6m/s = 40° 7-13m/s = 30° > 14m/s = 20°	r2 = 2km	0.20	0.44	0.17
	r2 = 3km	0.20	0.44	0.17
	r2 = 4km	0.20	0.44	0.17
	r2 = 5km	0.20	0.44	0.17
	r2 = 6km	0.20	0.44	0.17

Table 69. Correlation Results From Analysis Run 4 (Neutral Conditions). Upper Flow Surface Level 5 (Rainfall Station 9).

Wind Speed Thresholds to Determine the Cone Angle	Inner Radius (r2) (Outer Radius (r1) Proportional To Wind Speed)	All 360 Degree Wind Directions	Southeast Winds 90-180 Degrees	Southwest Winds 181-270 Degrees
0-3m/s = 40° 4-7m/s = 30° > 8m/s = 20°	r2 = 2km	-0.25	0.23	-0.16
	r2 = 3km	-0.26	0.13	-0.17
	r2 = 4km	-0.24	0.13	-0.16
	r2 = 5km	-0.24	0.21	-0.17
	r2 = 6km	-0.26	0.23	-0.19
0-4m/s = 40° 5-9m/s = 30° > 10m/s = 20°	r2 = 2km	-0.25	0.23	-0.16
	r2 = 3km	-0.26	0.13	-0.17
	r2 = 4km	-0.24	0.13	-0.16
	r2 = 5km	-0.24	0.21	-0.17
	r2 = 6km	-0.26	0.23	-0.19
0-5m/s = 40° 6-11m/s = 30° > 12m/s = 20°	r2 = 2km	-0.25	0.23	-0.16
	r2 = 3km	-0.26	0.13	-0.17
	r2 = 4km	-0.24	0.13	-0.16
	r2 = 5km	-0.24	0.21	-0.17
	r2 = 6km	-0.25	0.23	-0.18
0-6m/s = 40° 7-13m/s = 30° > 14m/s = 20°	r2 = 2km	-0.24	0.23	-0.15
	r2 = 3km	-0.25	0.13	-0.16
	r2 = 4km	-0.24	0.13	-0.16
	r2 = 5km	-0.24	0.21	-0.17
	r2 = 6km	-0.26	0.23	-0.19

Table 70. Correlation Results From Analysis Run 4 (Neutral Conditions). Upper Flow Surface Level 5 (Rainfall Station 18).

Wind Speed Thresholds to Determine the Cone Angle	Inner Radius (r2) (Outer Radius (r1) Proportional To Wind Speed)	All 360 Degree Wind Directions	Southeast Winds 90-180 Degrees	Southwest Winds 181-270 Degrees
0-3m/s = 40° 4-7m/s = 30° > 8m/s = 20°	r2 = 2km	0.22	0.39	0.16
	r2 = 3km	0.18	0.39	0.12
	r2 = 4km	0.18	0.39	0.12
	r2 = 5km	0.19	0.38	0.13
	r2 = 6km	0.19	0.43	0.13
0-4m/s = 40° 5-9m/s = 30° > 10m/s = 20°	r2 = 2km	0.22	0.39	0.16
	r2 = 3km	0.18	0.39	0.12
	r2 = 4km	0.18	0.39	0.12
	r2 = 5km	0.19	0.38	0.13
	r2 = 6km	0.19	0.43	0.13
0-5m/s = 40° 6-11m/s = 30° > 12m/s = 20°	r2 = 2km	0.22	0.39	0.16
	r2 = 3km	0.18	0.39	0.12
	r2 = 4km	0.18	0.39	0.12
	r2 = 5km	0.19	0.38	0.12
	r2 = 6km	0.19	0.43	0.12
0-6m/s = 40° 7-13m/s = 30° > 14m/s = 20°	r2 = 2km	0.19	0.39	0.13
	r2 = 3km	0.16	0.39	0.10
	r2 = 4km	0.15	0.39	0.09
	r2 = 5km	0.17	0.38	0.10
	r2 = 6km	0.17	0.43	0.11

Table 71. **Correlation Results From Analysis Run 4 (Neutral Conditions). Upper Flow Surface Level 4 (Rainfall Station 1).**

Wind Speed Thresholds to Determine the Cone Angle	Inner Radius (r2) (Outer Radius (r1) Proportional To Wind Speed)	All 360 Degree Wind Directions	Southeast Winds 90-180 Degrees	Southwest Winds 181-270 Degrees
0-3m/s = 40° 4-7m/s = 30° > 8m/s = 20°	r2 = 2km	0.11	-0.33	0.11
	r2 = 3km	0.06	-0.37	0.06
	r2 = 4km	0.01	-0.31	0.01
	r2 = 5km	-0.11	-0.38	-0.10
	r2 = 6km	-0.05	-0.36	-0.04
0-4m/s = 40° 5-9m/s = 30° > 10m/s = 20°	r2 = 2km	0.10	-0.33	0.09
	r2 = 3km	0.05	-0.37	0.05
	r2 = 4km	0.01	-0.31	0.00
	r2 = 5km	-0.09	-0.38	-0.08
	r2 = 6km	-0.04	-0.36	-0.02
0-5m/s = 40° 6-11m/s = 30° > 12m/s = 20°	r2 = 2km	0.12	-0.33	0.12
	r2 = 3km	0.09	-0.37	0.08
	r2 = 4km	0.03	-0.31	0.02
	r2 = 5km	-0.06	-0.38	-0.05
	r2 = 6km	-0.05	-0.36	-0.03
0-6m/s = 40° 7-13m/s = 30° > 14m/s = 20°	r2 = 2km	0.12	-0.33	0.12
	r2 = 3km	0.12	-0.37	0.11
	r2 = 4km	0.01	-0.31	0.01
	r2 = 5km	-0.04	-0.38	-0.04
	r2 = 6km	-0.05	-0.36	-0.03

Table 72. Correlation Results From Analysis Run 4 (Neutral Conditions). Upper Flow Surface Level 4 (Rainfall Station 8).

Wind Speed Thresholds to Determine the Cone Angle	Inner Radius (r2) (Outer Radius (r1) Proportional To Wind Speed)	All 360 Degree Wind Directions	Southeast Winds 90-180 Degrees	Southwest Winds 181-270 Degrees
0-3m/s = 40° 4-7m/s = 30° > 8m/s = 20°	r2 = 2km	0.20	0.46	0.17
	r2 = 3km	0.20	0.46	0.17
	r2 = 4km	0.20	0.46	0.17
	r2 = 5km	0.20	0.46	0.17
	r2 = 6km	0.20	0.46	0.17
0-4m/s = 40° 5-9m/s = 30° > 10m/s = 20°	r2 = 2km	0.20	0.46	0.17
	r2 = 3km	0.20	0.46	0.17
	r2 = 4km	0.20	0.46	0.17
	r2 = 5km	0.20	0.46	0.17
	r2 = 6km	0.20	0.46	0.17
0-5m/s = 40° 6-11m/s = 30° > 12m/s = 20°	r2 = 2km	0.20	0.46	0.17
	r2 = 3km	0.20	0.46	0.17
	r2 = 4km	0.20	0.46	0.17
	r2 = 5km	0.20	0.46	0.17
	r2 = 6km	0.20	0.46	0.17
0-6m/s = 40° 7-13m/s = 30° > 14m/s = 20°	r2 = 2km	0.19	0.46	0.16
	r2 = 3km	0.19	0.46	0.16
	r2 = 4km	0.19	0.46	0.16
	r2 = 5km	0.19	0.46	0.16
	r2 = 6km	0.19	0.46	0.16

Table 73. Correlation Results From Analysis Run 4 (Neutral Conditions). Upper Flow Surface Level 4 (Rainfall Station 9).

Wind Speed Thresholds to Determine the Cone Angle	Inner Radius (r2) (Outer Radius (r1) Proportional To Wind Speed)	All 360 Degree Wind Directions	Southeast Winds 90-180 Degrees	Southwest Winds 181-270 Degrees
0-3m/s = 40° 4-7m/s = 30° > 8m/s = 20°	r2 = 2km	-0.20	-0.22	-0.12
	r2 = 3km	-0.22	-0.25	-0.14
	r2 = 4km	-0.18	-0.27	-0.10
	r2 = 5km	-0.17	-0.27	-0.10
	r2 = 6km	-0.22	-0.30	-0.15
0-4m/s = 40° 5-9m/s = 30° > 10m/s = 20°	r2 = 2km	-0.20	-0.22	-0.12
	r2 = 3km	-0.22	-0.25	-0.14
	r2 = 4km	-0.18	-0.27	-0.11
	r2 = 5km	-0.17	-0.27	-0.10
	r2 = 6km	-0.21	-0.30	-0.15
0-5m/s = 40° 6-11m/s = 30° > 12m/s = 20°	r2 = 2km	-0.20	-0.22	-0.11
	r2 = 3km	-0.21	-0.25	-0.13
	r2 = 4km	-0.18	-0.27	-0.11
	r2 = 5km	-0.17	-0.27	-0.10
	r2 = 6km	-0.20	-0.30	-0.13
0-6m/s = 40° 7-13m/s = 30° > 14m/s = 20°	r2 = 2km	-0.21	-0.22	-0.12
	r2 = 3km	-0.22	-0.25	-0.14
	r2 = 4km	-0.20	-0.27	-0.12
	r2 = 5km	-0.18	-0.27	-0.11
	r2 = 6km	-0.20	-0.30	-0.14

Table 74. Correlation Results From Analysis Run 4 (Neutral Conditions). Upper Flow Surface Level 4 (Rainfall Station 18).

Wind Speed Thresholds to Determine the Cone Angle	Inner Radius (r2) (Outer Radius (r1) Proportional To Wind Speed)	All 360 Degree Wind Directions	Southeast Winds 90-180 Degrees	Southwest Winds 181-270 Degrees
0-3m/s = 40° 4-7m/s = 30° > 8m/s = 20°	r2 = 2km	0.03	0.48	-0.03
	r2 = 3km	-0.01	0.50	-0.06
	r2 = 4km	-0.02	0.48	-0.07
	r2 = 5km	0.02	0.49	-0.04
	r2 = 6km	0.03	0.48	-0.03
0-4m/s = 40° 5-9m/s = 30° > 10m/s = 20°	r2 = 2km	0.03	0.48	-0.03
	r2 = 3km	-0.01	0.50	-0.06
	r2 = 4km	-0.02	0.48	-0.07
	r2 = 5km	0.02	0.49	-0.04
	r2 = 6km	0.03	0.48	-0.03
0-5m/s = 40° 6-11m/s = 30° > 12m/s = 20°	r2 = 2km	0.02	0.48	-0.04
	r2 = 3km	-0.01	0.50	-0.07
	r2 = 4km	-0.02	0.48	-0.07
	r2 = 5km	0.01	0.49	-0.05
	r2 = 6km	0.03	0.48	-0.04
0-6m/s = 40° 7-13m/s = 30° > 14m/s = 20°	r2 = 2km	0.02	0.48	-0.04
	r2 = 3km	-0.01	0.50	-0.07
	r2 = 4km	-0.02	0.48	-0.07
	r2 = 5km	0.01	0.49	-0.05
	r2 = 6km	0.02	0.48	-0.04

Table 75. Correlation Results From Analysis Run 4 (Neutral Conditions). Upper Flow Surface Level 3 (Rainfall Station 1).

Wind Speed Thresholds to Determine the Cone Angle	Inner Radius (r2) (Outer Radius (r1) Proportional To Wind Speed)	All 360 Degree Wind Directions	Southeast Winds 90-180 Degrees	Southwest Winds 181-270 Degrees
0-3m/s = 40° 4-7m/s = 30° > 8m/s = 20°	r2 = 2km	0.09	0.26	0.07
	r2 = 3km	0.06	0.20	0.05
	r2 = 4km	0.04	0.18	0.02
	r2 = 5km	-0.03	0.14	-0.04
	r2 = 6km	-0.05	0.05	-0.05
0-4m/s = 40° 5-9m/s = 30° > 10m/s = 20°	r2 = 2km	0.08	0.26	0.06
	r2 = 3km	0.05	0.20	0.04
	r2 = 4km	0.02	0.18	0.00
	r2 = 5km	-0.03	0.14	-0.04
	r2 = 6km	-0.05	0.05	-0.05
0-5m/s = 40° 6-11m/s = 30° > 12m/s = 20°	r2 = 2km	0.10	0.26	0.08
	r2 = 3km	0.07	0.20	0.05
	r2 = 4km	0.04	0.18	0.02
	r2 = 5km	0.00	0.14	-0.01
	r2 = 6km	-0.06	0.05	-0.06
0-6m/s = 40° 7-13m/s = 30° > 14m/s = 20°	r2 = 2km	0.10	0.26	0.08
	r2 = 3km	0.07	0.20	0.05
	r2 = 4km	0.04	0.18	0.03
	r2 = 5km	-0.01	0.14	-0.02
	r2 = 6km	-0.06	0.05	-0.06

Table 76. Correlation Results From Analysis Run 4 (Neutral Conditions). Upper Flow Surface Level 3 (Rainfall Station 8).

Wind Speed Thresholds to Determine the Cone Angle	Inner Radius (r2) (Outer Radius (r1) Proportional To Wind Speed)	All 360 Degree Wind Directions	Southeast Winds 90-180 Degrees	Southwest Winds 181-270 Degrees
0-3m/s = 40° 4-7m/s = 30° > 8m/s = 20°	r2 = 2km	0.19	0.05	0.16
	r2 = 3km	0.19	0.05	0.16
	r2 = 4km	0.19	0.05	0.16
	r2 = 5km	0.19	0.05	0.16
	r2 = 6km	0.19	0.05	0.16
0-4m/s = 40° 5-9m/s = 30° > 10m/s = 20°	r2 = 2km	0.19	0.05	0.16
	r2 = 3km	0.19	0.05	0.16
	r2 = 4km	0.19	0.05	0.16
	r2 = 5km	0.19	0.05	0.16
	r2 = 6km	0.19	0.05	0.16
0-5m/s = 40° 6-11m/s = 30° > 12m/s = 20°	r2 = 2km	0.19	0.05	0.16
	r2 = 3km	0.19	0.05	0.16
	r2 = 4km	0.19	0.05	0.16
	r2 = 5km	0.19	0.05	0.16
	r2 = 6km	0.19	0.05	0.16
0-6m/s = 40° 7-13m/s = 30° > 14m/s = 20°	r2 = 2km	0.19	0.05	0.16
	r2 = 3km	0.19	0.05	0.16
	r2 = 4km	0.19	0.05	0.16
	r2 = 5km	0.19	0.05	0.16
	r2 = 6km	0.19	0.05	0.16

Table 77. Correlation Results From Analysis Run 4 (Neutral Conditions). Upper Flow Surface Level 3 (Rainfall Station 9).

Wind Speed Thresholds to Determine the Cone Angle	Inner Radius (r2) (Outer Radius (r1) Proportional To Wind Speed)	All 360 Degree Wind Directions	Southeast Winds 90-180 Degrees	Southwest Winds 181-270 Degrees
0-3m/s = 40° 4-7m/s = 30° > 8m/s = 20°	r2 = 2km	-0.08	-0.05	-0.06
	r2 = 3km	-0.11	-0.05	-0.09
	r2 = 4km	-0.04	0.01	-0.06
	r2 = 5km	0.01	0.04	-0.04
	r2 = 6km	-0.03	0.05	-0.06
0-4m/s = 40° 5-9m/s = 30° > 10m/s = 20°	r2 = 2km	-0.06	-0.05	-0.03
	r2 = 3km	-0.09	-0.05	-0.06
	r2 = 4km	-0.03	0.01	-0.04
	r2 = 5km	0.02	0.04	-0.03
	r2 = 6km	-0.03	0.05	-0.05
0-5m/s = 40° 6-11m/s = 30° > 12m/s = 20°	r2 = 2km	-0.06	-0.05	-0.04
	r2 = 3km	-0.08	-0.05	-0.06
	r2 = 4km	-0.03	0.01	-0.05
	r2 = 5km	0.01	0.04	-0.04
	r2 = 6km	-0.03	0.05	-0.06
0-6m/s = 40° 7-13m/s = 30° > 14m/s = 20°	r2 = 2km	-0.07	-0.05	-0.05
	r2 = 3km	-0.09	-0.05	-0.07
	r2 = 4km	-0.04	0.01	-0.05
	r2 = 5km	0.00	0.04	-0.04
	r2 = 6km	-0.03	0.05	-0.06

Table 78. Correlation Results From Analysis Run 4 (Neutral Conditions). Upper Flow Surface Level 3 (Rainfall Station 18).

Wind Speed Thresholds to Determine the Cone Angle	Inner Radius (r2) (Outer Radius (r1) Proportional To Wind Speed)	All 360 Degree Wind Directions	Southeast Winds 90-180 Degrees	Southwest Winds 181-270 Degrees
0-3m/s = 40° 4-7m/s = 30° > 8m/s = 20°	r2 = 2km	-0.24	-0.76	-0.22
	r2 = 3km	-0.26	-0.76	-0.23
	r2 = 4km	-0.26	-0.76	-0.23
	r2 = 5km	-0.22	-0.76	-0.20
	r2 = 6km	-0.20	-0.76	-0.20
0-4m/s = 40° 5-9m/s = 30° > 10m/s = 20°	r2 = 2km	-0.25	-0.76	-0.22
	r2 = 3km	-0.27	-0.76	-0.24
	r2 = 4km	-0.26	-0.76	-0.23
	r2 = 5km	-0.23	-0.76	-0.21
	r2 = 6km	-0.20	-0.76	-0.20
0-5m/s = 40° 6-11m/s = 30° > 12m/s = 20°	r2 = 2km	-0.24	-0.76	-0.22
	r2 = 3km	-0.26	-0.76	-0.23
	r2 = 4km	-0.25	-0.76	-0.22
	r2 = 5km	-0.22	-0.76	-0.20
	r2 = 6km	-0.20	-0.76	-0.19
0-6m/s = 40° 7-13m/s = 30° > 14m/s = 20°	r2 = 2km	-0.27	-0.76	-0.24
	r2 = 3km	-0.28	-0.76	-0.25
	r2 = 4km	-0.27	-0.76	-0.24
	r2 = 5km	-0.24	-0.76	-0.22
	r2 = 6km	-0.22	-0.76	-0.21

Table 79. Correlation Results From Analysis Run 4 (Neutral Conditions). Upper Flow Surface Level 2 (Rainfall Station 1).

Wind Speed Thresholds to Determine the Cone Angle	Inner Radius (r2) (Outer Radius (r1) Proportional To Wind Speed)	All 360 Degree Wind Directions	Southeast Winds 90-180 Degrees	Southwest Winds 181-270 Degrees
0-3m/s = 40° 4-7m/s = 30° > 8m/s = 20°	r2 = 2km	0.11	0.02	0.03
	r2 = 3km	0.13	0.02	0.10
	r2 = 4km	0.22	0.00	0.37
	r2 = 5km	0.21	0.03	0.35
	r2 = 6km	0.15	0.07	0.37
0-4m/s = 40° 5-9m/s = 30° > 10m/s = 20°	r2 = 2km	0.08	0.00	-0.05
	r2 = 3km	0.09	-0.01	0.02
	r2 = 4km	0.18	-0.02	0.30
	r2 = 5km	0.15	-0.01	0.27
	r2 = 6km	0.09	0.00	0.28
0-5m/s = 40° 6-11m/s = 30° > 12m/s = 20°	r2 = 2km	0.06	0.00	-0.09
	r2 = 3km	0.08	-0.01	0.00
	r2 = 4km	0.13	-0.03	0.19
	r2 = 5km	0.13	-0.05	0.25
	r2 = 6km	0.08	-0.02	0.26
0-6m/s = 40° 7-13m/s = 30° > 14m/s = 20°	r2 = 2km	0.06	-0.02	-0.10
	r2 = 3km	0.08	-0.02	-0.02
	r2 = 4km	0.13	-0.04	0.19
	r2 = 5km	0.13	-0.05	0.25
	r2 = 6km	0.08	-0.02	0.25

Table 80. Correlation Results From Analysis Run 4 (Neutral Conditions). Upper Flow Surface Level 2 (Rainfall Station 8).

Wind Speed Thresholds to Determine the Cone Angle	Inner Radius (r2) (Outer Radius (r1) Proportional To Wind Speed)	All 360 Degree Wind Directions	Southeast Winds 90-180 Degrees	Southwest Winds 181-270 Degrees
0-3m/s = 40° 4-7m/s = 30° > 8m/s = 20°	r2 = 2km	-0.07	0.63	-0.11
	r2 = 3km	-0.07	0.63	-0.11
	r2 = 4km	-0.07	0.63	-0.11
	r2 = 5km	-0.07	0.63	-0.11
	r2 = 6km	-0.07	0.63	-0.11
0-4m/s = 40° 5-9m/s = 30° > 10m/s = 20°	r2 = 2km	-0.06	0.63	-0.11
	r2 = 3km	-0.06	0.63	-0.11
	r2 = 4km	-0.06	0.63	-0.11
	r2 = 5km	-0.06	0.63	-0.11
	r2 = 6km	-0.06	0.63	-0.11
0-5m/s = 40° 6-11m/s = 30° > 12m/s = 20°	r2 = 2km	-0.07	0.63	-0.12
	r2 = 3km	-0.07	0.63	-0.12
	r2 = 4km	-0.07	0.63	-0.12
	r2 = 5km	-0.07	0.63	-0.12
	r2 = 6km	-0.07	0.63	-0.12
0-6m/s = 40° 7-13m/s = 30° > 14m/s = 20°	r2 = 2km	-0.04	0.63	-0.08
	r2 = 3km	-0.04	0.63	-0.08
	r2 = 4km	-0.04	0.63	-0.08
	r2 = 5km	-0.04	0.63	-0.08
	r2 = 6km	-0.04	0.63	-0.08

Table 81. Correlation Results From Analysis Run 4 (Neutral Conditions). Upper Flow Surface Level 2 (Rainfall Station 9).

Wind Speed Thresholds to Determine the Cone Angle	Inner Radius (r2) (Outer Radius (r1) Proportional To Wind Speed)	All 360 Degree Wind Directions	Southeast Winds 90-180 Degrees	Southwest Winds 181-270 Degrees
0-3m/s = 40° 4-7m/s = 30° > 8m/s = 20°	r2 = 2km	0.06	0.17	0.12
	r2 = 3km	0.04	0.17	0.09
	r2 = 4km	0.09	0.19	0.15
	r2 = 5km	0.17	0.20	0.20
	r2 = 6km	0.16	0.23	0.18
0-4m/s = 40° 5-9m/s = 30° > 10m/s = 20°	r2 = 2km	0.07	0.21	0.12
	r2 = 3km	0.06	0.21	0.10
	r2 = 4km	0.12	0.24	0.16
	r2 = 5km	0.18	0.24	0.21
	r2 = 6km	0.18	0.28	0.18
0-5m/s = 40° 6-11m/s = 30° > 12m/s = 20°	r2 = 2km	0.08	0.23	0.12
	r2 = 3km	0.06	0.22	0.10
	r2 = 4km	0.11	0.24	0.15
	r2 = 5km	0.17	0.24	0.19
	r2 = 6km	0.17	0.29	0.16
0-6m/s = 40° 7-13m/s = 30° > 14m/s = 20°	r2 = 2km	0.08	0.24	0.12
	r2 = 3km	0.07	0.24	0.10
	r2 = 4km	0.12	0.25	0.15
	r2 = 5km	0.18	0.27	0.19
	r2 = 6km	0.18	0.30	0.17

Table 82. Correlation Results From Analysis Run 4 (Neutral Conditions). Upper Flow Surface Level 2 (Rainfall Station 18).

Wind Speed Thresholds to Determine the Cone Angle	Inner Radius (r2) (Outer Radius (r1) Proportional To Wind Speed)	All 360 Degree Wind Directions	Southeast Winds 90-180 Degrees	Southwest Winds 181-270 Degrees
0-3m/s = 40° 4-7m/s = 30° > 8m/s = 20°	r2 = 2km	-0.21	0.11	-0.27
	r2 = 3km	-0.30	0.10	-0.35
	r2 = 4km	-0.30	0.13	-0.36
	r2 = 5km	-0.23	0.16	-0.32
	r2 = 6km	-0.21	0.14	-0.33
0-4m/s = 40° 5-9m/s = 30° > 10m/s = 20°	r2 = 2km	-0.18	0.11	-0.23
	r2 = 3km	-0.30	0.10	-0.36
	r2 = 4km	-0.29	0.13	-0.35
	r2 = 5km	-0.23	0.16	-0.32
	r2 = 6km	-0.21	0.15	-0.34
0-5m/s = 40° 6-11m/s = 30° > 12m/s = 20°	r2 = 2km	-0.19	0.08	-0.23
	r2 = 3km	-0.30	0.08	-0.35
	r2 = 4km	-0.30	0.11	-0.35
	r2 = 5km	-0.24	0.14	-0.32
	r2 = 6km	-0.23	0.12	-0.34
0-6m/s = 40° 7-13m/s = 30° > 14m/s = 20°	r2 = 2km	-0.21	0.08	-0.26
	r2 = 3km	-0.32	0.08	-0.38
	r2 = 4km	-0.31	0.11	-0.37
	r2 = 5km	-0.25	0.14	-0.34
	r2 = 6km	-0.24	0.12	-0.36

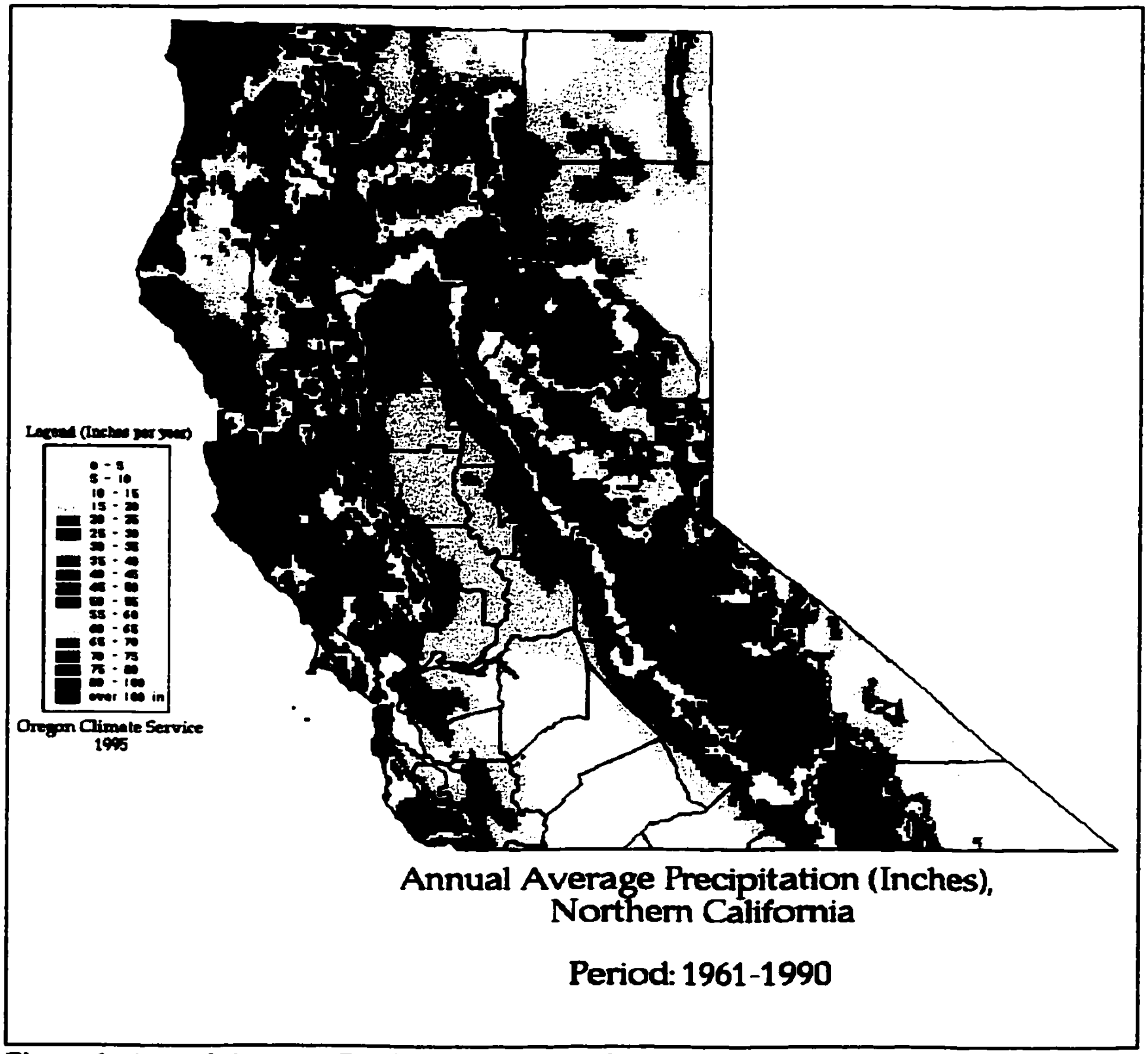

Figure 1 Annual Average Precipitation for Northern California (From PRISM data).

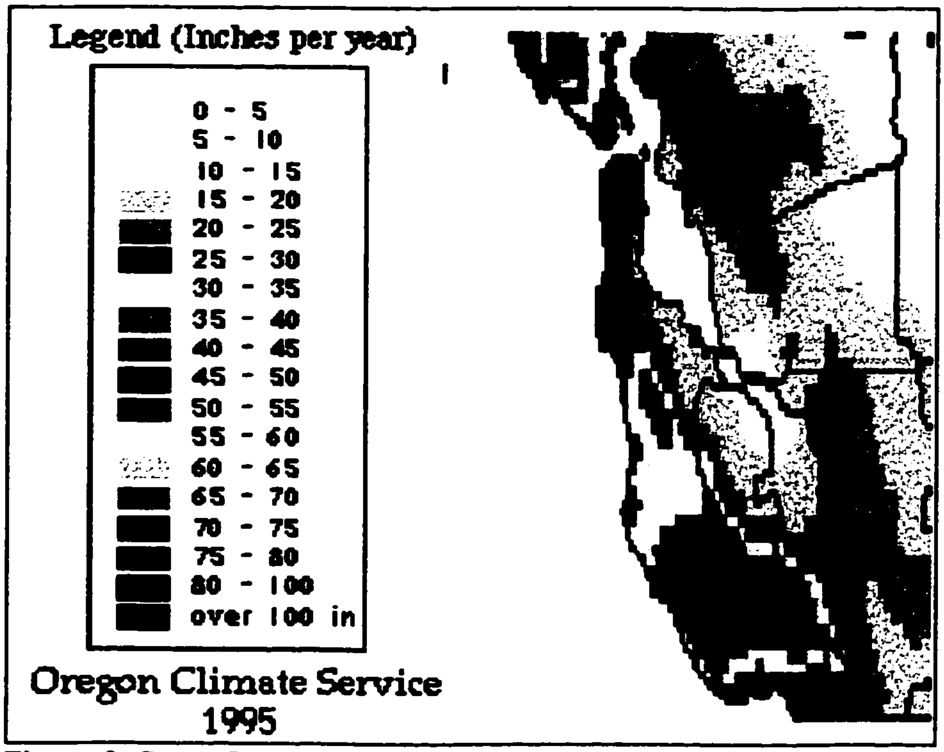

Figure 2 Santa Cruz Mountains Annual Precipitation Distribution (From PRISM Data).

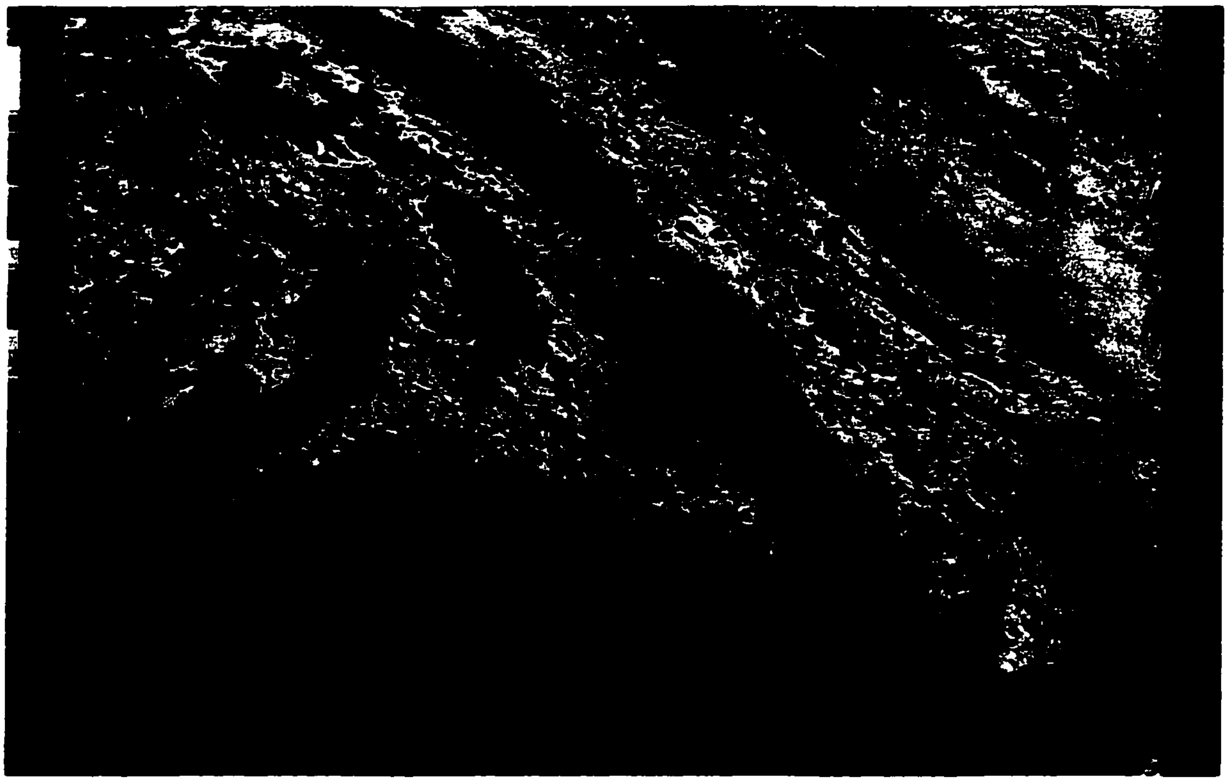

Figure 3 National Weather Service Eastern Pacific Infared Satellite Picture at 0000Z February 1st 1998.

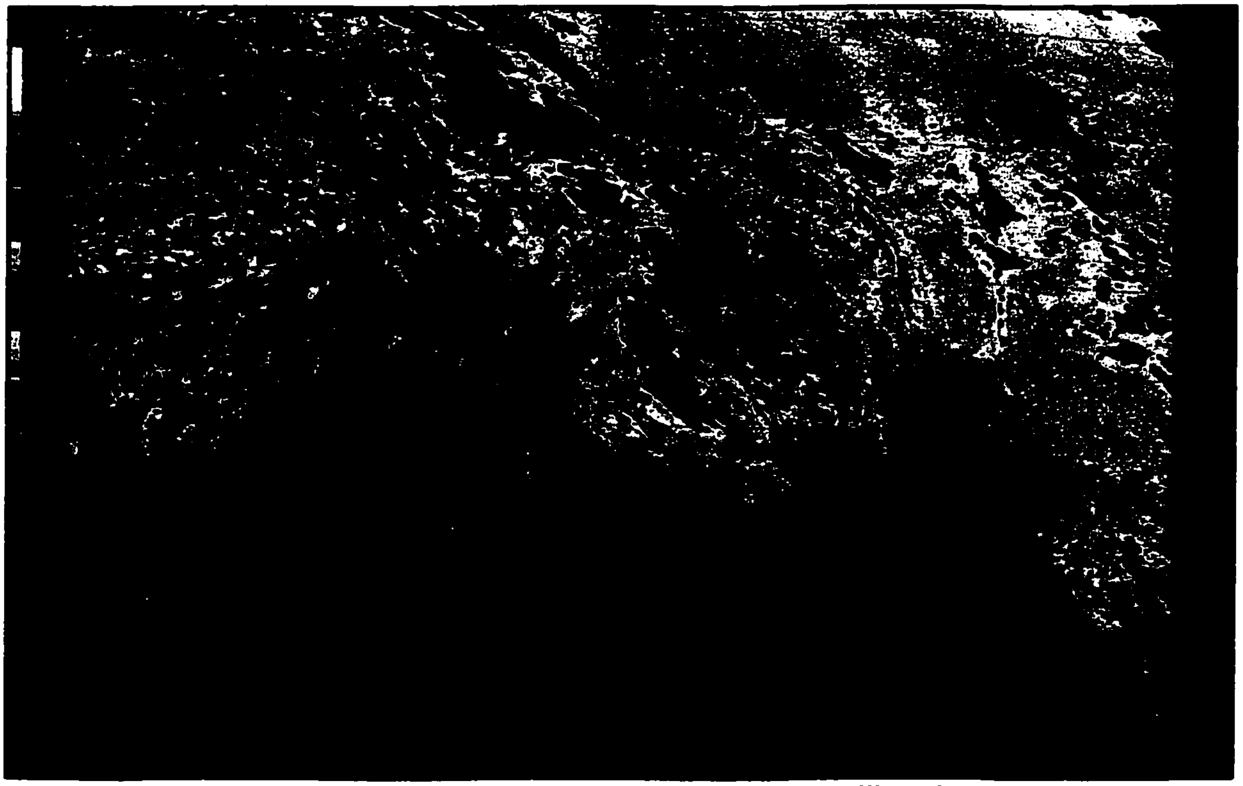

Figure 4 National Weather Service Eastern Pacific Infared Satellite Picture at 1200Z February 1st 1998.

Figure 5 National Weather Service Eastern Pacific Infared Satellite Picture at 0000Z February 2nd 1998.

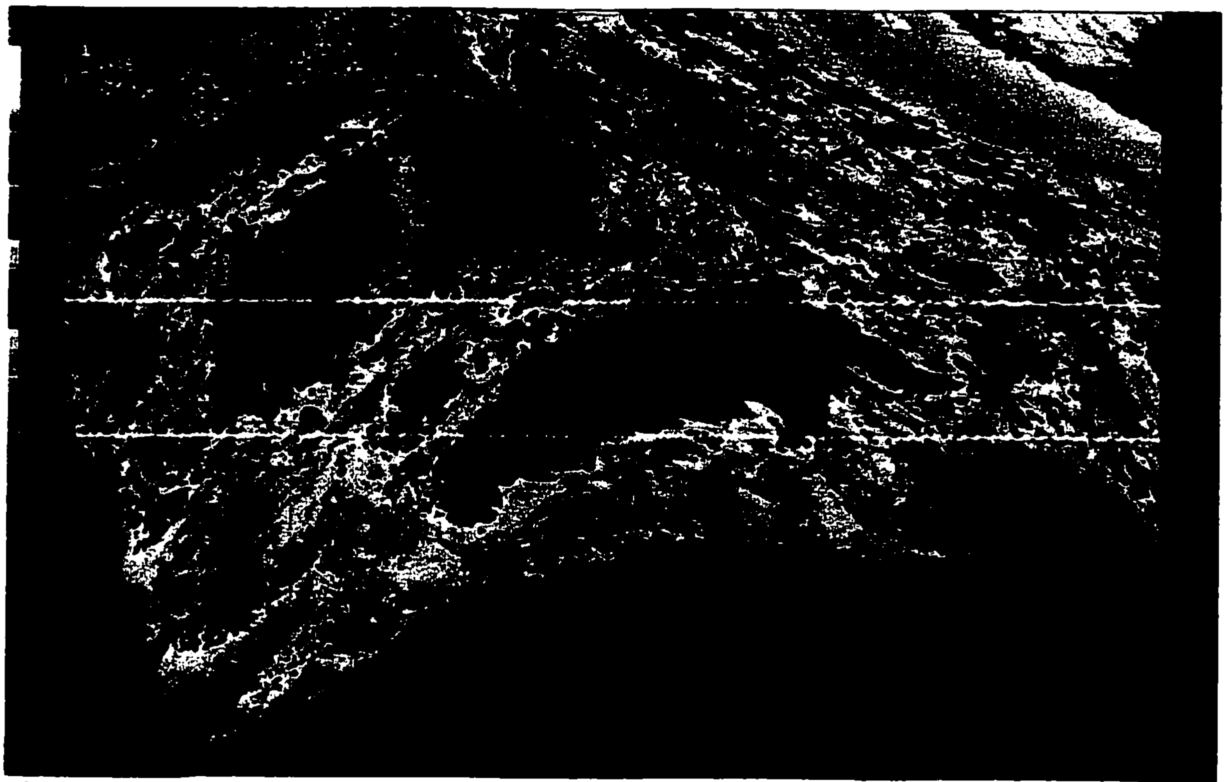

Figure 6 National Weather Service Eastern Pacific Infared Satellite Picture at 1200Z February 2nd 1998.

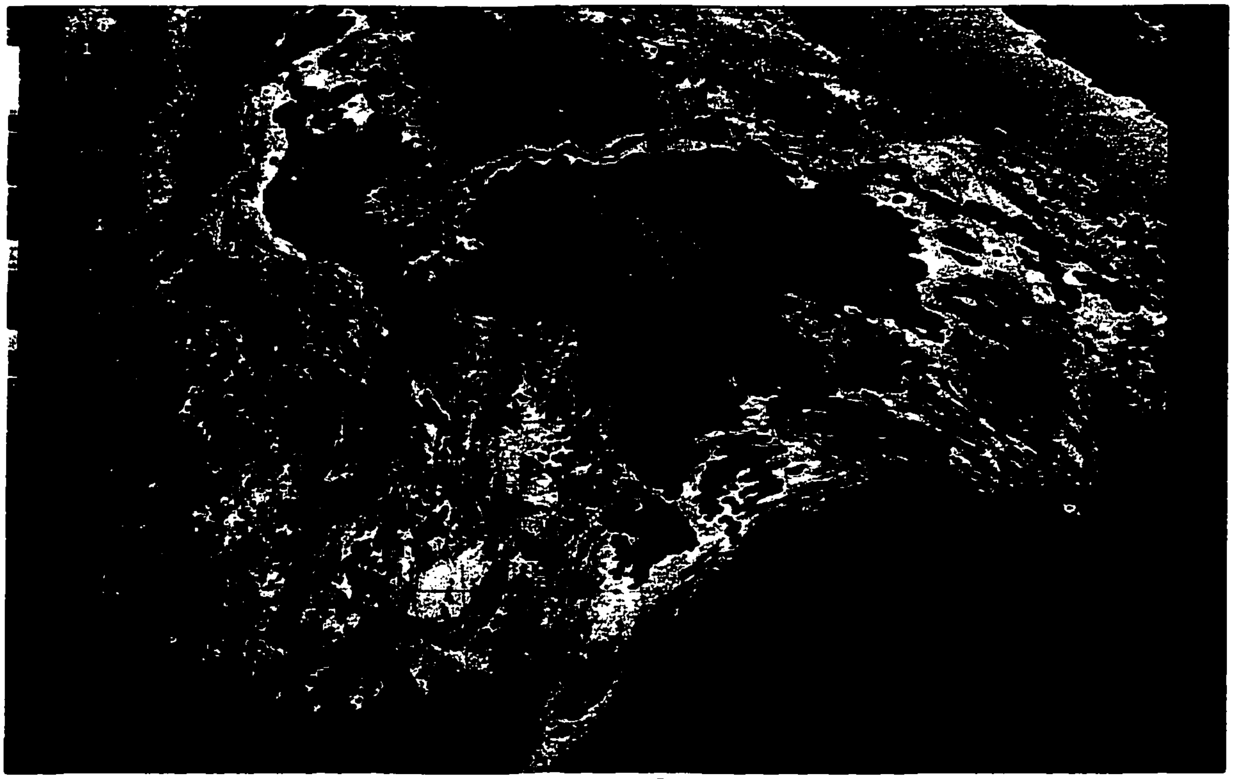

Figure 7 National Weather Service Eastern Pacific Infared Satellite Picture at 0000Z February 3rd 1998.

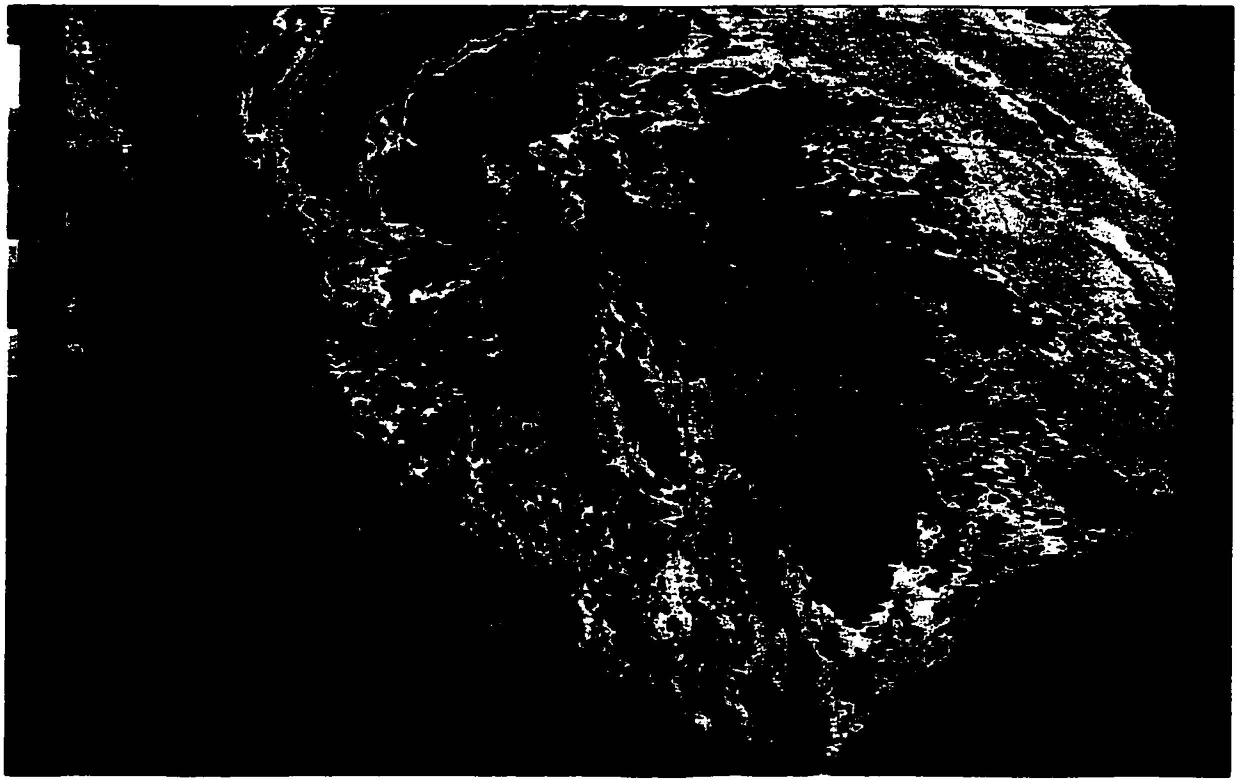

Figure 8 National Weather Service Eastern Pacific Infared Satellite Picture at 1200Z February 3rd 1998.

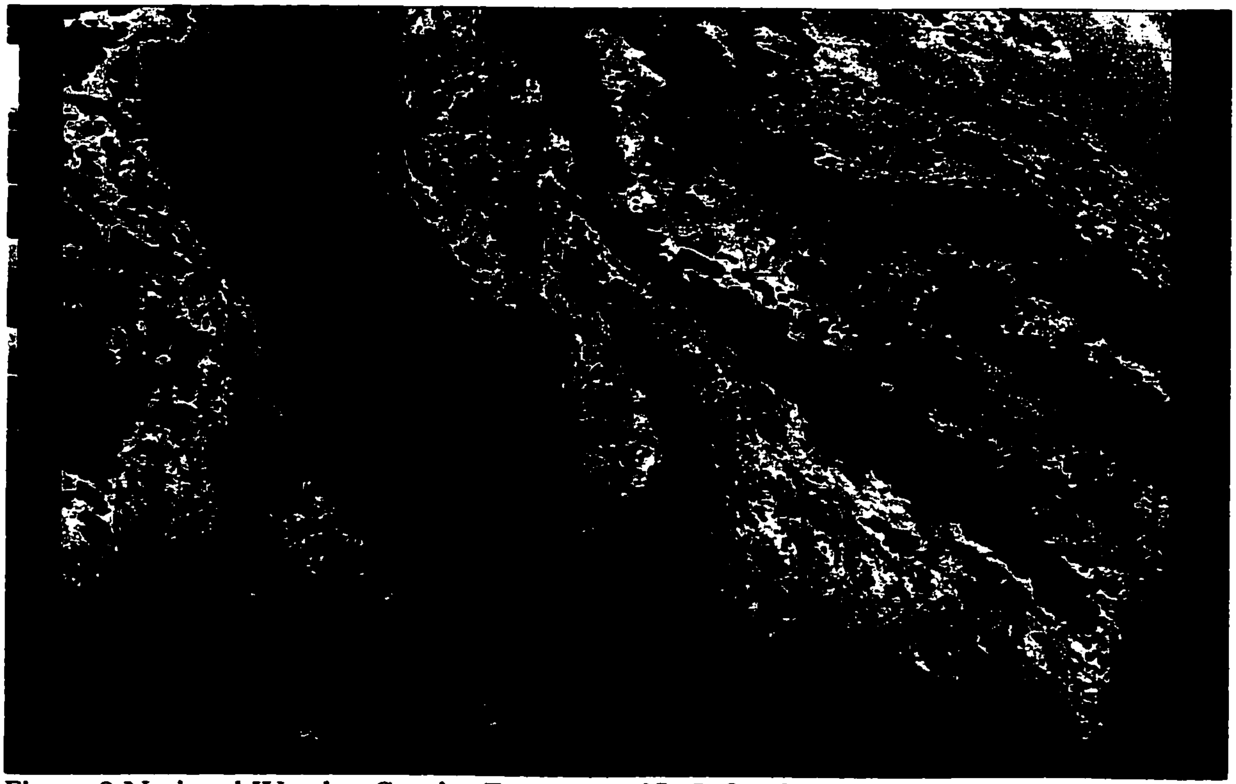

Figure 9 National Weather Service Eastern Pacific Infared Satellite Picture at 0000Z February 4th 1998.

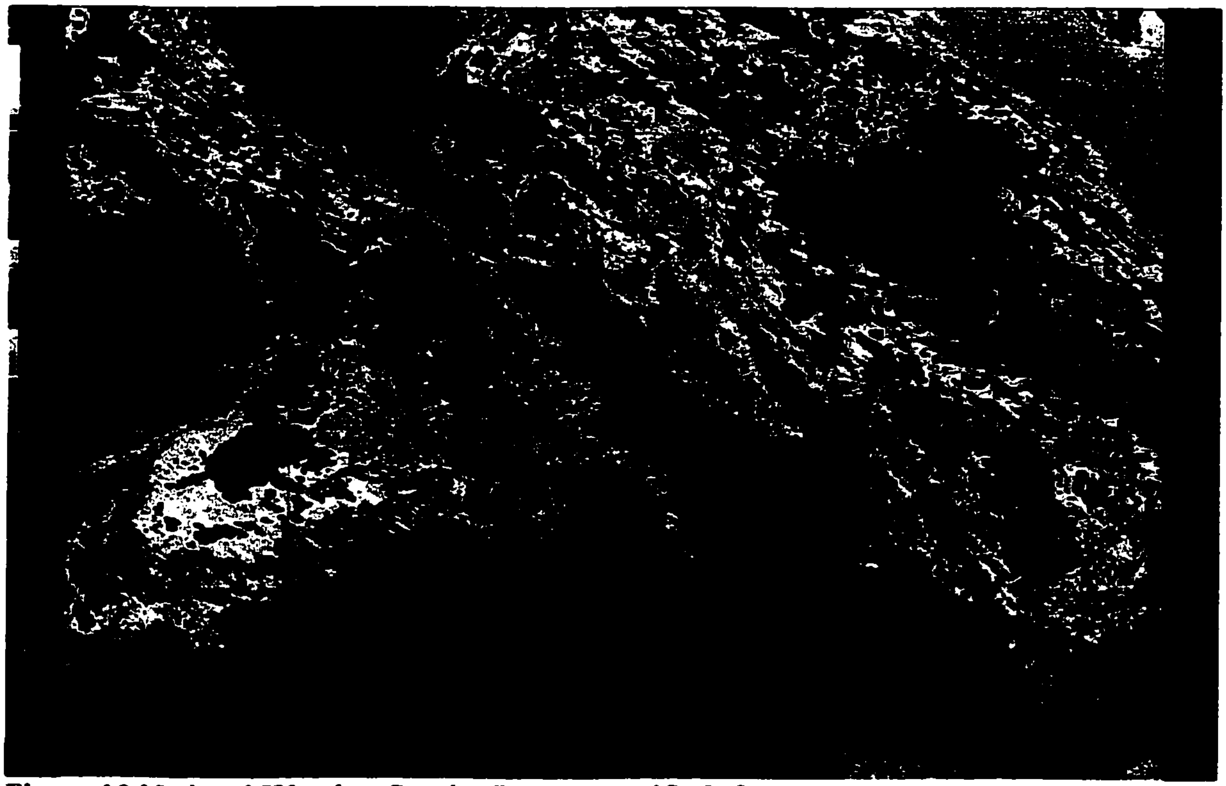

Figure 10 National Weather Service Eastern Pacific Infared Satellite Picture at 1200Z February 4th 1998.

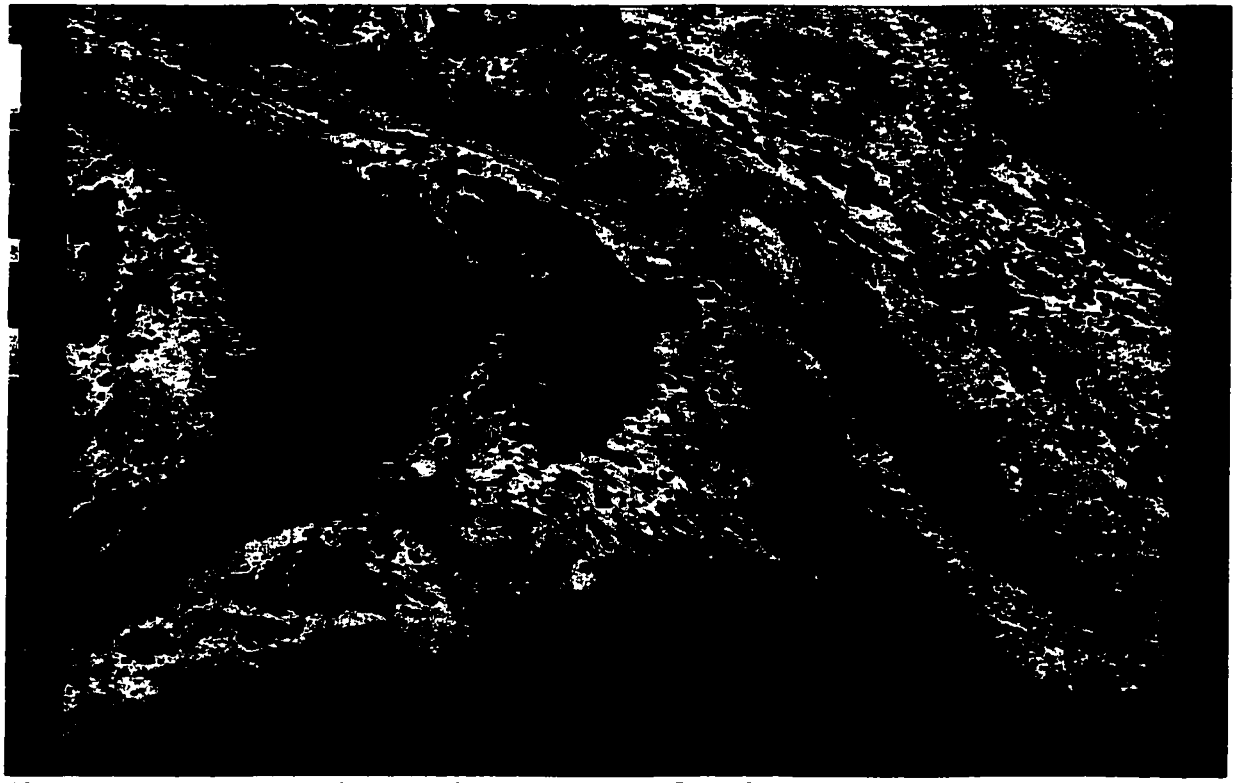

Figure 11 National Weather Service Eastern Pacific Infared Satellite Picture at 0000Z February 5th 1998.

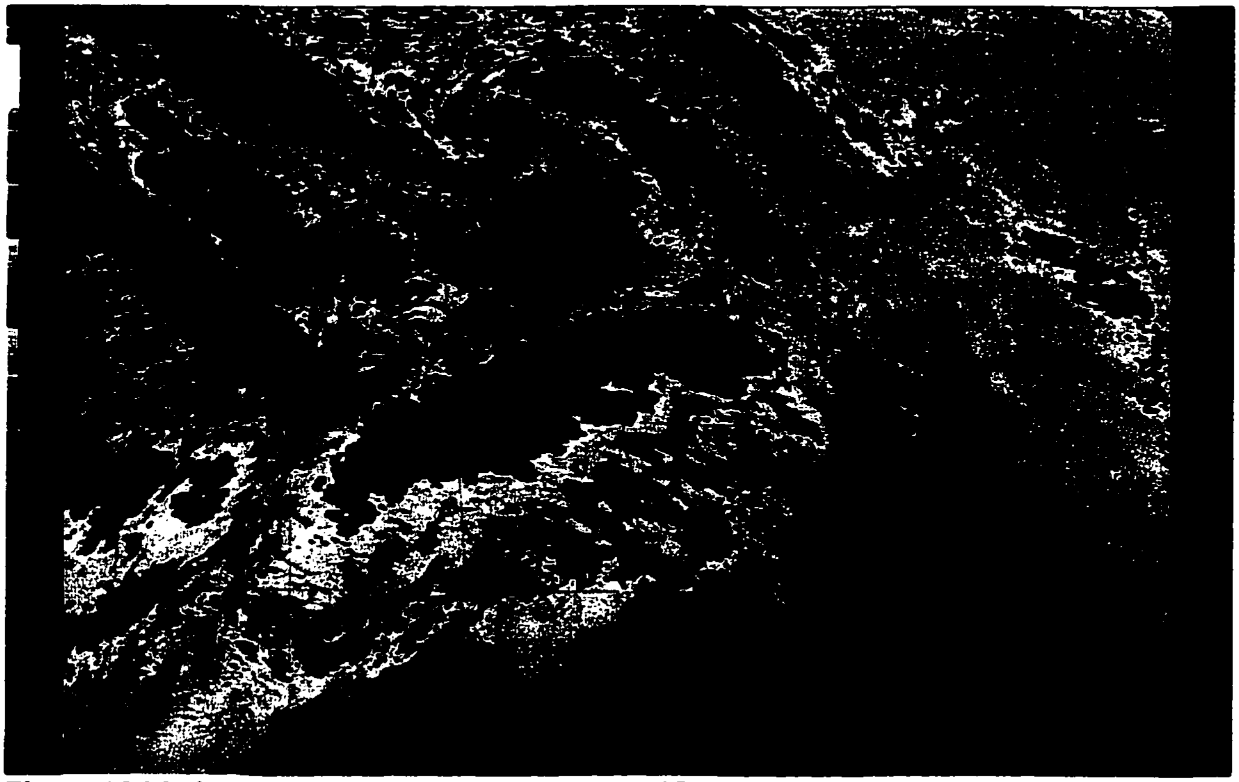

Figure 12 National Weather Service Eastern Pacific Infared Satellite Picture at 1200Z February 5th 1998.

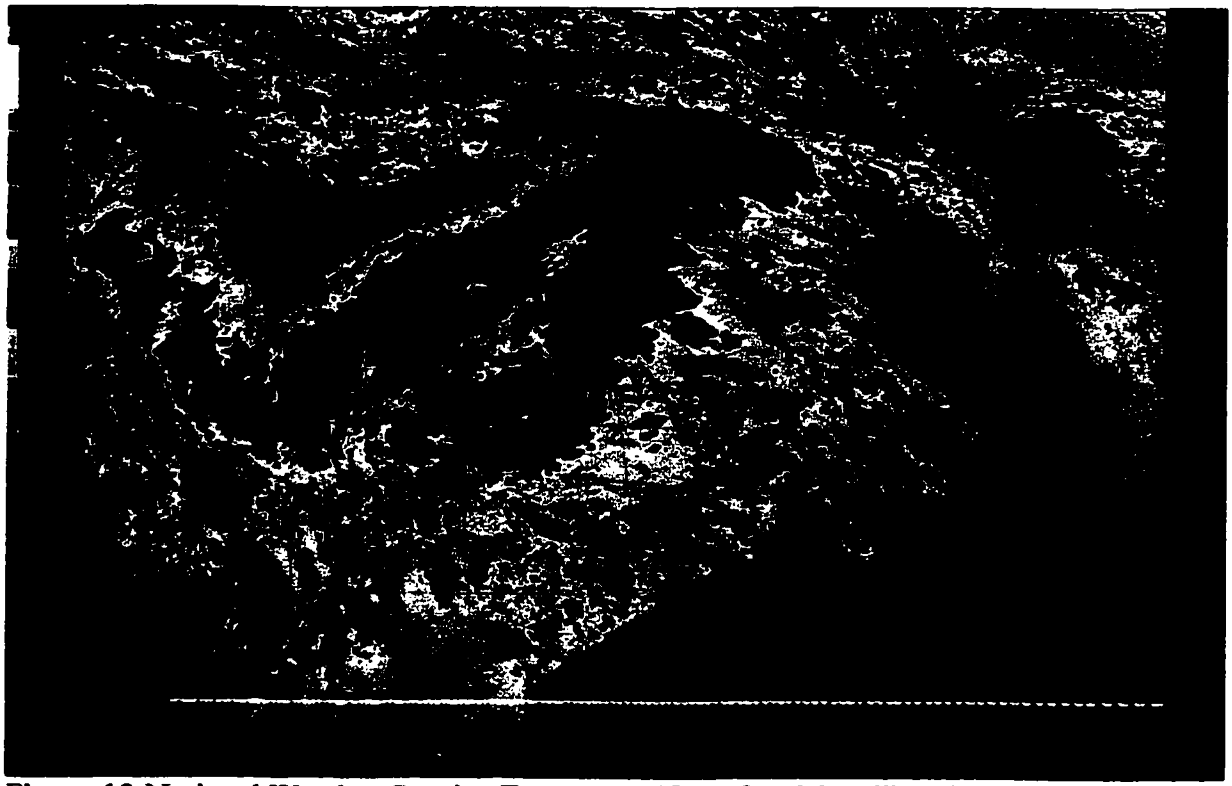

Figure 13 National Weather Service Eastern Pacific Infared Satellite Picture at 0000Z February 6th 1998.

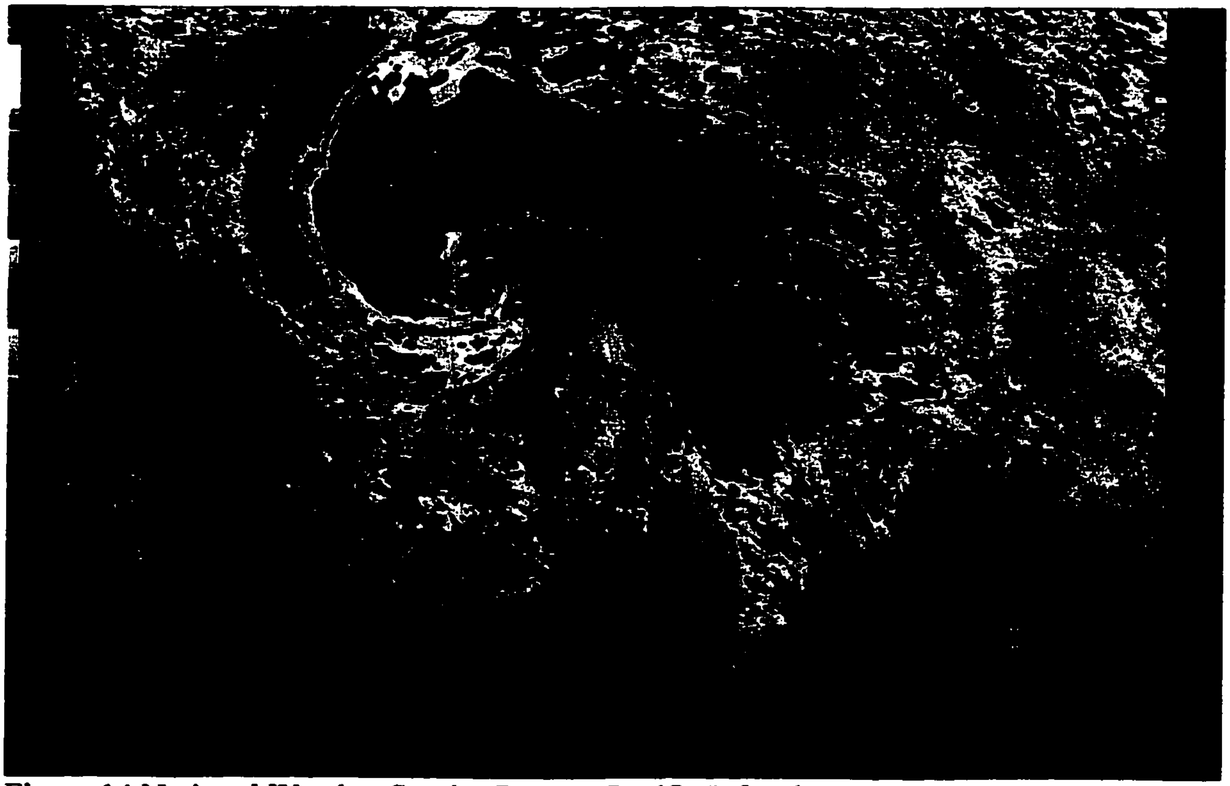

Figure 14 National Weather Service Eastern Pacific Infared Satellite Picture at 1200Z February 6th 1998.

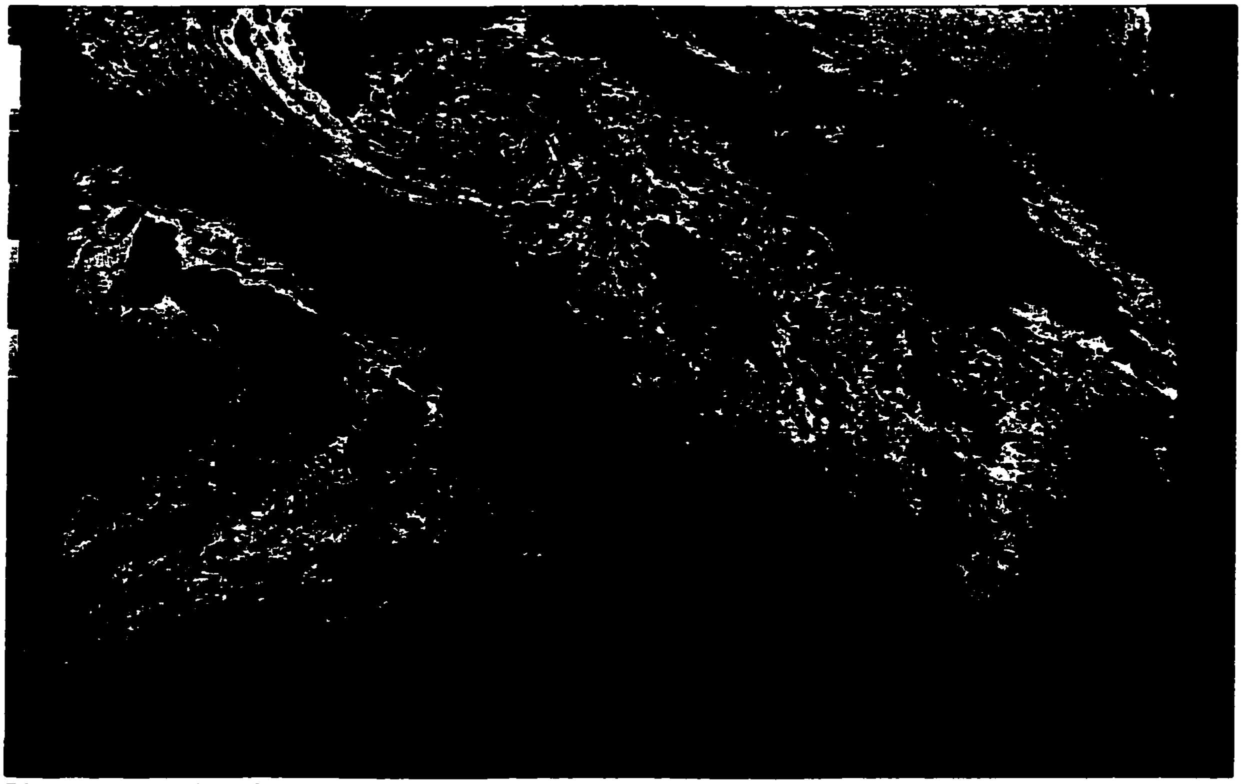

Figure 15 National Weather Service Eastern Pacific Infared Satellite Picture at 0000Z February 7th 1998.

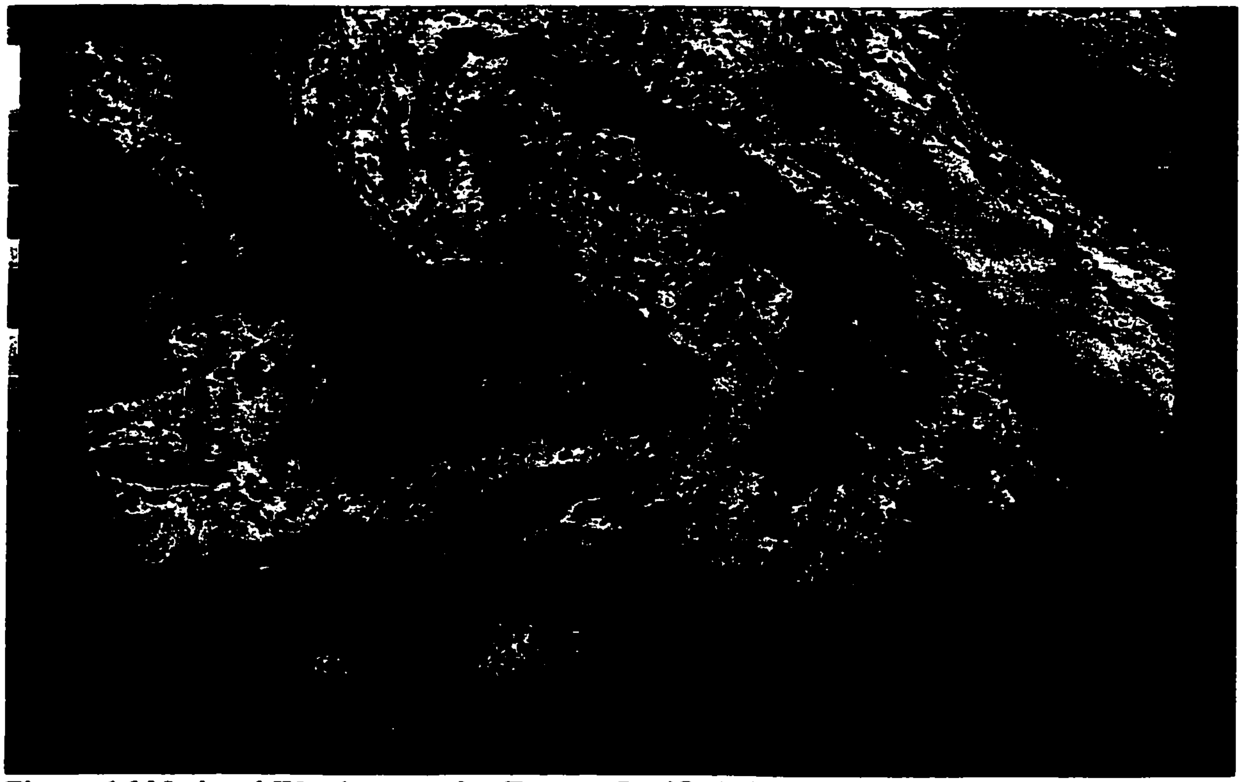

Figure 16 National Weather Service Eastern Pacific Infared Satellite Picture at 0000Z February 8th 1998.

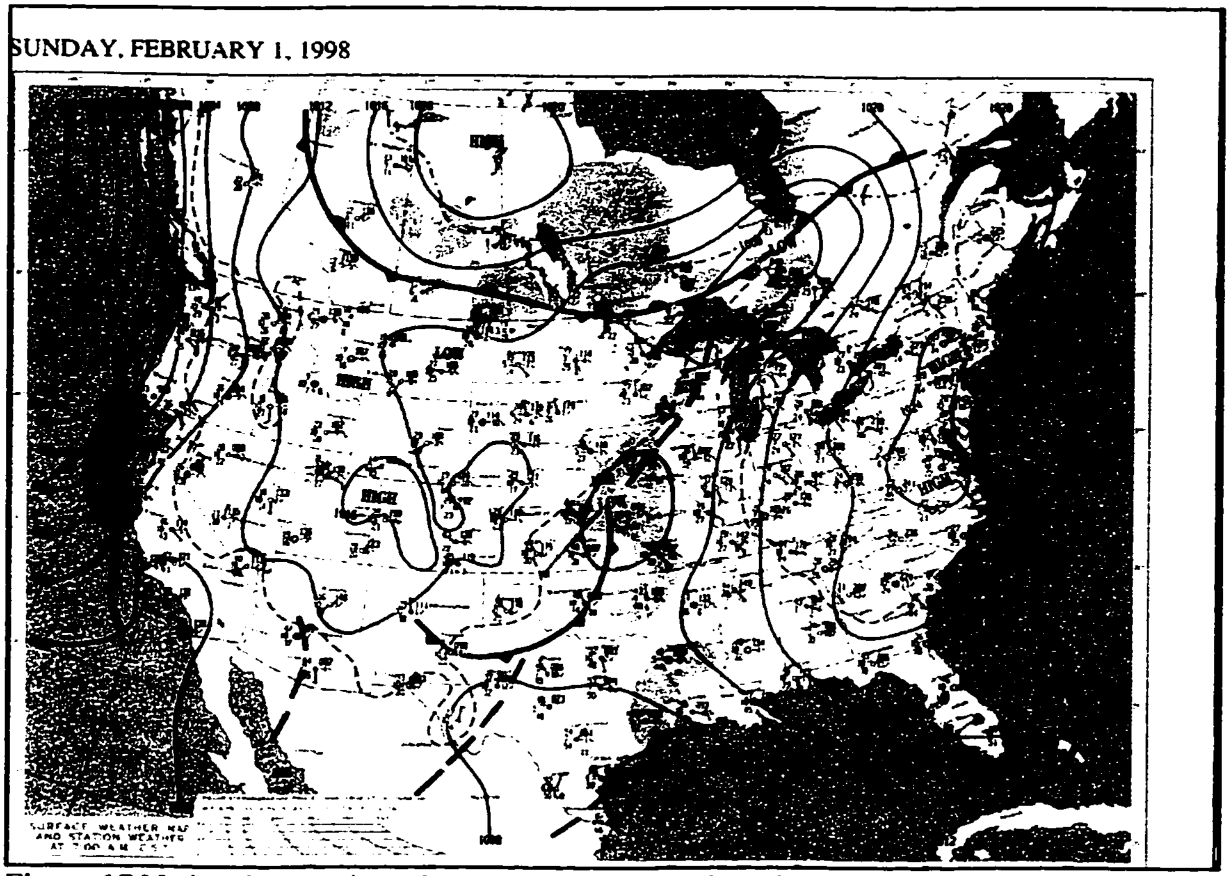

Figure 17 National Oceanic and Atmospheric Administration Daily Weather Map at 1200Z February 1st 1998.

MONDAY, FEBRUARY 2, 1998

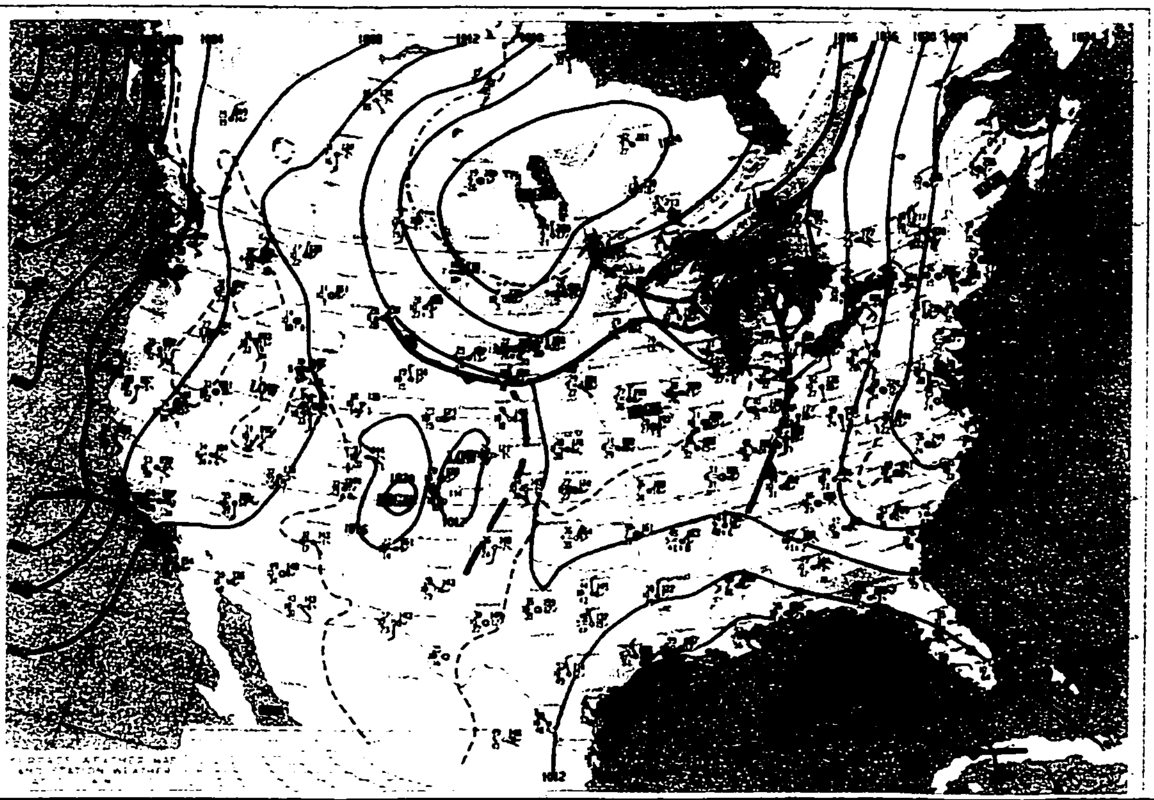

Figure 18 National Oceanic and Atmospheric Administration Daily Weather Map at 1200Z February 2nd 1998.

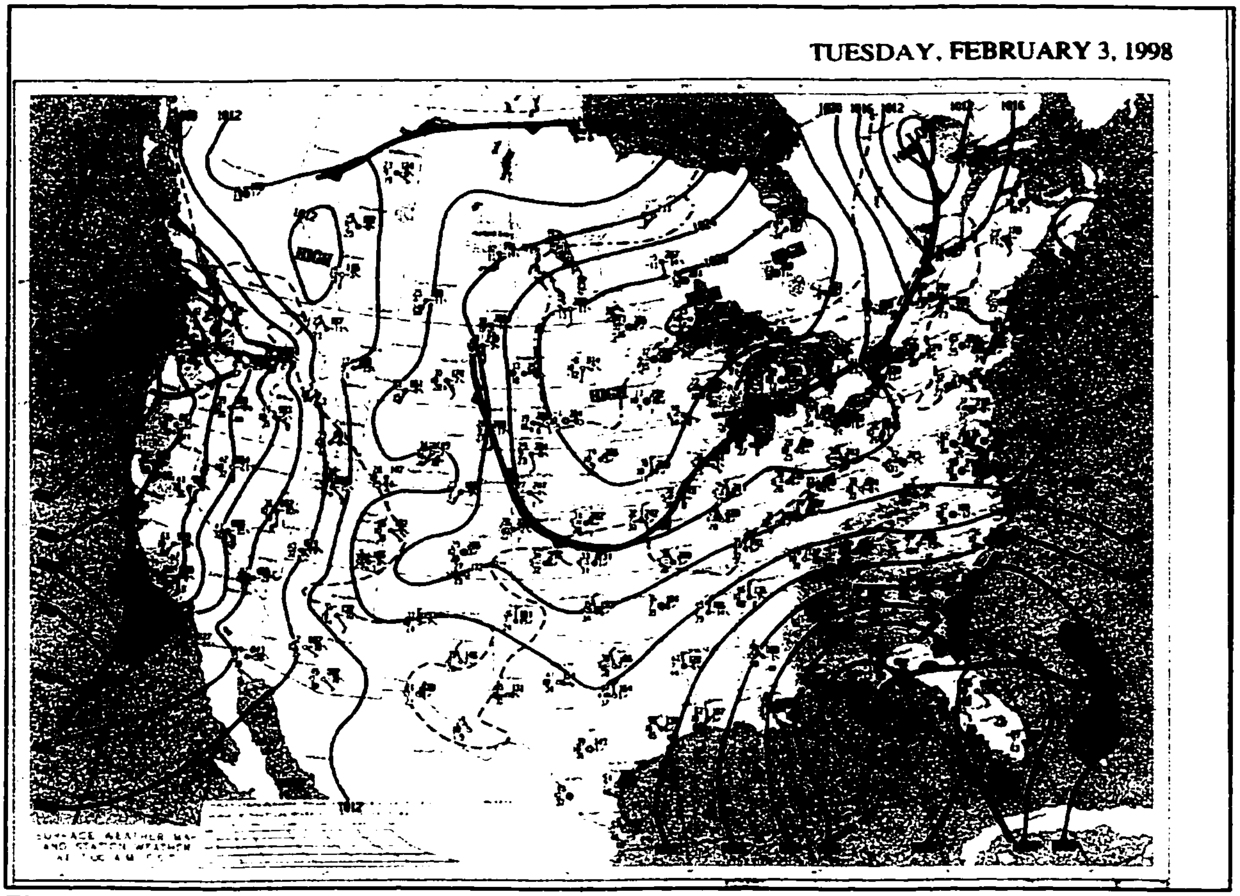

Figure 19 National Oceanic and Atmospheric Administration Daily Weather Map at 1200Z February 3rd 1998.

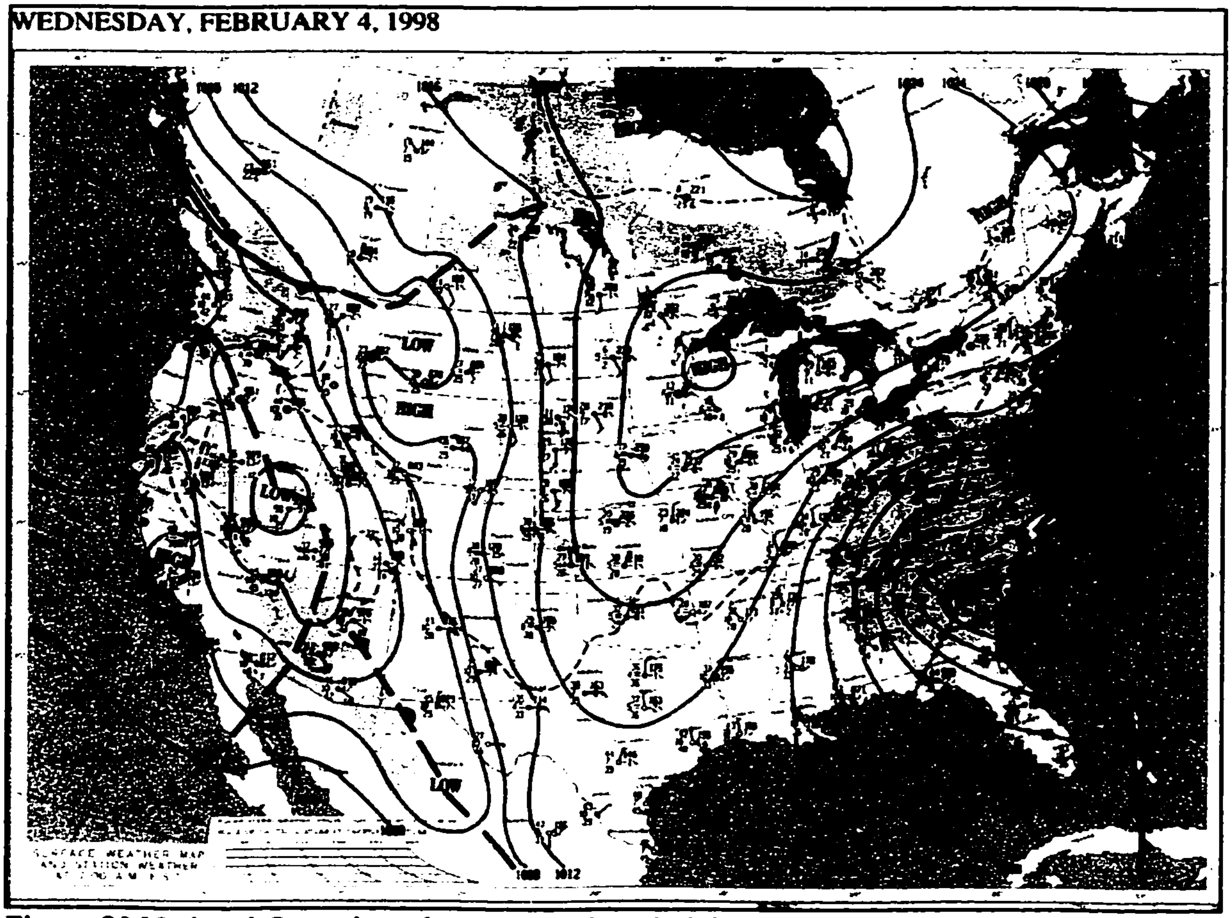

Figure 20 National Oceanic and Atmospheric Administration Daily Weather Map at 1200Z February 4th 1998.

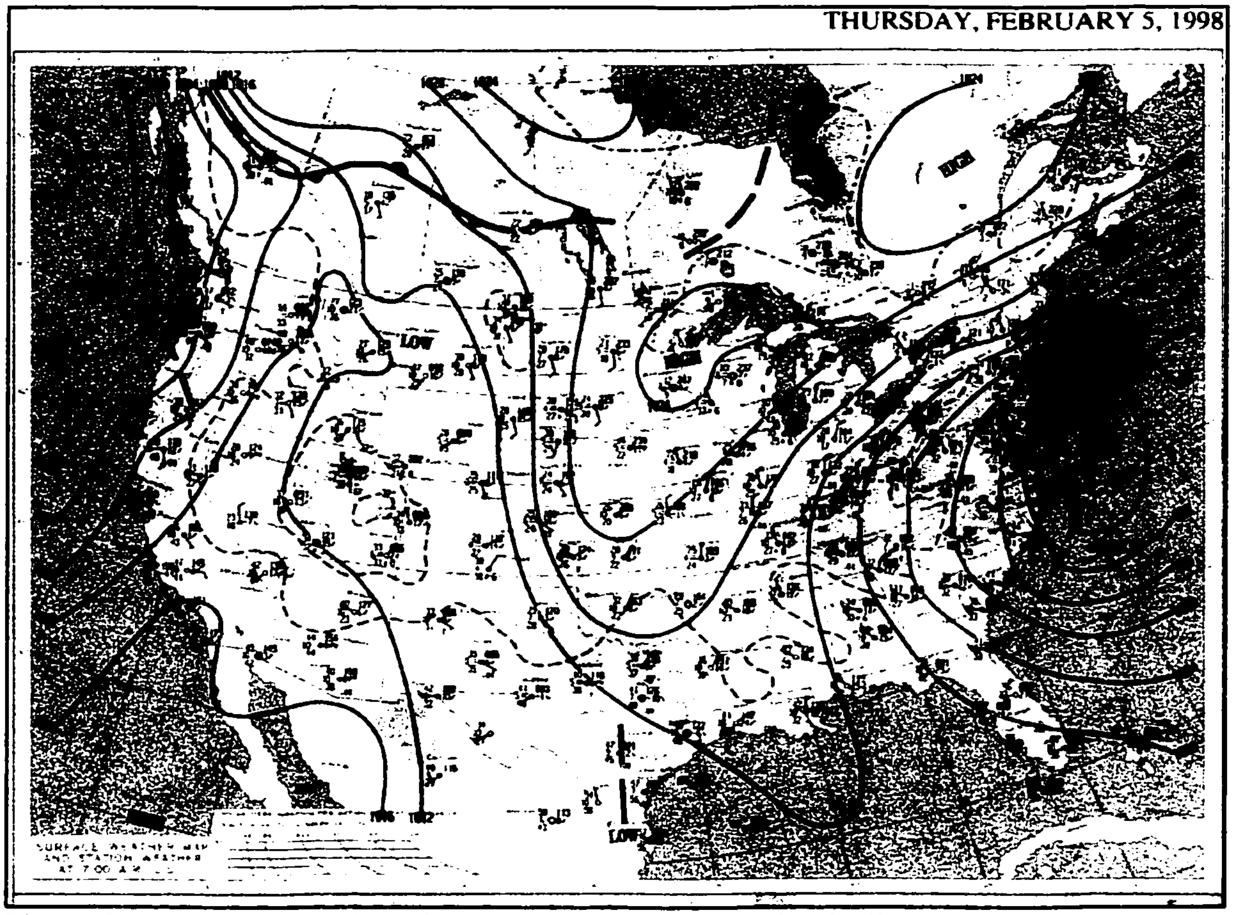

Figure 21 National Oceanic and Atmospheric Administration Daily Weather Map at 1200Z February 5th 1998.

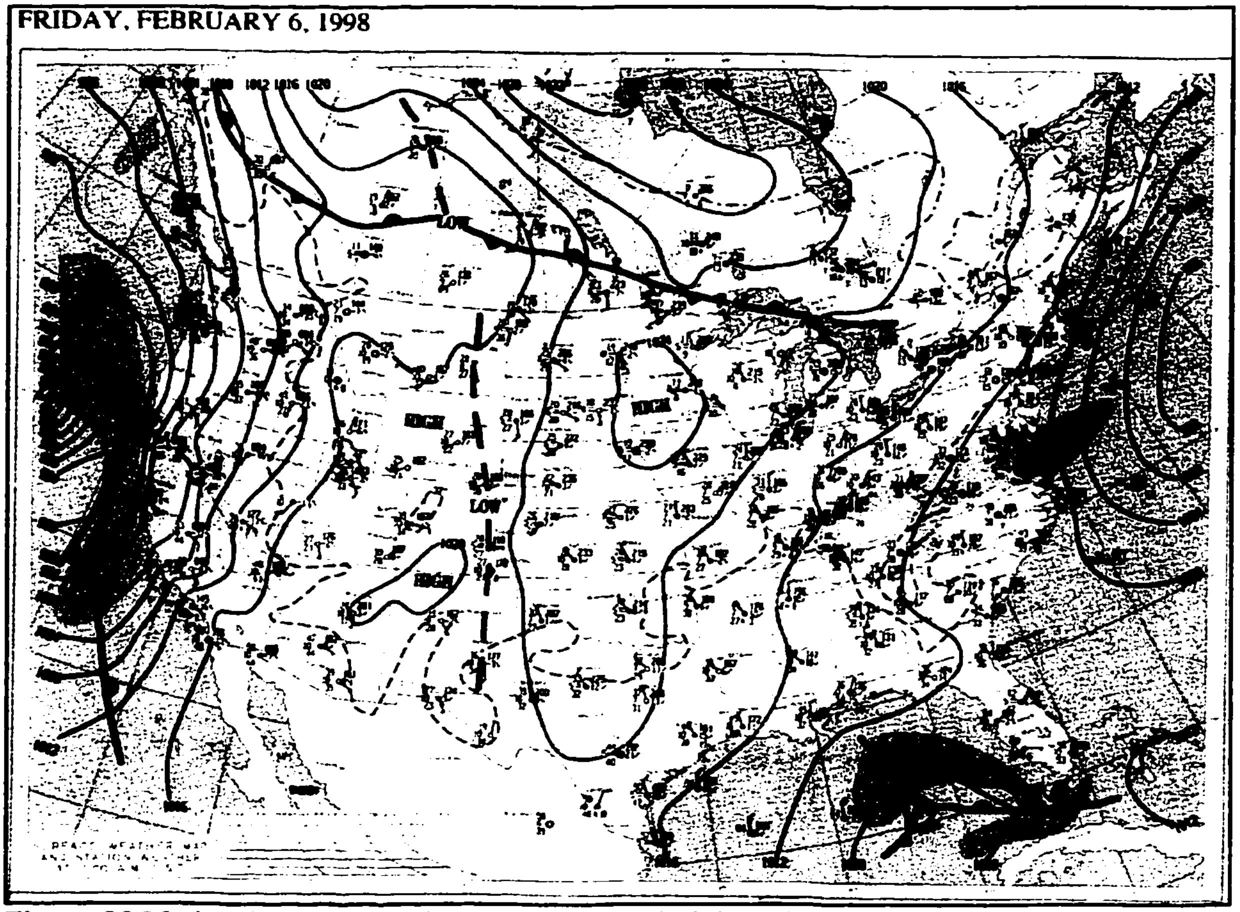

Figure 22 National Oceanic and Atmospheric Administration Daily Weather Map at 1200Z February 6th 1998.

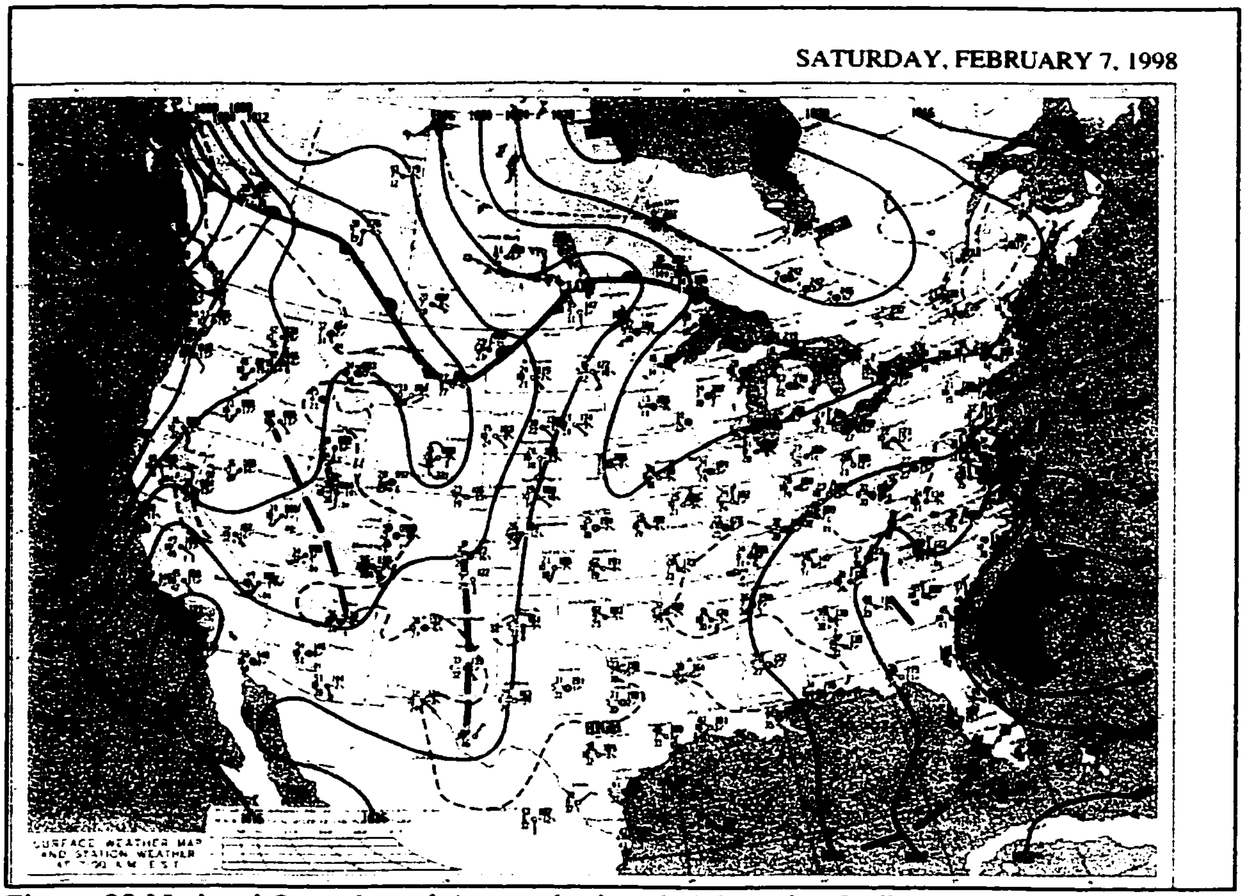

Figure 23 National Oceanic and Atmospheric Administration Daily Weather Map at 1200Z February 7th 1998.

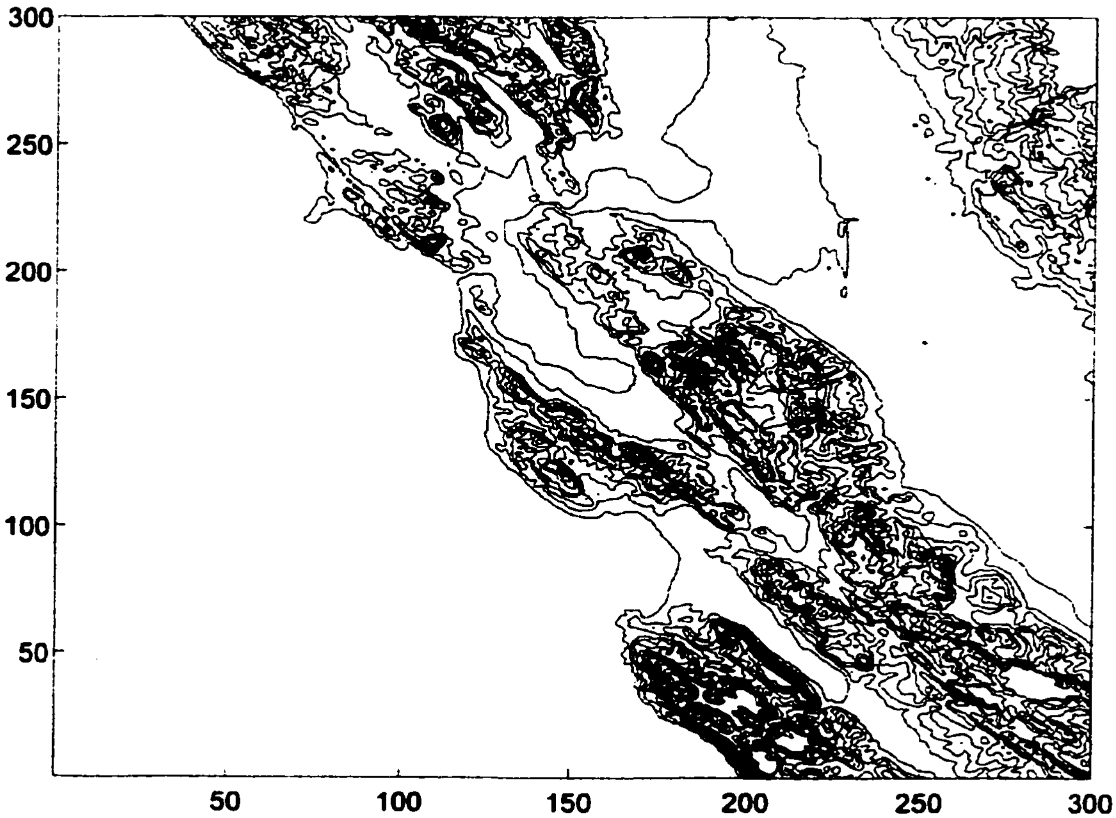

Figure 24 300km by 300km Topographic Map of the Model Domain. UTM Coordinates of Southwest Corner are 3993N and 426E. Contour Interval is 100m.

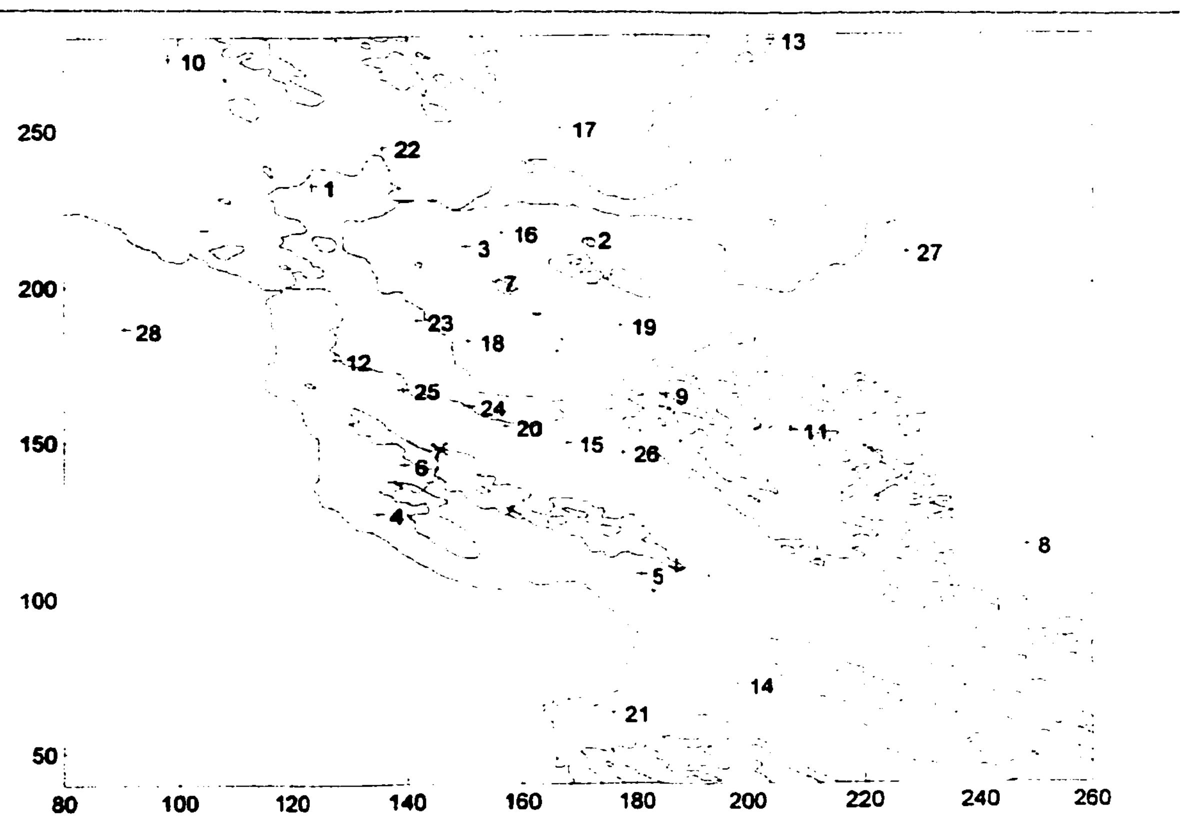

Figure 25 Map Showing location of Input Meteorological Surface Stations. Units are km North and East of UTM 3993N and 426E. Contour Interval is 500m.

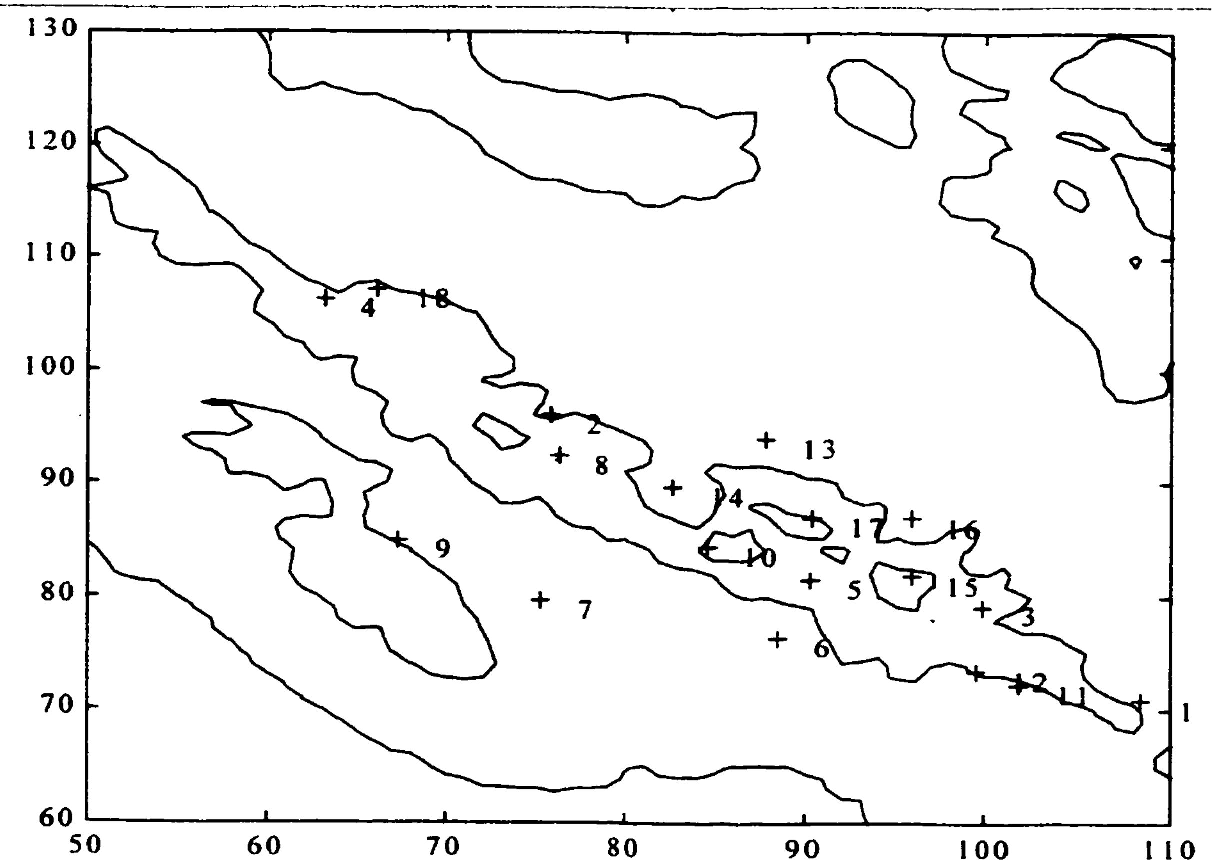

Figure 26 Rainfall Station Distribution. Units are km North and East of UTM 4026N 507E. Terrain Contour Interval is 500m.

Figure 27 Horizontal Dispersion Coefficient (Slade 1968).

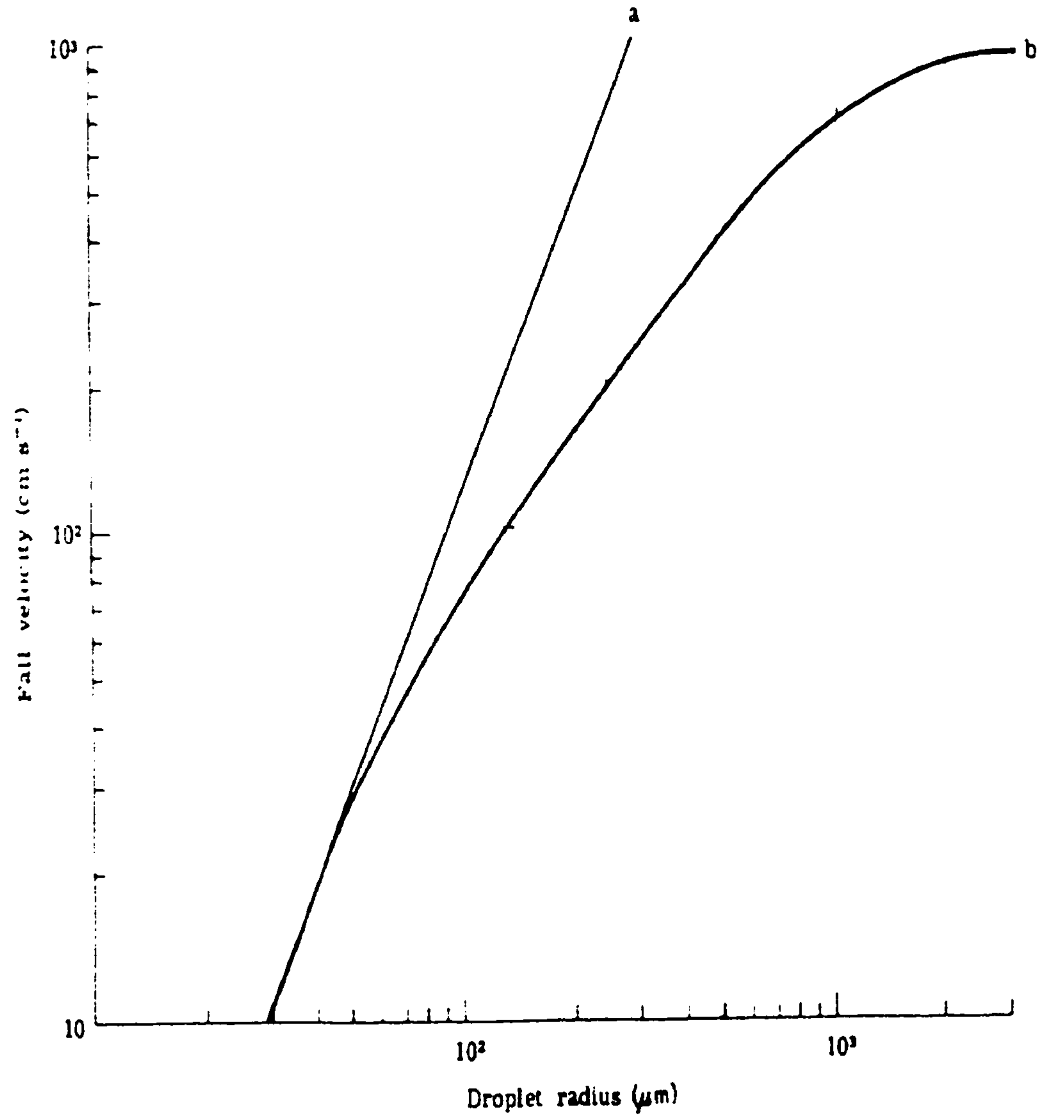

Figure 28 Theoretical Graph of Droplet Radius vs. Fall Velocity (Fleagle and Businger 1980).